

# Sphingolipids in *Physcomitrella patens*

## Dissertation

to acquire the doctoral degree in mathematics and natural science

‘Doctor rerum naturalium’

at the Georg-August-Universität Göttingen

in the doctoral degree program

GGNB Microbiology and Biochemistry

at the Georg-August University School of Science (GAUSS)

Submitted by

**Hanno Christoph Resemann**

from Göttingen

Göttingen, 2018

## Thesis Committee

**Prof. Dr. Ivo Feußner**

Department for Plant Biochemistry, Albrecht-von-Haller Institute for Plant Sciences,  
University of Göttingen

**Prof. Dr. Volker Lipka**

Department of Plant Cell Biology, Albrecht-von-Haller Institute for Plant Sciences,  
University of Göttingen

**Prof. Dr. Andrea Polle**

Department for Forest Botany and Tree Physiology, Büsgen Institute,  
University of Göttingen

## Members of the Examination Board:

**Referee:**      **Prof. Dr. Ivo Feußner**, Department for Plant Biochemistry, Albrecht-von-Haller  
Institute for Plant Sciences, University of Göttingen

**Co-referee:**   **Prof. Dr. Volker Lipka**, Department of Plant Cell Biology, Albrecht-von-Haller  
Institute for Plant Sciences, University of Göttingen

Other members of the Examination Board:

**Prof. Dr. Andrea Polle**, Department for Forest Botany and Tree Physiology,  
Büsgen Institute, University of Göttingen

**PD Dr. Thomas Teichmann**, Department of Plant Cell Biology, Albrecht-von-  
Haller Institute for Plant Sciences, University of Göttingen

**Prof. Dr. Christiane Gatz**, Department of Plant Molecular Biology and  
Physiology, Albrecht-von-Haller Institute for Plant Sciences, University of  
Göttingen

**Prof. Dr. Jörg Stülke**, Department of General Microbiology, Institute for  
Microbiology and Genetics, University of Göttingen

Date of the oral examination: 31.05.2018

# Table of contents

---

Abstract .....	V
List of abbreviations .....	VI
List of figures .....	IX
List of tables .....	XI
<b>1. Introduction .....</b>	<b>1</b>
1.1. <i>Physcomitrella patens</i> – a non-vascular plant model organism .....	1
1.2. Lipids in plants & microalgae .....	4
1.3. Modification of lipids in response to stress .....	8
1.4. Evolution of desaturases .....	10
1.5. The putative sphingolipid desaturase PpSFD .....	12
1.6. Analysis of lipids .....	14
1.7. Aims of this study .....	15
<b>2. Material &amp; Methods .....</b>	<b>17</b>
2.1. Material .....	17
2.1.1. Chemicals .....	17
2.1.2. Plants .....	17
2.1.3. Bacteria .....	18
2.2. Methods .....	18
2.2.1. Cultivation of <i>P. patens</i> cultures .....	18
2.2.2. Cultivation of <i>A. thaliana</i> plants .....	21
2.2.3. Cultivation of bacteria cultures .....	22
2.2.4. Complementing <i>A. thaliana</i> plants .....	22
2.2.5. Transcript analysis .....	24
2.2.6. Lipidomic analysis .....	26
2.2.7. Double bond position analysis .....	28
2.2.8. Fatty acid profile analysis .....	29
2.2.9. Chlorophyll content analysis .....	31
<b>3. Results .....</b>	<b>32</b>
3.1. Lipid composition in <i>P. patens</i> .....	32
3.1.1. Fatty acid composition of <i>P. patens</i> .....	33
3.1.2. Establishing a MRM-based UPLC-ESI-MS approach for the lipidome analysis of <i>P. patens</i> .....	34
3.1.3. Phospholipids in <i>P. patens</i> .....	39
3.1.4. Glycolipids and betaine lipids in <i>P. patens</i> .....	39
3.1.5. Neutral glycerolipids in <i>P. patens</i> .....	39
3.1.6. Sterol lipids in <i>P. patens</i> .....	41

3.1.7. Sphingolipids in <i>P. patens</i> .....	44
3.1.8. Lyso-lipids in <i>P. patens</i> .....	44
3.2. <i>PpSFD</i> - a <i>P. patens</i> sphingolipid fatty acid desaturase.....	46
3.2.1. <i>PpSFD</i> is a bifunctional cytochrome- <i>b5</i> fusion protein related to front-end desaturases.....	46
3.2.2. <i>Ppsfd</i> knock-out lines do not contain any mono-unsaturated C24 fatty acids in sphingolipids and some phospholipids, except for phosphatidyl-serine.....	49
3.3. Effects of cold stress on <i>P. patens</i> wild type and <i>Ppsfd</i> .....	51
3.3.1. Cold stressed <i>P. patens</i> wild type significantly adjust FA composition of most glycerolipids, <i>sfd</i> does not.....	52
3.3.2. Ceramides in <i>P. patens</i> accumulate more C24 FAs at cold stress while glycosyl-ceramides are not affected.....	56
3.3.3. Total amount of 5 major lipid groups is not affected in cold stressed <i>P. patens</i> wild type, but in <i>sfd</i> .....	57
3.3.4. Long time exposure to cold stress and continuous light shows enhanced chlorophyll degradation of <i>Ppsfd</i> .....	59
3.4. Complementation of <i>A. thaliana ads2.1</i> KO-mutant with <i>PpSFD</i> .....	63
3.4.1. Establishment of a rapid method for identifying transformed <i>A. thaliana</i> lines by chemotype analysis via LC-MS.....	63
3.4.2. Lines of <i>ads2.1</i> complemented with <i>PpSFD</i> have strongly elevated transcript levels of <i>PpSFD</i> .....	65
3.4.3. Transgenic <i>ads2.1/35S::PpSFD</i> lines show recovered phenotype at cold stress growth, similar to <i>ads2.1/35S::AtADS2</i> .....	66
3.4.4. Levels of unsaturated C24 FA moieties in cold stressed complementation lines is similar to cold stressed <i>A. thaliana</i> wild type.....	66
3.4.5. <i>AtADS2</i> desaturates at <i>n-9</i> position, while <i>PpSFD</i> (in the <i>ads2.1</i> background) desaturates at both <i>n-8</i> and <i>n-9</i> position.....	69
<b>4. Discussion.....</b>	<b>72</b>
4.1. Lipid composition in <i>P. patens</i> is far more diverse compared to <i>A. thaliana</i> due to higher FA variety.....	72
4.1.1. <i>P. patens</i> does not require the fatty acid 20:4 for survival at normal and cold conditions.....	72
4.1.2. Lipid species in <i>P. patens</i> are far more diverse than in <i>A. thaliana</i> , largely due to the additional FA moiety 20:4.....	74
4.1.3. Sphingolipids in <i>P. patens</i> differ strongly from <i>A. thaliana</i> .....	76
4.2. Cold stress in <i>P. patens</i> affects lipid composition differently depending on the lipid class.....	77
4.3. <i>PpSFD</i> is a sphingolipid FA desaturase acting on ceramides and some phospholipids.....	79
4.4. <i>Ppsfd</i> mutant does not significantly adjust lipid composition like wild type <i>P. patens</i> at cold stress.....	80
4.5. <i>PpSFD</i> and <i>AtADS2</i> function similarly in <i>A. thaliana</i> .....	82
4.6. <i>PpSFD</i> might be part of a yet unknown class of bi-functional desaturases.....	84
4.7. Outlook.....	84
<b>5. References.....</b>	<b>87</b>
<b>6. Appendix.....</b>	<b>95</b>
Curriculum vitae.....	<b>Error! Bookmark not defined.</b>

# Acknowledgements

---

Zuerst möchte ich Prof. Ivo Feußner danken für die Möglichkeit in seiner Abteilung und an diesem interessanten Thema zu arbeiten. Die Doktorarbeit hatte ihre Höhen und Tiefen, aber ich fühlte mich immer fair und gut von Ihnen betreut. Vielen Dank für das Vertrauen, dass sie mir in mehr als 5 Jahren geschenkt haben!

Vielen Dank auch an Kirstin, die sich immer aufopferungsvoll und geduldig um mich gekümmert hat. Von der Labrotation bis zur Doktorarbeit warst du immer für mich da, hast mich angetrieben und unterstützt. Nicht zuletzt deine positive Einstellung hat mich oft dazu gebracht noch mehr aus meiner Arbeit rauszuholen.

Conny möchte ich danken für die gute Betreuung an den Maschinen. Messungen waren nicht immer einfach und ohne deine Expertise wäre ich wahrscheinlich nicht so weit gekommen! Vielen Dank!

Ein besonderer Dank gebührt auch Ellen! Du hast mich immer gut beraten wenn es ums Klonieren ging, aber vor allem war es deine nette Art die mir immer sehr geholfen hat! Und du hast immer einen Muffin ohne Obst für mich mitgebacken, das war sehr lieb 😊

Pia möchte ich danken für die lange Zeit, in der du dich um meine Moos-Kulturen gekümmert hast. Und Susanne, meine Arabidopsen waren bei dir immer in guten Händen!

Vielen Dank Sabine für die unzähligen Male wo du mich bei Extraktionen, Messungen und HPLC-Läufen unterstützt hast. Bei dir im Labor war es immer lustig! Tut mir leid, dass ich dich so oft erschreckt habe...

Den allergrößten Dank verdienen aber Mama, Papa, Rike und der Rest der Familie. Vielen Dank dass ihr all die Jahre so stark zu mir gestanden habt. Ich fühlte mich immer unterstützt in allem was ich getan hab und ohne euch wäre ich nicht hier. Ihr seid die Allerbesten!

Und ganz lieben Dank an dich, Franzi! Du musstest viel meiner gestressten Stimmung ertragen in den letzten Monaten, aber jetzt ist es geschafft! Danke dass du für mich da bist!

**And finally: Big thanks to all of you from the Feußner department! All of you guys made this a really nice place to be! Thanks for all the laughter, cross-word puzzles, barbeques, hikes and overall good working atmosphere!**

# Abstract

---

The model organism *Physcomitrella patens* is a bryophyte in the group of non-vascular plants. Evolutionary, bryophytes evolved shortly after the event when plants developed the ability to grow on land. *P. patens* can therefore be considered a link between marine plants and vascular plants, which makes it interesting for research into how plants adapted to terrestrial conditions. Nevertheless, 10 years after the *P. patens* genome was sequenced there is still much research to be done on this organism, especially on the analysis of metabolites like lipids.

In recent years, *P. patens* received more attention in genetic, transcriptomic and proteomic studies. The study of lipids, a class of biological compounds that is crucial for all living cells, has however remained very superficial in *P. patens*. In order to close the gap in research between this organism and plant model organisms like *Arabidopsis thaliana* we analyzed for the first time the lipid composition of *P. patens* in 5 different lipid groups and 19 lipid classes. In the analysis, we discovered more than 700 individual lipid species in *P. patens* via a liquid-chromatography mass-spectrometry approach.

Lipids are important in the plants' reaction to environmental stresses, like cold. When grown at low temperatures, it was observed in this work that *P. patens* modifies lipids by adjusting the number of double bonds and the length of fatty acids (FA). Lipid modification hereby occurs differently when comparing phospholipids and glycolipids. One lipid-modifying enzyme in *P. patens*, the cold-induced putative desaturase PpSFD, was analyzed in this work for its phenotype at normal and cold conditions. *Ppsfd* knock-out (KO) mutants were incapable of producing mono-unsaturated C24-FAs in ceramides and some phospholipids and appeared drier and less viable compared to wild type moss. It was observed that cold-stressed *Ppsfd* plants do not adjust their lipid composition regarding FA desaturation and length as the wild type moss does.

The cold-sensitive *A. thaliana* KO-mutant *Atads2* has a similar disruption of FA desaturation as the *Ppsfd* KO-mutant in *P. patens*. PpSFD and AtADS2 were compared on a functional and evolutionary level to understand the relation between these two enzymes. It was discovered that PpSFD and AtADS2 are not closely related and probably have evolved independently from each other. Expressing PpSFD under an overexpression promoter in *Atads2* plants complemented the cold-sensitive phenotype. It was observed that the lipid composition in complemented plants is similar to *A. thaliana* wild type, but the double bond position of unsaturated C24-FAs differs slightly.

Overall, this work shed light on the lipid composition in *P. patens* and how it is adjusted at cold stress conditions. It was observed that the desaturase PpSFD is involved in this mechanism and evolved independently from the functionally similar desaturase AtADS2 from *A. thaliana*.

# List of abbreviations

---

- aa:** Amino acid  
***A. tumefaciens:*** *Agrobacterium tumefaciens*  
**ARA:** Arachidonic acid (20:4)  
**ASG:** Acylsterol-glycoside  
**AtACT8:** *A. thaliana* actin-8  
**AtADS2:** Acyl-coenzyme A desaturase-like 2  
**AtSLD1:** *A. thaliana* long-chain base desaturase 1  
**AtSLD12:** *A. thaliana* long-chain base desaturase 2  
***A. thaliana:*** *Arabidopsis thaliana*  
***B. napus:*** *Brassica napus*  
***B. officinalis:*** *Borago officinalis*  
**bp:** Base pair  
**BSTFA:** *N,O*-Bis(trimethylsilyl)trifluoroacetamide  
**CaMV:** Cauliflower-mosaic-virus  
**Cer:** Ceramide  
**Chl:** Chlorophyll  
**CoA:** Coenzyme A  
***C. purpureus:*** *Ceratodon purpureus*  
***C. reinhardtii:*** *Chlamydomonas reinhardtii*  
***C. sativa:*** *Camelina sativa*  
**DAG:** Diacyl-glyceride  
**DGCC:** Diacylglycerol-carboxyhydroxy-methylcholine  
**DGDG:** Digalactosyl-diacylglyceride  
**DGTA:** Diacylglycerol-*O*-(*N,N,N*-trimethyl)-alanine  
**DGTS:** Diacylglycerol-*O*-(*N,N,N*-trimethyl)-homoserine  
**DGTS/A:** Diacylglycerol-*O*-(*N,N,N*-trimethyl)-homoserine/alanine  
**DHA:** Docosahexaenoic acid (22:6)  
**DMDS:** Dimethyl disulfide  
**DNA:** Desoxy-ribonucleic acid  
**DPA:** Docosapentaenoic acid (22:5)  
**EDTA:** Ethylenediaminetetraacetic acid  
**EI:** Electron ionization  
**EPA:** Eicosapentaenoic acid (20:5)  
**ER:** Endoplasmic reticulum  
***E. coli:*** *Escherichia coli*  
**ESI:** Electrospray ionization  
**FA:** Fatty acid  
**FADS:** FA desaturase  
**FAME:** FA methyl-ester  
**FID:** Flame ionization detection  
**GC:** Gas chromatography  
**GIPC:** Glycosylinositolphospho-ceramide

**Glc:** Glucose  
**GlcCer:** Glycosyl-ceramide  
**Gln:** Glutamine  
**H:** Histidine  
**Hex:** Hexose  
**HexA:** Glucuronic acid  
**HexNAc:** *N*-Acetylglucosamine  
**His:** Histidine  
**HPLC:** High-performance liquid chromatography  
**IPC:** Inositolphospho-ceramide  
**JA:** Jasmonic acid  
**KO:** knock-out  
**LC:** Liquid chromatography  
**LCB:** Long-chain base  
***L. incisa:*** *Lobosphaera incisa*  
**LDGDG:** Lyso-digalactosyl-diacylglyceride  
**LMGDG:** Lyso-monogalactosyl-diacylglyceride  
**LSWDG:** Lyso-sulfoquinovosyl-diacylglyceride  
**LPA:** Lyso-phosphatidic acid  
**LPC:** Lyso-phosphatidic acid  
**LPE:** Lyso-phosphatidic acid  
**LPG:** Lyso-phosphatidyl-glycerol  
**LPI:** Lyso-phosphatidyl-inositol  
**LPS:** Lyso-phosphatidyl-serine  
***M. alpina:*** *Mortierella alpina*  
**MGDG:** Monogalactosyl-diacylglyceride  
***M. polymorpha:*** *Marchantia polymorpha*  
**MRM:** Multiple reaction monitoring  
**MS:** Mass spectrometry  
***M. squamata:*** *Mantoniella squamata*  
**MTBA:** Methyl *tert*-butyl ether  
***N. gaditana:*** *Nannochloropsis gaditana*  
***N. tabacum:*** *Nicotiana tabacum*  
**PA:** Phosphatidic acid  
**PC:** Phosphatidic acid  
**PCR:** Polymerase chain reaction  
**PE:** Phosphatidyl-ethanolamine  
**PG:** Phosphatidyl-glycerol  
**PI:** Phosphatidyl-inositol  
***P. patens:*** *Physcomitrella patens*  
**PpSFD:** *P. patens* sphingolipid FA desaturase  
**PS:** Phosphatidyl-serine  
***P. tricornutum:*** *Phaeodactylum tricornutum*  
**PUFA:** Poly-unsaturated fatty acid  
**Q:** Glutamine  
**qRT-PCR:** quantitative real-time PCR  
***R. allomyces:*** *Rozellida allomyces*  
**RP:** Reversed-phase



***S. cerevisiae***: *Saccharomyces cerevisiae*  
**SE**: Sterol-ester  
**SG**: Sterol-glycoside  
***S. moellendorffii***: *Selaginella moellendorffii*  
**SQDG**: Sulfoquinovosyl-diacylglyceride  
***S. rosetta***: *Salpingoeca rosetta*  
**TAG**: Triacyl-glyceride  
**TLC**: Thin-layer chromatography  
***T. oceanica***: *Turbonilla oceanica*  
***T. pseudonana***: *Thalassiosira pseudonana*  
**UPLC**: Ultra-performance liquid chromatography  
**UV**: Ultra-violet  
**VLC-PUFA**: Very-long-chain poly-unsaturated fatty acid  
**WT**: wild type  
***Z. mays***: *Zea mays*

# List of figures

---

Figure 1.1. Different types of growth conditions for <i>Physcomitrella patens</i> cultures.	3
Figure 1.2. Five most common lipid classes in plants.	4
Figure 1.3. Number-based nomenclature system for describing lipids.	6
Figure 1.4. Classification of membrane-bound desaturases in plants.	12
Figure 1.5. Mean expression fold change of <i>PpSFD</i> (Phypa_171332) in <i>P. patens</i> wild type at various time points of cold stress treatment.	13
Figure 1.6. Phenotypic analysis of <i>P. patens PpSFD</i> knockout lines (gKO25) in comparison to wild type.	13
Figure 3.1. Fatty acid profile of lipid classes in <i>P. patens</i> & <i>A. thaliana</i> wild type.	33
Figure 3.2. Lipid profile of glycerophospholipids in <i>P. patens</i> wild type.	40
Figure 3.3. Lipid profile of glycerolglycolipids in <i>P. patens</i> wild type.	41
Figure 3.4. Lipid composition of neutral glycerolipids in <i>P. patens</i> wild type.	42
Figure 3.5. Lipid composition of sterol lipids in <i>P. patens</i> wild type.	43
Figure 3.6. Sphingolipid composition in <i>P. patens</i> wild type.	45
Figure 3.7. Peptide sequence comparison between <i>PpSFD</i> (XP_024359978) and the most closely related desaturases in <i>A. thaliana</i> and <i>P. patens</i> ( <i>PpΔ5-FADS</i> , <i>PpΔ6-FADS</i> , <i>PpΔ8-SLD</i> , <i>AtΔ8-SLD1</i> & <i>AtΔ8-SLD2</i> ).	48
Figure 3.8. Phylogeny of <i>PpSFD</i> compared with closely related desaturases from other organisms.	49
Figure 3.9. Comparison of sphingolipids that contain C24-fatty acid moieties in <i>P. patens</i> wild type & <i>sfd</i> -KO line.	50
Figure 3.10. Comparison of phospholipids that contain the fatty acid 24:1 in <i>P. patens</i> WT & <i>sfd</i> -KO line.	51
Figure 3.11. Lipid composition changes in <i>P. patens</i> wild type after cold stress treatment.	54
Figure 3.12. Effects of cold stress on FAs chain length in combined lipid species of PC and MGDG.	54
Figure 3.13. Effects of cold stress on total number of double bonds in combined lipid species of PC and MGDG.	55
Figure 3.14. Effects of cold stress on the amount of the FA 20:4 in combined lipid species of PC and MGDG.	56
Figure 3.15. Ceramide composition changes in <i>P. patens</i> wild type & <i>sfd</i> -KO after cold stress treatment.	57
Figure 3.16. Relative peak area of combined detected lipid species in <i>P. patens</i> wild type & <i>sfd</i> -KO at normal & cold stress conditions ordered into 5 major lipid groups.	58
Figure 3.17. Total peak area of all detected TAG lipid species in <i>P. patens</i> wild type & <i>sfd</i> -KO at normal & cold stress conditions.	59
Figure 3.18. Moss plate cultures at normal temperature (24 °C) and protonema-inducing growth conditions (with tartrate).	60

Figure 3.19. Moss plate cultures at cold stress temperature (6°C) and protonema-inducing growth conditions (with tartrate).	61
Figure 3.20. Chlorophyll content of normal grown (24°C) and cold stressed (6°C) of <i>P. patens</i> wild type and KO-lines from protonema-inducing growth conditions (with tartrate).	62
Figure 3.21. Scheme for rapid chemotype analysis of transformation lines.	64
Figure 3.22. Relative transcript levels of genes <i>AtADS2</i> & <i>PpSFD</i> in different cold-stressed <i>A. thaliana</i> complementation lines.	65
Figure 3.23. Cold stress experiment with <i>A. thaliana</i> complementation lines.	67
Figure 3.24. C24 and C26 containing sphingolipids in <i>A. thaliana</i> mutant <i>ads2.1</i> and its complementation lines with <i>AtADS</i> and <i>PpSFD</i> .	68
Figure 3.25. Relative peak area of C24 fatty acid PC, PE & PS in <i>A. thaliana</i> complementation lines.	69
Figure 3.26. Analysis of double bond position in 24:1;1 in <i>A. thaliana</i> wild type, <i>P. patens</i> wild type & <i>A. thaliana ads2.1/35S::PpSFD</i> (C11).	71
Appendix 1. Structure of plasmid constructs used for <i>Agrabacterium</i> -mediated transformation in <i>A. thaliana ads2.1</i> lines.	95
Appendix 2. Free LCB composition in <i>P. patens</i> wild type.	96
Appendix 3. Lyso-lipid composition in <i>P. patens</i> wild type.	96
Appendix 4. Sphingolipid composition in <i>P. patens</i> wild type & <i>sfd</i> -KO line.	97
Appendix 5. Effects of cold stress on FAs chain length in combined lipid species of glycerolipids (phospholipids, glycolipids, neutral lipids).	98
Appendix 6. Effects of cold stress on total number of double bonds in combined lipid species of glycerolipids (phospholipids, glycolipids, neutral lipids).	99
Appendix 7. Effects of cold stress on the amount of the FA 20:4 in combined lipid species of glycerolipids (phospholipids, glycolipids, neutral lipids).	100
Appendix 8. Protein IDs of peptides used for building a phylogenetic tree (see Figure 3.8)	101
Appendix 9. Moss plate cultures at normal temperature and gametophore-inducing growth conditions (without tartrate).	102
Appendix 10. Moss plate cultures at cold stress temperature (6°C) and gametophore-inducing growth conditions (without tartrate).	103
Appendix 11. Moss plate cultures at normal grown (24°C) and cold stress temperature (6°C) and gametophore-inducing growth conditions (without tartrate).	104
Appendix 12. Moss plate cultures at normal grown (24°C) and cold stress temperature (6°C) and protonema-inducing growth conditions (with tartrate).	105

# List of tables

---

Table 2.1.: Composition of 1 L Wang medium	18
Table 2.2.: Composition of 1 L TES (Trace element solution)	18
Table 2.3.: Composition of 1 L vitamin solution	19
Table 2.4.: Composition of 1 L BCD medium	19
Table 2.5.: Composition of 1 L Knop medium	20
Table 2.6.: Composition of 1 L LB medium	20
Table 2.7.: Composition of 1 L CTAB extraction solution	22
Table 2.8.: qRT-PCR cyclers settings	25
Table 2.9.: Starting conditions for LC separation of different lipid classes	25
Table 2.10.: Ionization voltages for analyzing different lipid classes	27
Table 2.11.: Linear gradient of FAME HPLC separation	28
Table 3.1. Survey of all lipid species used for screening the <i>P. patens</i> lipidome.	36
Table 3.2. Lipids species detected in <i>P. patens</i> wild type.	38

# 1. Introduction

---

## 1.1. *Physcomitrella patens* – a non-vascular plant model organism

Photosynthesis, one of the most important biosynthesis pathways for life on earth, has its roots in ancient microorganisms living in water. When these organisms, like cyanobacteria, merged with eukaryotic cells the first step towards the evolution of plants was set. Photosynthetic unicellular organisms (microalgae) became multicellular organisms (macroalgae), forming tissues adapted for better light absorption or attachment to surfaces. About 450 million years ago, some of these plants evolved the ability to move away from their former habitat in the Ordovician oceans and settle on land (Clarke, Warnock et al. 2011). Life on land provided many challenges compared to life under water. Organisms have to be resistant against inconsistent water availability, stronger temperature fluctuations, desiccation of tissue, higher concentration of oxygen, and many more abiotic stresses to thrive under these conditions. The first kind of plants to adapt to terrestrial conditions (embryophyta) are the early ancestors of a diverse group called bryophytes, including liverworts, mosses, and hornworts (Cuming 2011). Bryophytes in general are often called just “mosses”, even though this just describes one subgroup of bryophytes. Liverworts are considered the oldest branch of the plant phylogenetic tree, splitting about 420 million years ago to mosses and hornworts (Clarke, Warnock et al. 2011). These early plants still have a lot of similarities to algae, in that they need water to reproduce, do not have actual roots (for nutrient or water absorption) and do not have a fully developed waxy layer surrounding outer tissues (cuticula). The absence of specialized structures for water transport makes these organisms non-vascular plants, while later plants developed tissue for transport of nutrients and water (coining the term “vascular plants” or “tracheophytes” (Glime 2007)).

Mosses are common all over the world in all land habitats. They make up the second largest group in the plant kingdom, behind flowering plants (Glime 2007). In very cold climate zones like arctic tundra and boreal woodlands, mosses can make up a substantial part of the biomass in these regions. Mosses appear to be well adapted to low temperature conditions compared to other plants (Rutten and Santarius 1992). There are reports of frozen moss being successfully revived after thousands of years in hibernation (Roads, Longton et al. 2014) and they can survive loss of high amounts of water (Proctor, Ligrone et al. 2007). For some animals, mosses can make up the majority of seasonal diets (Karunen and ARO 1979, Eskelinen 2002). However, mosses are commonly not a preferred food source for most organism, which is in part credited to the high content of defensive components like phenols (Xie and Lou 2009). Mosses grow predominantly in a haploid growth stage, the gametophyte, while the diploid sporophyte is only formed for producing spores (Cove 2005). This is in contrast to vascular plants, where the haploid gametophyte is strongly reduced, while the diploid sporophyte represents the dominant life cycle. Industrial usage of mosses is not strongly developed, focusing historically mostly

on its capability of water retainment as absorbents, as decoration, and a fuel for burning as peat.

*Physcomitrella patens* is a moss that was chosen as a model organism for non-vascular plants. *P. patens* is a leafy moss from the family of Funariaceae, a small plant that grows in all climate zones on all continents (Hodgetts 2010). In nature, it finishes a complete life cycle in several months (Cove 2005). It grows on wet soil that is exposed when water levels of small ponds fall after prolonged periods of sunshine in summer. It survives winter periods as spores (Engel 1968, Hohe and Reski 2002). The most commonly studied strain of *P. patens*, “Gransden”, has been continuously grown under laboratory conditions for over half a decade at this point (Ashton and Cove 1977, Cove 2005). The initial genomic analysis of *P. patens* was done in 1968 (Engel 1968) and was eventually chosen for genome sequencing (Cove 2005), which was completed in 2008 (Rensing, Lang et al. 2008). Since then, *P. patens* has been analyzed extensively concerning development, metabolism, adaptation to abiotic stresses and genetic relationship to other plants.

The main reason why *P. patens* was chosen as a model organism is its high accessibility for loss-of-function genetic experiments via homologous recombination (Schaefer, Zryd et al. 1991). *P. patens* possesses a highly effective DNA repair mechanism that is capable of inserting foreign DNA into protoplasts (cells without a cell wall) and integrating it in the genomic DNA (homologous recombination). It was shown that the rate of transformation via homologous recombination in *P. patens* is comparable to that of *Saccharomyces cerevisiae*, making it the only model plant known today to have this ability. This makes *P. patens* very interesting for the formation of targeted genomic knock-out mutants, which in vascular plants have to be produced by random mutations and managed via seed banks. The effectiveness of the genetic modification in *P. patens* is furthermore amplified due to the haploid-dominant life cycle of non-vascular plants. Mutations that occur in the genome therefore immediately take effect if they are functional, subsequent test crossings of transformed plants are not necessary. This all led to the development of a *P. patens* strain in which the plant-specific N-glycosylation of proteins is not functional anymore (Karg and Kallio 2009). This line is capable of producing proteins for medical purposes without risking severe allergic reactions that would normally be caused by non-human-specific glycosylations (Decker, Gorr et al. 2003) ([www.greenovation.com](http://www.greenovation.com)).

*P. patens* can be grown at a variety of different cultivation techniques. The use of plate cultures has been established early (Cove 2005), where moss colonies can be grown at room temperature and varying lighting conditions, even continuous light. The formation of spores is usually not desired in most experiments, but it can be easily avoided because sporulation is only induced at lower temperatures (15 °C) and short-day lighting conditions (Cove 2005). *P. patens* grows under long-day conditions and room temperature continuously as the haploid gametophyte and can remain in this growth stage indefinitely. The gametophyte tissue in *P. patens* comes in two different forms: the filament-like and fast-growing protonema and the leaf-like gametophore. If *P. patens* is grown from spores, the protonema is the first kind of tissue that is formed. At standard medium conditions, the protonema spreads out on an agar plate, while the gametophores are formed as branches from this filament (Cove 2005). *P. patens* can also be grown in liquid conditions without trouble, ranging from shaken flask cultures to more sophisticated bioreactors (Decker and Reski 2004). The fast-growing protonema stage of the moss is hereby preferred, which can be maintained by adding tartrate to the liquid growth medium and

regularly disrupting the moss tissue mechanically. Different growth conditions of *P. patens* cultures are depicted in Figure 1.1.

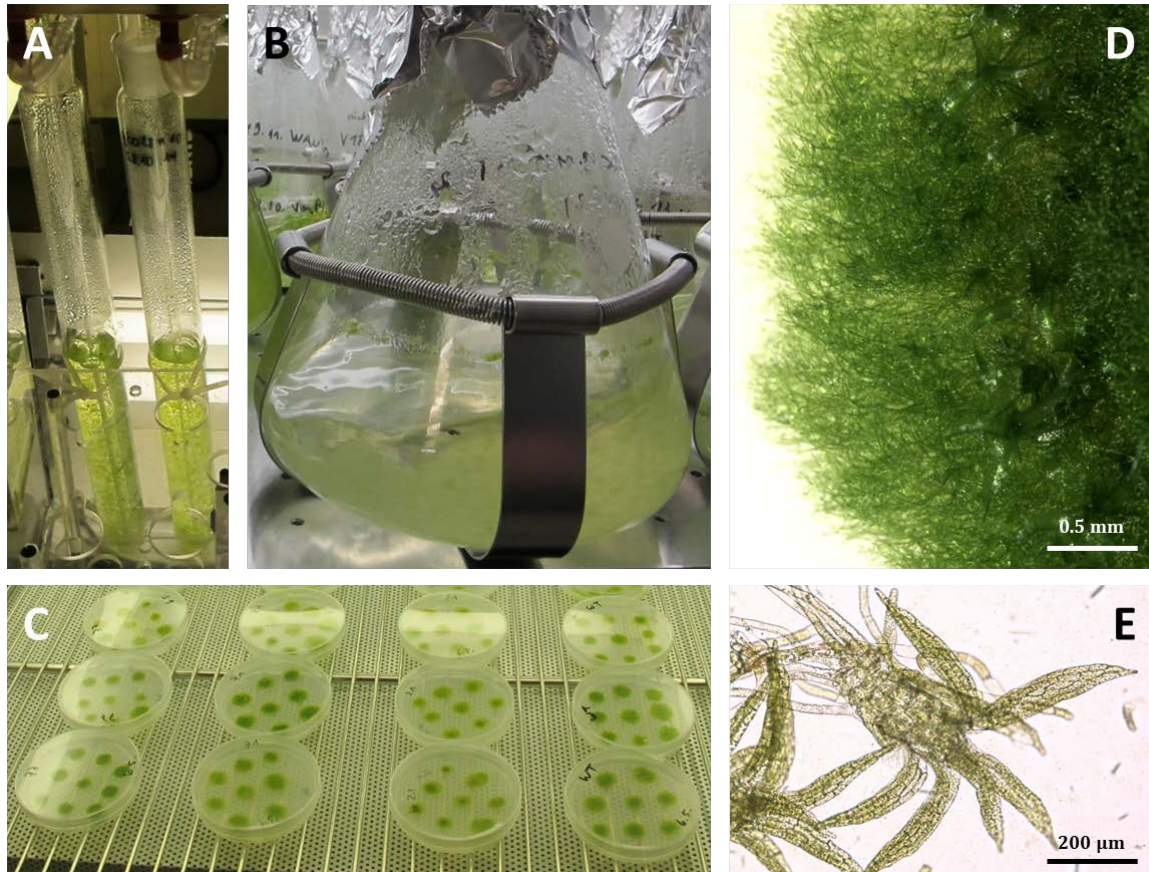


**Figure 1.1. Different types of growth conditions for *Physcomitrella patens* cultures.** A: Aerated liquid culture (air substituted with 1% CO<sub>2</sub>). B: shaken liquid cultures (not gassed). C: agar plate culture. D: Close-up of a protonema tissue on a plate culture. E: Plate moss culture at cellular level, showing a gametophore. All cultures are inoculated with disrupted moss material.

Despite the increased interest in *P. patens* as a model plant and an evolutionary connection between marine and vascular plants, research on a variety of topics is still quite scarce. One notable area of research that has not been explored a lot up to now in *P. patens* is the analysis of lipids. In parts, *P. patens* and other bryophytes have been studied regarding their lipid composition (Dembitsky 1993), but these analyses are mostly focusing on only a few lipid species or are several decades old (Grimsley, Grimsley et al. 1981). To this day, an analysis of a complete overview of all kinds of lipid classes in *P. patens* has not been published.

## 1.2. Lipids in plants & microalgae

Lipids are a very important class of metabolites that are present in all kinds of organisms, including plants. They are defined by their mostly hydrophobic nature, often combined with hydrophilic head group residues, making them amphiphilic compounds. Purely hydrophobic lipids are used as storage molecules in fats and oils, while amphiphilic lipids may form bilayers in aquatic solutions. These bilayers, or membranes, are one of the defining characteristics of living cells, establishing the “inside” of a cell against the “outside” of the environment (Voet and Voet 2004). Lipids can also function as signaling molecules, for example as precursors for the formation of oxylipins (Andreou, Brodhun et al. 2009). The five most common lipid groups in plants are depicted in Figure 1.2.

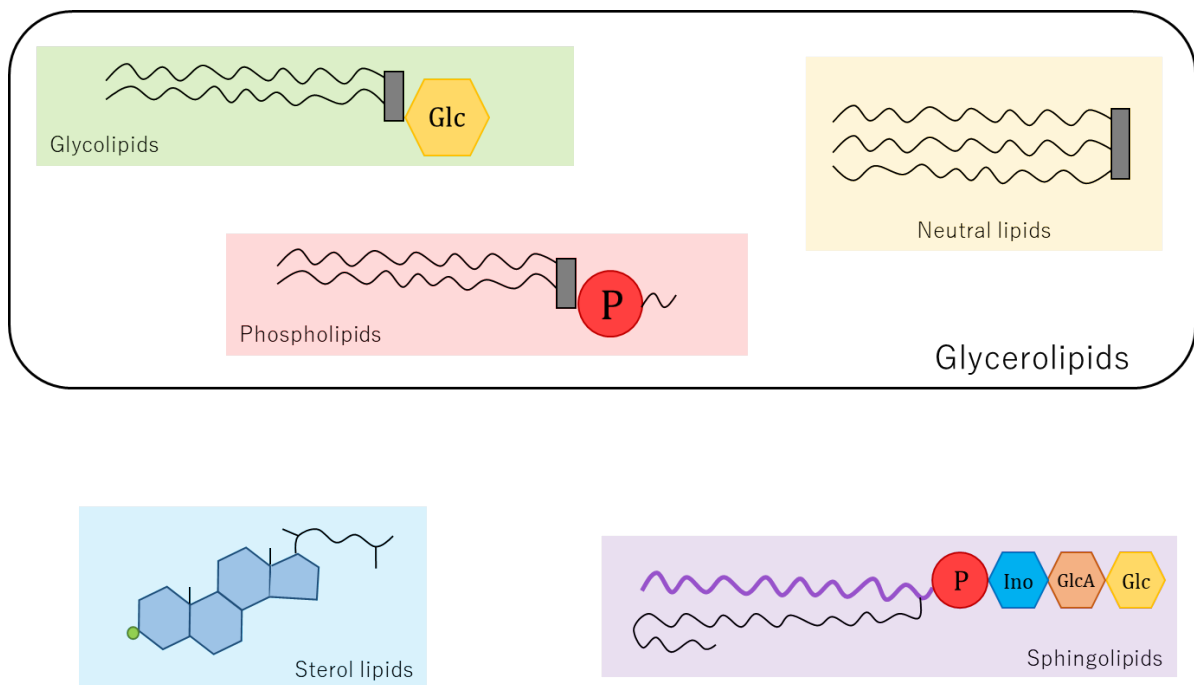


**Figure 1.2. Five most common lipid classes in plants.** Glc: Glycosyl residue, P: phosphate residue, Ino: inositol residue, GlcA: glucuronic acid residue. Grey boxes represent the glycerol backbone of glycerolipids. The purple lines represents the long-chain base (LCB) backbone of sphingolipids. Black lines represent acyl- and isoprenyl-residues.

Lipids can come in a variety of different forms. In general, lipids can be defined by their backbone molecule (glycerol, long-chain base, sterol etc.) and the type of head group attached to it (sugars, phosphates, no head groups). In plants, lipids are present most abundantly as glycerolipids (which in this work we divide into glycolipids, phospholipids and neutral lipids), sterol lipids and sphingolipids. The three types of glycerolipids all have in common that they contain the backbone molecule glycerol, to which fatty acid (FA) moieties are connected to (via ester bonds) as well as different polar head groups. These head groups can consist of sugars (in glycolipids) or phosphate-containing residues (in phospholipids), or they can be completely absent (in neutral lipids). Depending on the exact molecular makeup of the head group, these lipid groups can be further divided into lipid classes (see Figure 1.2.). Glycolipids can be divided into monogalactosyl-



diacylglycerides (MGDG), digalactosyl-diacylglycerides (DGDG), and sulfoquinovosyl-diacylglycerides (SQDG). Phospholipids are divided into phosphatidic acid (PA), phosphatidyl-choline (PC), phosphatidyl-ethanolamine (PE), phosphatidyl-serine (PS), phosphatidyl-glycerol (PG), and phosphatidyl-inositol (PI) (Buchanan 2015). Neutral lipids are only defined by the number of FA moieties attached to the glycerol backbone, either two for diacyl-glycerides (DAG) or three for triacyl-glycerides (TAG). Another type of glycerolipid found in microalgae and bryophytes are the betaines, which have a trimethyl-homoserine (DGTS), a trimethyl-alanine (DGTA) or a carboxy-choline (DGCC) as a headgroup (Dembitsky 1996). All these lipids can also be present as so-called lyso-lipids, meaning a lipid that contains only one acyl-chain while the remaining hydroxyl-group of the glycerol backbone is left unoccupied. Lyso-lipids may be biosynthesis intermediates, induce curvature in membranes, and are typically not present in high amounts in cells.

Lipids that do not contain a glycerol backbone are sterols and sphingolipids. Sterols consist of a type of steroid backbone (which in plants can be one of 5 different types, (Wewer, Dombrink et al. 2011)), as well as a possible residue connected to the hydroxyl-group of that sterol. This residue can either be a FA moiety in sterol-esters (SE), a sugar moiety in sterol-glycosides (SG) or both in acylsterol-glycosides (ASG). Sterols are very commonly encountered as free sterols without any head groups or acyl-chains. Sphingolipids have as a backbone a long-chain base (LCB), a molecule consisting of a long acyl-chain with 2 – 3 hydroxy-groups and an amino-residue. At the amino-residue, FA moieties can be attached, forming a ceramide (Cer). If additionally a sugar moiety is connected at the C<sub>1</sub> hydroxy-group, the molecule is called a glycosyl-ceramide (GlcCer). If instead of a sugar moiety a complex head group consisting of sugars and phosphate is added, the resulting sphingolipid class is called a glycosylinositolphospho-ceramide (GIPC). LCBs without FA moieties attached to it (free LCBs) are not encountered in high amounts in living organisms, since they can also act as an apoptosis signal to the cell (Buchanan 2015).

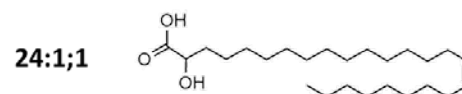
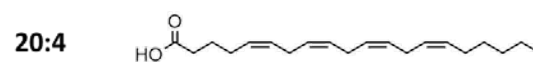
Since there are so many different lipid species present in any organism, it is important to have an easily understandable system of nomenclature at hand to describe a single lipid molecule as accurately as possible. In Figure 1.3., a number-based system is displayed that can be used to define FAs, LCBs and complex lipids accurately. A FA in a glycerolipid is hereby described as X:Y, where X represents the number of carbon atoms and Y the number of double bonds in the FA moiety. When describing LCBs and FAs in sphingolipids, the nomenclature X:Y:Z is used, where Z additionally stands for the number of hydroxyl-groups in the FA or LCB moiety. Complex lipids are described as H(R<sub>1</sub>/R<sub>2</sub>), where H stands for the shortcut of the specific head group of the lipid class (e.g. PC), R<sub>1</sub> stands for the first FA moiety of the lipid or the LCB species in sphingolipids, and R<sub>2</sub> stands for the other FA residue.

The position of a double bond in a FA can be stated in two ways: 1) Δ#, which means that the double bond is located at the # C counting from the carboxyl-end of the FA, 2) ω# or *n*-, which means the double bond is located the # C counting from the methyl-end of the FA. For poly-unsaturated FAs (PUFAs), it is common to only state the position of the double bond nearest to the methyl-end (as *n*-#). The other double bonds in the FAs are then located towards the carboxyl-end of the FAs each 3 Cs apart from the next double bond.

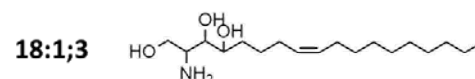
Lipids fulfill different functions in plants, depending on their head group structure and acyl-residues. The size and polarity of head groups has influence on the curvature of the

membranes they are part of, as well as the surface charge of these membranes. Acyl-chains in lipids can vary in length and in the number of double bonds present in these chains, which influences properties like membrane thickness and fluidity (Holthuis and Menon 2014). In most glycerolipids in plants, FA residues are between 16 and 18 carbons long and contain between 0 and 3 double bonds. The presence of very-long-chain polyunsaturated FAs (VLC-PUFAs) is, unlike in animals or microalgae, usually low in plants. The in animals common VLC-PUFA arachidonic acid (20:4 *n*-3) has so far only been found in major amounts in microalgae like *Lobosphaera incisa* (Bigogno, Khozin-Goldberg et al. 2002) and in bryophytes (Dembitsky 1993), but not in vascular plants. The FA hexadecatrienoic acid (16:3 *n*-3) is commonly only found in plants, and there only in glycolipids (Buchanan 2015). FAs with even longer chain-lengths are typically only found in some specific lipid classes in higher amounts, like neutral lipids. Most prominently, sphingolipids contain these very long FAs, which are usually present saturated or mono-unsaturated, and are commonly hydroxylated at the  $\alpha$ -position (Luttgeharm, Kimberlin et al. 2016).

### Fatty acids



### Long-chain bases



### Glycerolipids

FA-1 FA-2  
Head(16:0/18:3)



### Sphingolipids

LCB FA  
Head(18:1;3/24:1;1)

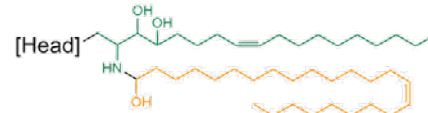


**Figure 1.3. Number-based nomenclature system for describing lipids.** Head group shortcuts are depending on the lipid class.

Polar glycerolipids make up most of the lipids found in green tissues, while in plant seeds, non-polar lipids like sterols and neutral glycerolipids are the dominant lipid class as the principal component of fats and oils (Buchanan 2015). There, they serve as energy storage compounds that do not influence the osmotic potential of the cell when they accumulate. A defining lipid class in plants are the glycolipids, which make up most of all membrane lipids. Glycolipids are only found in plants and are produced in chloroplasts where they

make up the various plastid membranes. Phospholipids are found in almost all membranes of plants cells, but are primarily located in membranes of organelles outside of chloroplasts. Phospholipids are mostly produced in the endoplasmic reticulum (ER) and are shipped from there to other membranes, also to chloroplasts. In green plant tissue like leaves where a lot of chloroplasts are present, glycolipids are the most abundant membrane lipid class, while phospholipids are most abundant in roots (Buchanan 2015). Sphingolipids are produced mainly in the ER, GIPCs furthermore in the Golgi apparatus (Luttgeharm, Kimberlin et al. 2016). They usually take up only a very small portion of total lipids in cells, but accumulate significantly in plasma membranes, specifically in the outer leaflet (Tjellström, Hellgren et al. 2010). It has been theorized that sphingolipids together with sterols can form membrane microdomains of higher density and thickness, so-called lipid rafts. These microdomains might be important for the recruitment of certain proteins to the plasma membrane (Nagano, Ishikawa et al. 2016). Sterols in plants are present in different membranes and also play part as precursors for a variety of hormones like brassinosteroids (Li, Nagpal et al. 1996). Sterol synthesis mainly takes place in the ER and the plasma membrane (Benveniste 2004).

The evolutionary ancestors of land plants are unicellular marine photosynthetic organisms, or microalgae. It is assumed that after developing multicellular tissues marine plants eventually evolved to survive on land (Kenrick and Crane 1997). Compared to vascular plants, microalgae have commonly a reduced composition of lipid classes, but do also contain some lipids not found in vascular plants. The model algae *Chlamydomonas reinhardtii* has been studied extensively in this regard, but many other species of microalgae are also of interest nowadays, as algae are considered interesting for producing VLC-PUFAs at an industrial scale (Spolaore, Joannis-Cassan et al. 2006). In *C. reinhardtii*, the phospholipid classes PC and PS are absent, while instead the betaine DGTS plays a role as a major membrane lipid (Guschina and Harwood 2006). Similar to plants, however, the major membrane lipids found in this organism are glycolipids, making up combined more than 70 % of total acyl lipids (Harwood and Guschina 2009). Other microalgae have similar compositions of lipids. Another feature of lipids in microalgae is the high abundance of VLC-PUFAs. Microalgae regularly contain high amounts of FAs with more than 18 carbons and more than 3 double bonds. This includes the fatty acids arachidonic acid (20:4, ARA), eicosapentaenoic acid (20:5, EPA), docosapentaenoic acid (22:5, DPA), and docosahexaenoic acid (22:6, DHA), which are all considered interesting for nutritional purposes (Harwood and Guschina 2009). The terrestrial glacial microalga *L. incisa* accumulates high amounts of 20:4 in neutral lipids when exposed to a nitrogen deficient diet (Bigogno, Khozin-Goldberg et al. 2002). The accumulation of neutral lipids under stress is a well-known phenomenon in microalgae (Guschina and Harwood 2006).

Bryophytes, the intermediates between marine plants and vascular plants, have so far only superficially been analyzed in regards to lipid composition, especially compared to vascular plants and microalgae. Often, lipid composition was only conducted on a FA level without identifying individual classes of lipids (Dembitsky 1993). What we know so far is that most bryophytes have a broadly similar lipid compositions than vascular plants, with some exceptions. Most notably is the presence of VLC-PUFAs like 20:4 and 20:5, which are apparently present in most bryophyte species, yet at varying relative amounts (Beike, Jaeger et al. 2014). Analysis of lipids in bryophytes is best described for the model organism *P. patens*. The FA species 16:0, 18:2 and 18:3 were described by several different works to be present in *P. patens* (Grimsley, Grimsley et al. 1981, Beike, Jaeger et al. 2014)

as the most abundant FAs next to 20:4, yet the amount of 16:3 has been described in varying amounts, being a very abundant FA when analyzed by Grimsley (Grimsley, Grimsley et al. 1981), but only present in low amounts when analyzed by Beike (Beike, Jaeger et al. 2014). Beike (Beike, Jaeger et al. 2014) also compared the FA composition in different tissue types in *P. patens* (protonema vs gametophore) and found that the overall amount of lipids goes down in gametophores compared to protonema while 20:4 accumulates slightly in this tissue type. The phospholipid classes PC, PG, PE, PI and PA have been described to be present in *P. patens* (Grimsley, Grimsley et al. 1981), for other mosses the presence of MGDG, DGDG and SQDG were also reported (Karunen 1977, Karunen and ARO 1979, Hartmann, Beutelmann et al. 1986). Also the presence of betaine lipids has been reported (Dembitsky 1993). Sterols were described to be present in *P. patens* mostly as stigmasterol and campesterol, but traces of all 5 phytosterols were detected (Morikawa, Saga et al. 2009). Except for *P. patens*, most of the bryophytes analyzed in these studies were harvested in the wild and not grown under controlled conditions. Sphingolipids however are scarcely studied in any moss species. Buré (Buré, Cacas et al. 2014) cited unpublished data that detected GIPC in *P. patens*, but no further analysis was done and no other sphingolipid classes were analyzed. To this day, the knowledge we have about lipids in mosses like *P. patens* remains superficial.

### 1.3. Modification of lipids in response to stress

Lipids play a big part in how any organism deals with outside stresses, may it be biotic or abiotic ones. Biotic stresses are defined as attacks from other organisms, like viruses, bacteria, fungi and feeding insects. Lipids represent often the first barriers these organisms have to overcome in order to get access to nutrients kept inside cells. It has been reported that cuticular waxes and neutral lipids might be able to repel some herbivorous organism when they feed on plants (Buchanan 2015). Also, FAs can serve as precursors for phytohormones that are involved in plant defense (Wasternack 2007). The sphingolipids located in the plasma membrane are believed to be important for fending off invading organisms, also by initiating programmed cell death (Markham, Lynch et al. 2013). However, lipids are most prominently associated with plants reacting to abiotic stresses, like low or high temperatures, freezing, desiccation, or exposure to light. The research on how plants deal with these abiotic stresses is of high interest for agricultural industry, since drought and cold can have severe impact on the harvest yield of crop plants (Bohnert, Nelson et al. 1995).

For a variety of plants, the impact of drought on the lipid composition has been reported. In *Arabidopsis thaliana*, water stress reduces the overall total lipid content per dry weight severely, but returns to normal when the plants are rehydrated (Gigon, Matos et al. 2004). While the relative amount of PC and PG remains the same after dehydration, plants decrease substantially the amount of MGDG, the main lipid class in *A. thaliana*, while accumulating DGDG in dehydrated leaves. Similar results have been observed for other plants like coconut tree (Repellin, Thi et al. 1997) and rape (Benhassaine-Kesri, Aid et al. 2002). It was assumed that the ratio of MDGD to DGDG might be a way for the plant to maintain the membrane structure of chloroplasts under these conditions (Gigon, Matos et al. 2004). In many plants it was additionally observed that the amount of PUFAs in lipids

decreases, especially in glycolipids (Yordanov, Velikova et al. 2000). It is not yet clear what exact purpose the rearrangements of lipid composition have, but it is assumed that it is an overall reaction to slower metabolism, which requires changing the properties of the chloroplasts for less photosynthetic activity.

Related to drought stress in plants is cold stress, which can also cause a dehydration of tissues. In general, the stress of cold temperatures below 6 °C is to be differentiated from the stress of freezing temperatures below 0 °C (Buchanan 2015). Freezing causes the formation of ice crystals that can rupture cell membranes, leading to leaking cells when they thaw again. It was observed for plants that the exposure to freezing stress can be lethal in a short time frame, but can be partially avoided as long as the plants were exposed to non-freezing cold temperatures prior to freezing (Smallwood and Bowles 2002). This cold acclimatization phase is accompanied by reshuffling of lipid composition, which can be different depending on the species (Uemura, Joseph et al. 1995, Badea and Basu 2009). In *A. thaliana*, it was reported for different accessions that the overall lipid amount did not change significantly at cold acclimatization, but TAG content increased a lot (Degenkolbe, Giavalisco et al. 2012). TAG makeup also changed to longer FAs after cold stress. Variants of *A. thaliana* with a higher resistance against freezing generally also accumulated TAGs faster compared to freezing-sensitive accessions. Similar to observations at drought stress, MGDG lipids decreased significantly after cold acclimatization, an effect also observable for PC, PE and ceramides, while DGDG remained stagnant and glycosylceramides decreased (Degenkolbe, Giavalisco et al. 2012). Similar effects have been reported by Tarazona (Tarazona, Feussner et al. 2015), where also an increase in certain phospholipid species, sterols and sphingolipids was observed.

One of the most important impacts of cold stress on lipids does not take place on a lipid class level, but at the makeup of their FA moieties. Vascular plants have a relatively small variety of carbon chain lengths in lipids, mostly ranging from 16 to 18 carbons (Buchanan 2015). This leaves only a small window for modifications in length of FAs at stress conditions. Instead, adaptation to cold is often done in plants by changing the number of double bonds found in these FAs (Badea and Basu 2009). In *A. thaliana*, cold stress leads to the accumulation of lipids with a higher degree of unsaturation, mainly in phospholipids and sphingolipids (Tarazona, Feussner et al. 2015). *A. thaliana* lines incapable of producing PUFAs (16:3 and 18:3) can grow normally at room temperature, but have strongly reduced photosynthesis at lower (< 10 °C) and higher (> 30 °C) temperatures. In wild type plants, these two FAs make up 70 % of lipids in chloroplasts. Variants of rapeseed that are tolerant to cold stress showed a faster accumulation of 18:2 and 18:3 FAs at low temperatures compared to sensitive variants (Tasseva, de Virville et al. 2004). Increases in unsaturation levels at cold stress have also been reported for potato (De Palma, Grillo et al. 2008), winter wheat (Bohn, Lüthje et al. 2007), rice (Zhu, Yu et al. 2007) and other plants (Badea and Basu 2009). But not only PUFAs play a role for cold stress response in plants. In sphingolipids, both FAs and LCBs can be present in unsaturated form, but in *A. thaliana*, both acyl-residues are commonly only monounsaturated. Both *A. thaliana* KO lines of a LCB desaturase (AtSLD1) (Chen, Markham et al. 2012) and a sphingolipid FA desaturase (AtADS2) (Chen and Thelen 2013) are sensitive to low temperatures and significantly smaller at cold stress conditions. The main unsaturated sphingolipid FA in *A. thaliana* is the very long 24:1;1 and not found in any other group of lipids. These FAs in sphingolipids might be also important for the function of secretory pathways in plants at any temperature (Markham, Molino et al. 2011).

In the bryophyte *P. patens*, some research has been done concerning reaction to cold stress, but only on a level of gene expression (Beike, Jaeger et al. 2014), proteome (Wang, Yang et al. 2009), or soluble compounds (Yuanyuan, Yali et al. 2009). Only limited research was conducted on how lipid levels are effected by cold stress in bryophytes. Anna Beike (Beike 2013) found that genes for some lipid desaturation were induced by cold stress, but no lipid analysis was conducted to compare normal and cold growth conditions in *P. patens*.

## 1.4. Evolution of desaturases

Desaturation of lipids is important for plants for regular function and for dealing with environmental stresses. Most FAs found in plant leaves are unsaturated and the level of unsaturation in lipids increases as a response to cold stress. It can therefore be concluded that the enzymes responsible for double bond insertion are of high importance for plants. These enzymes are called desaturases. Desaturases are enzymes that include a di-iron complex within their active site and use molecular oxygen to remove two hydrogen atoms from a FA or LCB carbohydrate chain (Shanklin and Cahoon 1998). This di-iron complex is coordinated by conserved histidine (His) and glutamine (Gln) residues in these enzymes. Furthermore, desaturases need access to an electron transport system for catalyzing the reaction. A final flavoprotein (either ferredoxin or cytochrome-*b5*) provides hereby the electrons for the desaturase reaction. The redox-reaction is performed when molecular oxygen is bound to the diiron center as a diferryl ( $\text{Fe}^{\text{IV}}\text{-Fe}^{\text{IV}}$ ) form and each oxygen atom abstracts a hydrogen from the target methylene group in the substrate. This results in the loss of  $\text{H}_2\text{O}$  and the formation of a resting stage diferric ( $\text{Fe}^{\text{III}}\text{-Fe}^{\text{III}}$ ) center with one bound oxygen atom, which is reactivated by electron transfer from the involved flavoprotein. The exact position of the double bond insertion is usually strictly defined for each type of desaturase with different types of mechanisms for determining the exact ethyl-group in the carbon-chain and commonly occurs in *cis*-conformation (Buchanan 2015).

In plants, desaturases are divided into two major groups: soluble desaturases and membrane-bound desaturases. Soluble desaturases are unique to plants and are not anchored to membranes as all other types of desaturases are. They are considered evolutionary to be completely separate from all other types of desaturases (Alonso, Garcia-Maroto et al. 2003). They can be found in chloroplasts and commonly catalyze the insertion of the very first double bond into FAs produced in chloroplasts, e.g. in 18:1, while all subsequent double bond insertions are formed by membrane-bound desaturases. Double bond insertion is commonly done at the  $\Delta 9$  position at substrates bound to acyl-carrier protein ACP (Shanklin and Cahoon 1998). The flavoprotein interacting with soluble desaturases is ferredoxin and there are two conserved His-boxes present in the enzyme's desaturase domain, responsible for fixating the catalytic diiron center of the enzyme (Shanklin and Cahoon 1998). Soluble desaturases only use saturated FAs as substrate that are present in chloroplasts, which include 16:0 and 18:0.

The other group of desaturases in plants are the membrane-bound desaturases, which include the vast majority of all plant desaturases. Membrane-bound desaturases may be characterized by four transmembrane domains (Murphy 1999) and can be found in plastids and the ER. They contain 3 conserved His-boxes and use cytochrome-*b5* as a final

electron donor. Most membrane-bound desaturase do not insert the first double bond into saturated FAs, but instead introduce double bonds adjacent to an existing double bond (which commonly is located at the  $\Delta 9$  position). The new double bond is placed usually 3 carbons next to the first one, either located towards the carboxyl- or the methyl-end of the FA. Membrane-bound desaturases can act on FAs connected to acyl-Coenzyme A (acyl-CoA) or on FAs bound to complex lipids (Buchanan 2015).

Depending on the protein domain structure, membrane-bound lipids can be further divided into mono-functional desaturases and bi-functional desaturases. Bi-functional desaturases in plants, contrary to mono-functional ones, contain additionally to a desaturase domain a cytochrome-*b5* domain towards the N-terminus. Bi-functional desaturases are located in the ER and catalyze either the desaturation of FAs or LCBs (Meesapyodsuk and Qiu 2012). In LCBs, position of desaturation is fixed to either the  $\Delta 4$  or  $\Delta 8$  position and can also occur in *trans*-conformation, which is unusual for most other types of desaturases. In FAs, bi-functional desaturases insert double bonds counting from the carboxyl-end of a FA (called front-end), while mono-functional desaturases count from the methyl-end (see Figure 1.4.). This lead to the common differentiation between front-end desaturases and methyl-end desaturases (Meesapyodsuk and Qiu 2012).

In microalgae and bryophytes, bi-functional desaturases catalyze the insertion of double bonds into LCBs and into VLC-PUFAs. Vascular plants do not contain VLC-PUFAs in significant amounts and front-end desaturases are not present in these organisms at all. Instead, all bi-functional desaturases in vascular plants are exclusively LCB desaturases, not accepting FAs as substrates (Meesapyodsuk and Qiu 2012). For all other kinds of double bond insertion (except for those done by soluble desaturases), vascular plants use mono-functional desaturases, which are therefore all methyl-end desaturases (Alonso, Garcia-Maroto et al. 2003). In non-vascular plants and microalgae, bi-functional desaturases are present in two separate functions. The enzymes  $\Delta 5$  and  $\Delta 6$  desaturases in *P. patens* (Girke, Schmidt et al. 1998, Kaewsuwan, Cahoon et al. 2006) belong to the first group of front-end desaturases and are both necessary for the formation of 20:4, a major FA in *P. patens*. The second group of desaturases in microalgae and bryophytes are the LCB desaturases necessary for the formation of saturated LCB in sphingolipids. Both groups of enzymes are bi-functional desaturases containing a cytochrome-*b5* domain.

The importance of any given desaturase on the viability of an organism can usually not be predicted beforehand. KO-mutants of desaturases for the formation of PUFAs in *A. thaliana* have varying degrees of effect on phenotypes. Triple-KO-mutants of *fad3*, *fad7* and *fad8* which are unable to produce 16:3 and 18:3 FAs grow normally at room temperature, but are less viable at high or low temperatures. Additionally, the mutant is male sterile because the phytohormone jasmonic acid (JA) cannot be synthesized any more. The double-KO mutant *fas2*, *fad6* however can only produce mono-unsaturated FAs and is not able to maintain photosynthesis, requiring the presence of sucrose in the medium to survive (Buchanan 2015). In *P. patens*, KO-mutants that are unable to produce the VLC-PUFA 20:4 grow normally with no observed effect on phenotypes, even though 20:4 is a major FA in *P. patens* lipids (Girke, Schmidt et al. 1998, Zank, Zähringer et al. 2002, Kaewsuwan, Cahoon et al. 2006).

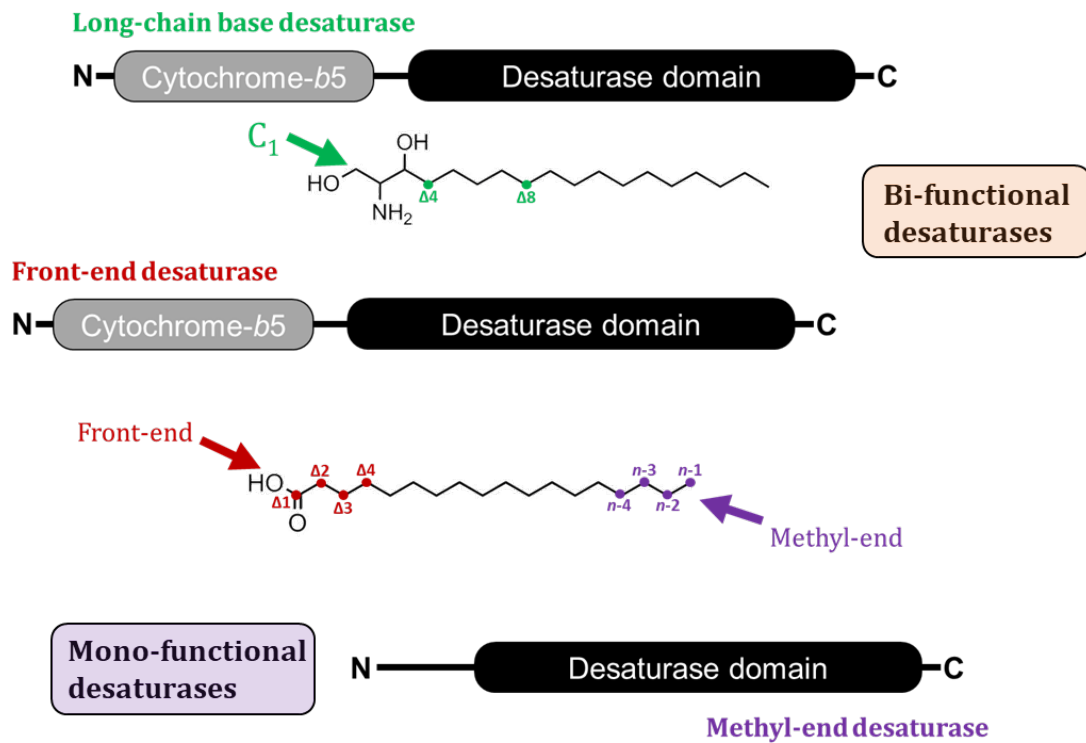


**Figure 1.4. Classification of membrane-bound desaturases in plants.** As subclasses, bi-functional desaturases include long-chain base desaturases and front-end desaturases, while mono-functional desaturases include methyl-end desaturases. Long-chain base desaturases use long-chain bases as substrates, double bonds are inserted at  $\Delta 4$  or  $\Delta 8$  position. Front-end desaturases count from the carboxyl-end of a fatty acid, the corresponding C-atom is referred to with  $\Delta \#$ . Methyl-end desaturases count from the opposing end for the fatty acid chain, the corresponding C-atom is designated with  $n\text{-}\#$  or  $\omega \#$ . Both front-end and methyl-end desaturases use either free fatty acids or acyl-CoAs as substrates. Bi-functional desaturases contain a cytochrome-*b5* fusion domain at the N-side, mono-functional desaturases do not.

## 1.5. The putative sphingolipid desaturase PpSFD

There is only a limited amount of research done on lipids in *P. patens*. In order to reveal the importance and possible functions of genes that were discovered after sequencing the *P. patens* genome, several groups worked however on transcriptome analysis in *P. patens*. Hiss (Hiss, Laule et al. 2014) analyzed gene expression in a great variety of different conditions, including tissue types, developmental stages, and stresses. The abiotic stress of low temperature exposure was not tested in this work, but this was analyzed by Beike (Beike 2013). There, a great variety of different genes were discovered whose transcripts accumulated in *P. patens* cultures after exposure to 4 °C over a time period of 24 h. One gene that was upregulated at these conditions was a putative sphingolipid desaturase with yet unknown functions: Phypa\_171332 (see Figure 1.5.). In this work, the protein for this gene is referred to as PpSFD.



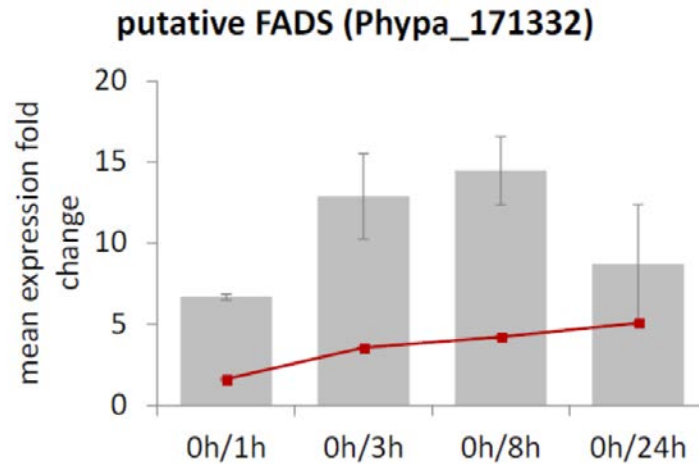


**Figure 1.5. Mean expression fold change of *PpSFD* (Phypa\_171332) in *P. patens* wild type at various time points of cold stress treatment.** Plate cultures were grown for 4 weeks under normal conditions before transfer on ice ( $\sim 3.5\text{ }^{\circ}\text{C}$ ) for 24 h. At least three biological replicates were analyzed. Grey bars represent qRT-PCR data, red lines microarray data. The experiment was performed by Beike (Beike 2013). The image corresponds to Figure 3.33 from that work.

Analysis of the peptide sequence of Phypa\_171332 revealed the presence of a desaturase domain and an N-terminal cytochrome-*b5* domain, identifying it as a bi-functional desaturase. Its function was assumed to be similar to either  $\Delta 5/\Delta 6$  desaturases or to sphingolipid LCB-desaturases, since it showed highest similarity to these types of desaturases when compared to a variety of different desaturases from vascular & non-vascular plants, microalgae, fungi, and protists (Beike 2013). *P. patens* knock-out (KO)-mutants of this gene did not show any visible phenotype at normal and cold stress conditions (see Figure 1.6.).

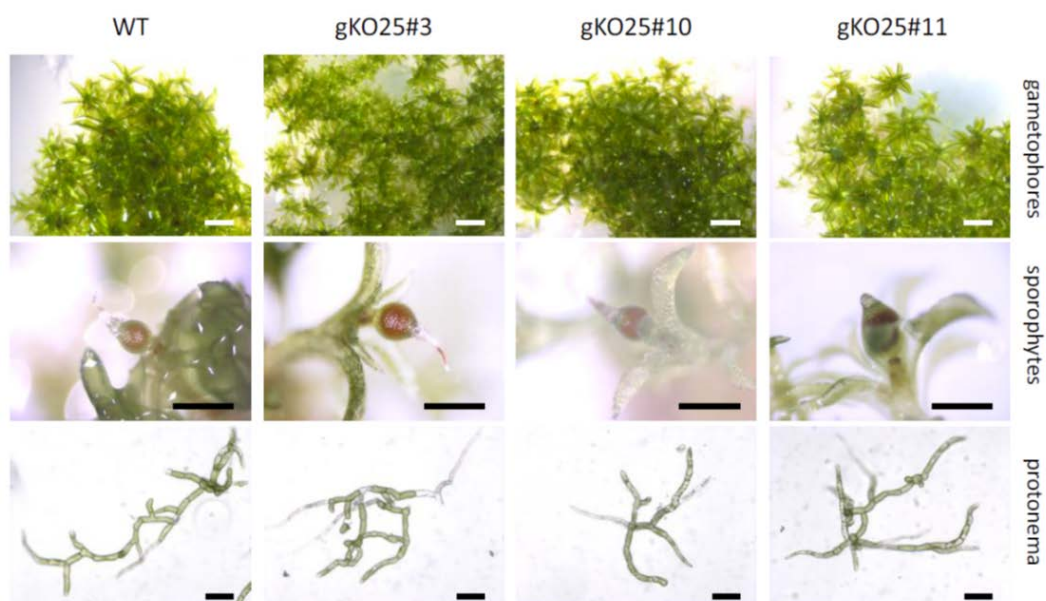


**Figure 1.6. Phenotypic analysis of *P. patens* *PpSFD* knockout lines (gKO25) in comparison to wild type.** Gametophores (scale bar = 1 mm), sporophytes (0.5 mm) & protonema (0.1 mm). The experiment was performed by Beike (Beike 2013). The image corresponds to Figure 3.36 from that work.

The FA profile in these KO-lines did also not show any differences to *P. patens* wild type. Further analysis of lipid classes or lipid molecular species in the KO-lines were not done in this or any other work. Therefore, the exact function of PpSFD remains unknown. It is also unclear if the desaturase uses FAs or LCBs as substrates, which are both reported targets for bi-functional desaturases.

## 1.6. Analysis of lipids

Lipid analysis has come a long way in analytical sciences. To this day, a great variety of different techniques have been developed to identify non-polar components in organisms, each with its own benefits and drawbacks. Analysis of lipids has always been more of a challenge compared to other types of compounds in living cells, like proteins or nucleic acids. Lipids have a high chemical diversity with often only subtle differences between them on a molecular level.

One of the oldest techniques of lipid analysis is thin-layer chromatography (TLC) and is still used often as a first step of analyzing lipids today (Touchstone 1995). TLC separates lipid classes according to how fast they travel via capillary forces on an absorbent material that is soaked with a solvent mixture. Depending on which solvent mixture and which absorbent material is used, different types of lipid classes travel at set speeds through the TLC plate (usually a glass sheet coated with silica gel). This however allows only the separation of entire lipid classes (like MGDG, PC, TAG), but not individual lipid molecules. Also, the separation resolution is quite low with this technique. An advancement from this technique is gas chromatography (GC), where instead of a planar TLC plate a very long column with small inner diameter is used, coated on the inside with the stationary phase (Christie 1989). As mobile phase, instead of a solvent mixture, samples are transported through the column with an inert gas. The length of the column as well as the regulation of temperature in the column allows a far better separation of samples and therefore causes a higher resolution. This technique is powerful enough to separate different FA species. However, this approach can only analyze compounds that are volatile enough to convert into a gaseous phase in the GC. This is not the case for unmodified diacyl-lipids or FAs. FAs have to be derivatized to FA methyl-esters (FAME) in order to be analyzed, more complex lipids are often not analyzable. A way to analyze not only the entirety of all FAs is to extract different lipid classes from a sample using different solvent mixtures. Then, analyze the lipid classes separately for their FA composition after converting them to FAMES.

Detection of lipids on a GC system is commonly done in two different ways. One is by flame ionization detection (FID), which basically burns the incoming compounds in order of separation and measures the intensity of that flame. This detection is very accurate in relation to the amount of compound present in the sample, but it does not allow a further analysis of the compound. As an alternative, GC systems can instead be equipped with a mass spectrometer. Instead of burning the compounds, they get ionized and the mass of the compound is measured in a variety of different ways (Griffiths and Wang 2009). The mass spectrometry (MS) device can be set up so that any compound additionally is also fragmented into various pieces and a spectrum of these fragments is measured for each

compound as well. This allows further analysis and identification of lipids, e.g. the determination of the double bond position (Christie 1998). However, this detection is commonly less sensitive than FID. Furthermore, the amount of the compound in the sample cannot be accurately determined from the signal intensity, since ionization of compounds can be drastically different for each compound and is prone to suppression in complex samples. Quantification of a small group of compounds is however possible if genuine internal standards for each molecule are used as reference and samples do not contain too many compounds. Ionization in GC-MS systems is commonly done via electron ionization (EI), where electrons bombard compounds, therefore charging them. This ionization method is considered hard ionization, fragmenting molecules strongly into small fragments. As mass spectrometers, quadrupole MS devices or ion-traps are commonly used (Christie 1998). GC and GC-MS analysis techniques are the most common ways to analyze lipids and are relatively easy to use in most laboratory setups.

An advancement from GC-MS analysis is the use of MS systems coupled to liquid chromatography (LC). For lipid analysis, the use of ultra-performance liquid chromatography (UPLC) has been broadly established for lipid analysis, since here the separation of complex lipids can be accomplished with a high separation power (Griffiths and Wang 2009). In LC systems, solvent mixtures are again used as mobile phases, while tightly packed columns of shorter length are used as stationary phase. For lipid analysis, most commonly columns with reversed-phase (RP) stationary phase are used, which means that the compounds interact with non-polar long-chain hydrocarbons while being transported on mobile phases that contain more polar solvents (like water, methanol or acetonitrile). Lipid species are separated based on their hydrophobicity, causing lipids with longer and more saturated FAs to remain longer in the column. The solvents of the mobile phase can be adjusted so that lipid classes with different degrees of head group polarity can be analyzed on the same type of column. Lipids are ionized after going through the column most commonly via electrospray ionization (ESI), a soft ionization method. Similar to GC-MS, molecules can also be analyzed for their mass fragment spectra via MS-MS, allowing further means of lipid identification. This technique can be very powerful, allowing the identification of single lipid molecules for their exact FA/LCB moieties and their head groups for many different lipid classes (Tarazona, Feussner et al. 2015). Most advanced lipid analyses are nowadays done with UPLC-ESI-MS-MS systems. Like all MS analysis techniques, accurate quantitative lipid analysis cannot be done without the extensive use of genuine standards for each compound analyzed (Griffiths and Wang 2009). Therefore, GC techniques are still used to acquire data about absolute lipid amounts in samples.

## 1.7. Aims of this study

The bryophyte *P. patens* is gaining more and more attention as a model organism for non-vascular plants. Lipids however are still only scarcely studied in this organism, as for all other bryophytes. *P. patens* represents as a bryophyte an evolutionary link between land plants and marine plants. The transition for plants to live outside of water must have come with severe adaptations on many different levels. The environmental conditions that are present on land, like drought and stronger temperature shift, cause major stress on cells.

Lipids are a key component in adjusting to these conditions and lipid composition probably underwent a lot of changes from marine organisms to early land plants to vascular plants. To understand this evolutionary transition in plants, we need to compare the differences and similarities in lipid composition between bryophytes and vascular plants.

The first aim of this work was therefore to analyze lipids in *P. patens* as extensively as possible. Lipids in *P. patens* should be analyzed with the tools and methods developed by Tarazona (Tarazona, Feussner et al. 2015) using a UPLC-ESI-MS-MS setup. This allows to have insight into glycerolipids, sterol lipids and sphingolipids of this organism and compare it to what is known in vascular plants, represented by *A. thaliana*. The lipid analysis would furthermore be supplemented by GC and GC-MS analysis to establish a FA profile for different lipid groups to make assumptions about the absolute amounts of lipids in *P. patens*. In order to observe how *P. patens* adjusts lipid composition in response to environmental stress, lipids should be further analyzed in *P. patens* cultures exposed to low temperatures.

The second aim of this work focuses on the analysis of the *P. patens* KO-line of the cold-stress-induced putative sphingolipid desaturase PpSFD. The protein should be compared to desaturases with similar structure from other organisms and analyzed for their specific enzymatic activity *in vivo*. The impact of the KO-mutation should be analyzed for the complete lipidome in *P. patens*, at normal and cold stressed growth conditions. It should be observed if *Ppsfd* KO-lines show a phenotype at prolonged growth at low temperature and how the adjustment of the lipid composition differs to wild type *P. patens*.

The third part of this work aims on comparing PpSFD with the enzyme AtADS2 from *A. thaliana*, which could catalyze a similar reaction as PpSFD. Evolutionary origins of both proteins should be discussed by comparing their peptide sequences and protein structure to similar proteins from other organisms. The exact effect of KO-mutation should be compared between the *P. patens sfd* KO-mutant and *A. thaliana ads2* KO-mutant. Furthermore, it should be analyzed if PpSFD is capable of complementing the phenotype and chemotype of *ads2* lines when expressed in this line heterologously under a overexpression promoter. Lastly, it should be compared at which exact position both enzymes insert double bond into their substrates and if PpSFD can maintain its position specificity when expressed in *A. thaliana*.

## 2. Material & Methods

---

### 2.1. Material

#### 2.1.1. Chemicals

All general chemicals used were purchased either from Roth (Karlsruhe, Germany) or from Merck (Darmstadt, Germany). Solvents were purchased either from Fisher Scientific (Schwerte, Germany) or from Merck (Darmstadt, Germany). Water was drawn from an Arium pro Ultrapure Water Systems device (Sartorius, Göttingen, Germany) if not noted otherwise.

#### 2.1.2. Plants

Plant samples were obtained from the organisms *A. thaliana* (Col-0 strain), *P. patens* (Gransden strain) and mutants in these genetic backgrounds.

The following KO-lines were used in this work:

*A. thaliana* KO-lines:

**ads2.1:** *Atads2.1*, provided by Jonathan Markham, University of Nebraska-Lincoln; described by Smith (Smith, Dauk et al. 2013)

*P. patens* KO-lines:

**sfd3:** *Ppsfd3*, labelled gko25#3, provided by Ralf Reski, University of Freiburg

**sfd10:** *Ppsfd10*, labelled gko25#10, provided by Ralf Reski, University of Freiburg

**sfd11:** *Ppsfd11*, labelled gko25#11, provided by Ralf Reski, University of Freiburg

Lines were described by Beike (Beike 2013).

**elo:** *Ppelo/Pppse1*, generated in-house by Pia Meyer; described by Zank (Zank, Zähringer et al. 2002)

(two lines: elo35, elo131)

The following complementation lines were generated & analyzed in this work:

**ads2.1/AtADS2:** *Atads2.1/CaMV-35S::AtADS2*; lines: F01, F03, F09

**ads2.1/PpSFD:** *Atads2.1/CaMV-35S::PpSFD*; lines: C05, C10, C11

Plasmid constructs for all transformation lines produced are shown in Appendix 1.

### 2.1.3. Bacteria

Bacteria strains were used from the organisms *Escherichia coli* and *Agrobacterium tumefaciens*.

The following *E. coli* strains were used for cloning:

- XL1-Blue
- NEB-DH5- $\alpha$

The *A. tumefaciens* strain used for transforming *A. thaliana* plants is:

- EHA 105

## 2.2. Methods

### 2.2.1. Cultivation of *P. patens* cultures

Cultures of *P. patens* were grown using three different cultivation methods: plate culture, shaken liquid culture, or aerated liquid culture. Each cultivation method included different growth parameters (see below).

All moss cultures were inoculated with moss material that was homogenized in Wang medium (see 2.2.1.1.) using an Ultra Turrax T25 basic homogenizer (IKA, Staufen, Germany) at 19,000 min<sup>-1</sup>. Homogenized moss was then either dropped as spots on agar plates or resolved in Wang medium (depending on method of growth).

#### 2.2.1.1. Moss liquid culture

All liquid cultures were grown on Wang medium (modified from Wang (Wang, Cove et al. 1980) and Ashton & Cove (Ashton and Cove 1977)).

**Table 2.1.: Composition of 1 L Wang medium**

Ca(NO <sub>3</sub> ) <sub>2</sub> * 4 H <sub>2</sub> O	59 mg
MgSO <sub>4</sub> * 7 H <sub>2</sub> O	250 mg
KH <sub>2</sub> PO <sub>4</sub>	250 mg
KNO <sub>3</sub>	1040 mg
Di-NH <sub>4</sub> -tartrate	920 mg
TES (see Table 2.2.)	1 mL
Vitamin solution (see below)	1 mL
FeSO <sub>4</sub> * 7 H <sub>2</sub> O	12.5 mg

pH was adjusted to 6.5 with 1 M KOH solution.

**Table 2.2.: Composition of 1 L TES (Trace element solution)**

H <sub>3</sub> BO <sub>3</sub>	614 mg
MnCl <sub>2</sub> * 4 H <sub>2</sub> O	389 mg
NiCl <sub>2</sub> * 6 H <sub>2</sub> O	59 mg
CoCl <sub>2</sub> * 6 H <sub>2</sub> O	55 mg
CuSO <sub>4</sub> * 5 H <sub>2</sub> O	55 mg
ZnSO <sub>4</sub> * 7 H <sub>2</sub> O	55 mg
Al(SO <sub>4</sub> ) <sub>3</sub> * 18 H <sub>2</sub> O	38.6 mg
KBr	28 mg
KI	28 mg
LiCl	28 mg
SnCl <sub>2</sub> * H <sub>2</sub> O	28 mg

**Table 2.3.: Composition of 1 L vitamin solution**

4-aminobenzoic acid	0.25 g
Niacin	1 g
Thiamin/HCl	5 g

#### 2.2.1.1.1. Shaken liquid culture

Intermediate cultures and pre-cultures for plate cultures & aerated liquid cultures were grown in Erlenmeyer flasks filled with 200 – 400 mL Wang medium (see 2.2.1.1.). Cultures were inoculated with about 100 – 200 mg homogenized fresh moss, taken from either plate cultures or other liquid cultures. Erlenmeyer flasks were sealed with cotton balls and aluminum foil and autoclaved before use. Shaken liquid cultures were cultivated at long-day conditions (16 h/25 °C day, 8 h/18 °C night) at 55 µmol/m<sup>2</sup> light exposure in Percival climate chambers (Intellus environmental controller, Percival Scientific, Perry, USA). Cultures were constantly shaken at 100 – 130 rpm under normal air atmosphere.

Flask cultures were homogenized & transferred to fresh medium every 4 weeks.

#### 2.2.1.1.2. Aerated liquid culture

For lipid analytics, moss cultures were grown as aerated liquid cultures. About 0.5 g freshly homogenized moss (from 4 week old shaken liquid cultures) was mixed in about 200 mL Wang medium (see 2.2.1.1.) and filled in special glass vials that were equipped with a gas inlet and outlet (Ochs GmbH, Bovenden, Germany). Growth temperature was set at 22 °C. During cultivation, the moss culture was constantly aerated with air containing 1% CO<sub>2</sub>. Aeration also continuously stirred the moss culture. Lighting conditions were similar to shaken liquid cultures (see 2.2.1.1.1.). After 7 d, cultures were harvested.

#### 2.2.1.1.3. Moss liquid culture harvest & sample storage

Liquid cultures were harvested by pouring the moss culture through a steel filter, then pressing remaining liquid out with a spoon and drying the moss pellet with filter paper. The moss pellet was then transferred to a falcon reaction tube and frozen in liquid nitrogen. The fresh sample was stored at -80 °C. After lyophilizing the sample, it was stored under Argon atmosphere at -20 °C.

#### 2.2.1.1.4. *P. patens* liquid cold stress experiment

Liquid cultures for cold stress experiments were grown as described under 2.2.1.1.2. as aerated liquid cultures. After 7 d of growth, cultures were chilled by submerging the culture vials in crushed ice, cooling them down to about 4 °C in 30 min. The temperature was maintained for 24 h, adding fresh ice when necessary. Aeration and light cycle was maintained similar to 2.2.1.1.2. until the samples were harvested.

#### 2.2.1.2. Plate culture

For wounding & phenotype analysis, moss was grown on agar plates. Two types of medium composition were used for agar plates: BCD medium (for phenotype analysis, modified from Knight (Knight, Cove et al. 2002) or Knop medium (for wounding analysis, modified from Reski (Reski and Abel 1985).

**Table 2.4.: Composition of 1 L BCD medium**

MgSO <sub>4</sub> * 7 H <sub>2</sub> O	250 mg
KH <sub>2</sub> PO <sub>4</sub>	250 mg
KNO <sub>3</sub>	1010 mg
FeSO <sub>4</sub> * 7 H <sub>2</sub> O	12.5 mg
TES (see Table 2.2.)	1 mL
CaCl <sub>2</sub>	111 mg
Di-NH <sub>4</sub> -tartrate (optional)	920 mg
Agar	8 g

pH was adjusted to 6.5 with 1 M KOH solution.

**Table 2.5.: Composition of 1 L Knop medium**

Ca(NO <sub>3</sub> ) <sub>2</sub> * 4 H <sub>2</sub> O	1000 mg
KCL	250 mg
KH <sub>2</sub> PO <sub>4</sub>	250 mg
MgSO <sub>4</sub> * 7 H <sub>2</sub> O	250 mg
FeSO <sub>4</sub> * 7 H <sub>2</sub> O	12.5 mg
Agar	15 g

pH was adjusted to 5.8 with 1 M KOH solution.

Moss plate cultures were cultivated under similar light conditions as shaken liquid cultures in Percival climate chambers (see 2.2.1.1.1.).

#### 2.2.1.2.1. *P. patens* wounding experiment

For the moss wounding experiment, *P. patens* lines were grown on Knop medium plates for 1 month, sealed with parafilm (PM-996, Bemis, Neenah, USA). 100 mg of fresh moss was then scraped off the plate with sterile forceps and transferred into a 1.5 mL reaction tube. Wounding stress was simulated by grinding & squashing the moss on the inside of the reaction tube with a plastic pestle to a smooth, liquid paste. The pestle was then washed with 1 mL sterile tap water and the water collected in the same reaction tube. The sample was then incubated under light & 22 °C for 30 min, before freezing it in liquid nitrogen. Control samples were not wounded but directly frozen in liquid nitrogen after harvesting.



#### 2.2.1.2.2. *P. patens* plate cold stress experiment

Plate moss cultures for analyzing cold stress response were grown on BCD medium plates, both with and without tartrate. Plates were grown at continuous light & 25 °C, sealed with surgical tape (3M Deutschland GmbH, Neuss, Germany), for 2 weeks. Plates were then resealed with parafilm and transferred to cold stress conditions (6 °C, continuous light).

### 2.2.2. Cultivation of *A. thaliana* plants

All *A. thaliana* plants were grown on soil and cultivated at long-day conditions (16 h light/22 °C, 8 h night/22 °C) with 60 % humidity (except were stated differently). Seeds were planted directly on the soil, kept in the dark at 4 °C for 2 days, and transferred to climate chambers.

#### 2.2.2.1. *A. thaliana* cold stress experiment

For analyzing effects of low temperature on *A. thaliana*, plants were first cultivated at 22 °C at long-day conditions. After 15 d, plants were moved to a growth chamber and grown under continuous light at 6 °C for another 59 d. Pictures were taken directly before the transfer and after finishing the experiment. All plant parts above soil level were harvested and frozen in liquid nitrogen.

#### 2.2.2.2. Transforming *A. thaliana* plants

For complementation experiment, *A. thaliana* was transformed via *A. tumefaciens* mediated flower dip transformation. 500 mL of heat-shock transformed *A. tumefaciens* EHA 105 cells (see 2.2.4.5.) was grown for 2 days, sedimented by centrifugation and resuspended in 300 mL 5 % sucrose solution. Then, 70 µL of Silwett L-77 (Momentive Performance Materials, Waterford, USA) was added to the solution. Flowering *A. thaliana* plants (1 – 2 months old) were then dipped into the bacterial solution for ~ 5 s. Dipped plants were moved to a greenhouse under plastic coverage and dipping repeated after 1 week. After the plants matured, seeds were harvested and sown out on soil. Seedlings were sprayed with 0.5 % Basta (Bayer CropScience, Monheim, Germany) solution 1 and 2 weeks after sowing. Surviving seedlings were planted in single pots and grown until seeds were harvested individually for each plant. These seed lines were used for growth and lipidomics experiments.

#### 2.2.2.3. *A. thaliana* fatty acid profile

For analyzing the FA composition in different lipid classes in *A. thaliana* wild type, plants were cultivated for 3 weeks and rosetta leaves were harvested for analysis.

### 2.2.3. Cultivation of bacteria cultures

All *E. coli* and *A. tumefaciens* cultures were cultivated in LB medium (Bertani 1951).

**Table 2.6.: Composition of 1 L LB medium**

Peptone	10 g
Yeast extract	5 g
NaCl	10 g

LB plates additionally contained 15 g agar per 1 L. For selecting transformants, antibiotics were added to the medium in varying amounts (carbenicillin: 100 µg/mL, kanamycin: 25 µg/mL, rifampicin: 50 µg/mL).

*E. coli* cultures were grown over night at 37 °C. *A. tumefaciens* cultures were grown for 2 days at 28 °C.

### 2.2.4. Complementing *A. thaliana* plants

Complementation of the *A. thaliana ads2.1* KO-line was performed by transforming via *A. tumefaciens*. The transformation vector contained the *P. patens* gene *PpSFD* behind either a 35S CaMV promoter or the native promoter region in front of the *A. thaliana* gene *AtADS2*. Plasmid constructs are shown in Appendix 1.

#### 2.2.4.1. Extracting genomic DNA from plant material

For extracting genomic DNA from plant samples, a modified protocol from Henry (Henry 1997) was used. A small amount of frozen leaf or moss material was put into a 1.5 mL reaction tube and grinded with a plastic pestle. 250 µL CTAB mix (see Table 2.7.) was added to the sample and incubated at 65 °C for 15 min. After adding 250 µL of chloroform/isoamyl alcohol (24:1, v/v), the mixture was centrifuged and the upper phase transferred into a new reaction tube. 250 µL isopropanol was added and the sample centrifuged. The supernatant was discarded and the pellet washed with 75 % ethanol (in water). The supernatant was again discarded and the pellet was dried completely before resolving it in 50 µL water.

**Table 2.7.: Composition of 1 L CTAB extraction solution**

Cetytrimethylammoniumbromide	20 g
Tris-HCl (1 M, pH: 8.0)	100 mL
EDTA (0.5 M, pH: 8.0)	40 mL
NaCl	81.82 g

#### 2.2.4.2. Synthesizing cDNA from plant material

RNA was extracted from plant samples using a modified protocol from Onate-Sanchez (Oñate-Sánchez and Vicente-Carbajosa 2008). A small amount of frozen leaf or moss material was put into a 1.5 mL reaction tube and grinded with a plastic pestle. Then, 1 mL trizol mixture (TRI Reagent, Sigma-Aldrich, St. Louis, USA) was added and incubated for 10 min. After addition of 200  $\mu$ L chloroform and another 5 min of incubation, the mixture was centrifuged at 4 °C. The upper phase was transferred to a new reaction tube and mixed with 250  $\mu$ l isopropanol. After centrifuging at 4 °C, the supernatant was discarded and the pellet washed with 75 % ethanol (in water). After centrifuging again at 4 °C and discarding the supernatant, the pellet was dried under a clean bench. The dry pellet was resolved in 50  $\mu$ L water.

RNA concentration was measured at 260 nm light absorption with a NanoDrop 2000 (Thermo Fisher Scientific, Waltham, USA). Synthesis of cDNA from the RNA was performed by using DNaseI and RevertAid H Minus reverse transcriptase (both from Thermo Fisher Scientific, Waltham, USA) following the instructions of the manufacturer.

#### 2.2.4.3. Construct design

The constructs for complementation were designed with support of the Genious R7 & R8 software (Biomatters, Auckland, New Zealand). Genome & transcript sequences were retrieved from NCBI (National Center for Biotechnology Information, www.ncbi.nlm.nih.gov).

For creating the *sfd* KO-line, the following primer pair was designed:

- PpSFD-for short (EcoRI): GAATTCATGGCGACATCTGAAGCT
- PpSFD-rev short (XhoI): CTCGAGTTAATCAGCATGTTCAATCTTTGTA

For *At-ads2*, the following primer pair was used:

- ADS2-for (BamHI): CGGATCCATGTCGGTGACATCAACGGT
- ADS2-rev (NotI): ATAAGAATGCGGCCGCACGA ACTATAGCCATACGACG

#### 2.2.4.4. Polymerase Chain Reaction (PCR)

Amplifying DNA sequences was done via Polymerase Chain Reaction (PCR) (Mullis 1987). For cloning, the Phusion Polymerase (New England Biolabs, Ipswich, USA) was used. For verifying cloning products & transformation efficiency, the RedTaq ReadyMix polymerase was used (Sigma-Aldrich, St. Louis, USA). Both enzymes were used according to the manufacturer's instructions. PCRs were performed on a Mastercycler personal or Mastercycler gradient thermocycler (Eppendorf, Hamburg, Germany).

PCR products were analyzed via agarose gel electrophoresis. Gels used contained 1 % agarose (w/v) in TAE buffer (40 mM Tris, 20 mM acetic acid, 1 mM EDTA). PCR products generated via RedTaq ReadyMix were applied directly to the gel, PCR products from Phusion polymerase were mixed with 1/5 volume 6 x DNA Gel loading dye (Thermo Fisher Scientific, Waltham, USA) prior to loading and run at 10 V/cm for ~ 20 min. Gels were then

stained in 2 µg/mL ethidium bromide solution (in TAE buffer) and visualized under UV light in a Biometra BioDocAnalyze gel documentation system (Analytik Jena, Jena, Germany).

#### 2.2.4.5. Cloning

Desired PCR products from PCR reaction were purified using the NucleoSpin Gel and PCR Clean-up kit (Macherey-Nagel, Düren, Germany). PCR products intended for subcloning were produced via Phusion Polymerase (see 2.2.4.4.) and therefore contained blunt ends. Blunt-end DNA was ligated into pJET1.2/blunt subcloning vector by using the CloneJET PCR cloning kit (Thermo Fisher Scientific, Waltham, USA). Ligation products were then inserted into chemically competent XL1-Blue *E. coli* cells (Agilent Technologies, Santa Clara, USA) by performing heat shock transformation (30 min incubation of competent cells with ligation mixture on ice, 45 s heat shock at 42 °C). Cells were then selected on antibiotics-containing LB medium plates.

Positive transformed *E. coli* colonies were picked from agar plates and grown over night in 5 mL antibiotic-containing liquid LB medium. Plasmids were then isolated from the liquid culture with the GenElute HP Plasmid Miniprep kit (Sigma-Aldrich, St. Louis, USA). Correct insertion of the desired PCR products into the pJET plasmid was confirmed via sequencing (performed by GATC Biotech, Konstanz, Germany; analyzed with Geneious R8 software, Biomatters, Auckland, New Zealand).

Correct inserts were cut out of the plasmid with various restriction enzymes (from Thermo Fisher Scientific, Waltham, USA). The digested DNA fragment was then ligated into the Entry vector pUC18-Entry (designed by Ellen Hornung, University of Göttingen) using the Gateway cloning system (Thermo Fisher Scientific, Waltham, USA). If two inserts were to be inserted into the Entry vector, digestion and ligation was performed twice, one after the other. The finished Entry vector construct was then used for Gateway cloning with the LR-clonase reaction mixture (according manufacturer's instructions). The target vector used was pCambia 33.1s-35S (already containing a CaMV-35S promoter in front of the multiple cloning site). The pCambia vectors contained resistance genes for kanamycin, as well as a Basta-resistance cassette.

The finished pCambia vector constructs were then transformed into competent *E. coli* cells for proliferation of the plasmid. Purified pCambia plasmid constructs from liquid *E. coli* cultures were then transformed into competent *A. tumefaciens* cells (EHA 105) via heat shock. Plasmid DNA was mixed with competent cells, incubated for 30 min, frozen at -80 °C for 2 min and rethawed at 37 °C. Cells were then resolved in LB medium, grown at 28 °C for 3 h and plated on selection plates.

#### 2.2.5. Transcript analysis

Complemented *A. thaliana* lines were analyzed for transcript levels via quantitative real-time PCR (qRT-PCR). For this purpose, cDNA was isolated (see 2.2.4.2.) from cold-stressed plant material (see 2.2.1.1.).

Primers for qRT-PCR were designed using the Primer3Prefold ((Markham and Zuker 2008) and Primer3Plus (Untergasser, Cutcutache et al. 2012) tools. Settings were as follows: Product size range 70 – 150, primer size 18 – 23, primer Tm 58 – 62 (max. Tm difference 3), primer GC % 30 – 80. Automatically designed results were tested via PCR and RT-PCR and best performing primer pairs used for the final qRT-PCR experiment.

The following primer pairs were used for qRT-PCR:

Actin *AtACT8* (reference gene, NM\_103814.4):

- Actin8-RT\_for: GGTTTTCCCCAGTGTTGTTG
- Actin8-RT\_rev: CTCCATGTCATCCCAGTTGC

*AtADS2* (NM\_128693.5):

- *AtADS2*\_qPCR\_left3: CAGTGTGGAAGAAGAGCAAACG
- *AtADS2*\_qPCR\_right3: ACATGCCACCAAGGTAGAAGAG

*PpSFD* (XM\_001780735.1):

- *PpSFD*-RT\_left4: TGAAGTGGTTGCCCATTCAC
- *PpSFD*-RT\_right4: TGTCAAGCCAAACTCAACCG

For qRT-PCR analysis, an iQ5 qPCR cycler (BioRad Laboratories, München, Germany) was used. Reaction mixtures were combined from the Takyon No Rox SYBR Core Kit blue dTTP (Eurogentec Biologics Division, Seraing, Belgium). PCR settings are shown in Table 2.8.

**Table 2.8.: qRT-PCR cycler settings**

PCR	1x	95 °C	3 min
	39x	95 °C	10 s
		58 °C	20 s
		72 °C	20 s
	1x	72 °C	4 min
Melting curve	1x	95 °C	1 min
	1x	55 °C	1 min
	81x	55 °C	10 s

## 2.2.6. Lipidomic analysis

Lipids from both *P. patens* and *A. thaliana* tissue were extracted via a one-phase extraction and analyzed for molecular species composition on a LC-MS system.

### 2.2.6.1. One-phase lipid extraction

All lipid analyses and fatty acid double bond analyses were performed on lipids extracted via a one-phase isopropanol/hexane/water extraction method from lyophilized plant material. The extraction protocol was originally developed by Markham (Markham, Li et al. 2006) and modified by Klug (Klug, Tarazona et al. 2014). 10 or 20 mg of lyophilized plant material were resolved in 6 mL pre-heated (60 °C) propan-2-ol/hexane/water (60:26:14, v/v/v) solution and incubated at 60 °C for 30 min while occasionally stirring. Afterwards, cell debris was centrifuged down and the supernatant collected. Solvents were dried under streaming nitrogen and the remaining lipids resolved in 800 µL tetrahydrofuran/methanol/water (4:4:1, v/v/v). Except for analysis of PA and lyso-PA (LPA), the extracted samples were ready for LC-MS analysis.

### 2.2.6.2. Methylation of samples

For PA and LPA analysis, 80 µL of the extract was dried under streaming nitrogen and resolved in 400 µL methanol. 6.5 µL trimethylsilyl-diazomethane was added to the solution and shaken at room temperature for 30 min. After adding 2 µL 10 % acetic acid solution, samples were dried under streaming nitrogen and resolved in 80 µL tetrahydrofuran/methanol/water (4:4:1, v/v/v). The samples were then analyzed via LC-MS.

### 2.2.6.3. Liquid chromatography mass spectrometry (LC-MS)

For analysis of the molecular composition of lipid species, extracts were analyzed via MRM-based UPLC-ESI-MS (multi reaction monitoring-based ultra-performance liquid chromatography-electrospray ionization-mass spectrometry) analysis. The method was developed by Tarazona (Tarazona, Feussner et al. 2015) and was used with some modifications.

Separation of lipid molecular species was carried out via reversed-phase UPLC using an ACQUITY UPLC I-class system (Waters, Milford, USA) with an ACQUITY UPLC HSS T3 column (100 mm x 1 mm, 1 µm; Waters, Milford, USA). 2 µL aliquots of sample extracts (see 2.2.6.1.) were injected. Flow rate was set at 0.1 mL/min at a separation temperature of 35 °C. Separation of lipids was performed via linear binary gradients using two solvent mixtures (A and B).

Solvent mixture composition was as follows: A) methanol/20 mM ammonium acetate (3:7, v/v), B) tetrahydrofuran/methanol/20 mM ammonium acetate (6:3:1, v/v/v).

Both solvent mixtures were substituted with 0.1 % (v/v) acetic acid. Linear gradients followed similar procedures were used for the respective lipid classes: Starting conditions (50 – 100 % B) for 2 min, linear increase to 100 % B for 8 min, holding 100 % B for 2 min,

returning to starting conditions for 4 min. Starting conditions vary between lipid classes analyzed (see Table 2.9).

**Table 2.9.: Starting conditions for LC separation of different lipid classes**

DGDG, MGDG, PA, PC, PE, PG, PI, PS, SQDG, GIPC, DGTS/A, SG	65 % B
ASG, Cer, GlcCer, DAG	80 % B
SE, TAG	90 % B
Lyso-lipids	50 % B

Lipids were ionized (positive and negative, respectively) by chip-based nanoelectrospray ionization with a TriVersa Nanomate (Advion, Ithaca, USA), using nozzles with 5  $\mu$ m internal diameter. Advion ChipSoftManager was used for ion source control. A post-column splitter was used to direct 255 nL/min of the eluent to the nanoESI chip. Ionization voltage was set according to the lipid classes of interest (see Table 2.10.). Detection of ions was performed with a 6500 QTRAP tandem mass spectrometer (AB Sciex Germany, Darmstadt, Germany) used in multiple reaction monitoring (MRM) mode. Dwell time was set to 5 ms and MS parameters were calibrated for maximum detector response. Analyst IntelliQuan (MQII) peak-finding algorithm was used for peak annotation.

**Table 2.10.: Ionization voltages for analyzing different lipid classes**

DGDG, MGDG, PA, PC, PE, PG, PI, PS, SQDG, GIPC, DGTS/A, SG	1.23 kV
ASG, Cer, GlcCer, DAG	1.30 kV
SE, TAG	1.45 kV
Lyso-lipids	1.41 kV

The lipid classes PA, PC, PE, PG, PI, PS, MGDG, DGDG, SQDG, GIPC, and lyso-lipids were analyzed in negative ionization mode. Cer, GlcCer, DAG, TAG, ASG, SG, SE and DGTS/A were analyzed in positive ionization mode.

Precursor ions that were measured for analysis were as follows for different lipid classes:

Cer, GlcCer:  $[M+H]^+$ ; GIPC:  $[M+2H]^{2+}$ ; sterol lipids, neutral glycerolipids:  $[M+NH_4]^+$ ; phospholipids (except PC), SQDG:  $[M-H]^-$ ; PC, glycolipids:  $[M-H+CH_3CO_2H]^-$ .

For lipid species with more than one acyl-chain, fragment ions were detected for either neutral loss of the acyl chain during positive ionization (neutral glycerolipids) or for formation of fatty acyl-related fragments during negative ionization (phospho- and glycol-glycerolipids). Fragmentation of Cer & GlcCer was detected for dehydrated LCB fragments in positive ionization. For GIPC, the loss of a phosphoinositol head group at positive ionization was detected.

All LC-MS data were analyzed using Analyst software (AB Sciex, Framingham, USA) and house-made software tools (developed by Pablo Tarazona).

### 2.2.7. Double bond position analysis

Analysis of double bond position in fatty acids was done with lyophilized plant material and a process involving several steps of derivatisation, HPLC-purification and measurement on GC-MS.

#### 2.2.7.1. Production of fatty acid methyl esters from sphingolipids via acidic methylation (after Christie (Christie 2009))

Lyophilized plant material (20 x 10 mg) were extracted as described in 2.2.6.1. and resolved in 1 mL hexane. The extracted sample was then transferred to smooth-top glass vials, dried under streaming nitrogen and resolved with 1 N methanolic HCl solution to hydrolyze FA residues from all lipid classes. Glass vials were closed air tight with aluminium lids and incubated for 20 h at 100 °C. FAMES were extracted from the solution by adding 1 mL hexane, centrifuging and transferring the upper phase to new glass vials. The sample was then dried down under streaming nitrogen and resolved in 30  $\mu$ L acetonitrile.

#### 2.2.7.2. Purification of FAMES via HPLC

In order to obtain desired C24 FAMES from the solution, samples were separated on a HPLC system (Agilent 1100 Series, Agilent Technologies, Santa Clara, USA) equipped with a Nucleosil 125-5 C18 column (Macherey-Nagel, Düren, Germany). Separation was applied by a linear binary gradient (see Table 2.11.) with the two solvent mixtures A) methanol and B) methanol/water (3:1, v/v), both substituted with 0.1 % (v/v) acetate.

**Table 2.11.: Linear gradient of FAME HPLC separation**

Time (min)	A (%)	B (%)	Flow (mL/min)
0	100	0	0.18
5	100	0	0.18
10	0	100	0.36
20	0	100	0.36
25	100	0	0.36
30	100	0	0.36

The retention time of desired C24 FAMES on this gradient was determined with a genuine 24:1;1 FAME standard and collected as a fraction over 1 min. FAMES were extracted from the fraction by adding hexane, centrifugation and transferring the upper phase to a new GC vial. The extract was dried under streaming nitrogen and resolved in 50  $\mu$ L acetonitrile.

#### 2.2.7.3. Derivatization of FAMES with DMDS (after Francis (Francis and Veland 1987))

For derivatization of the double bonds in FAMES, 50  $\mu$ L BSTFA (*N,O*-Bis(trimethylsilyl)trifluoroacetamide, from Sigma-Aldrich, St. Louis, USA) was added to the sample and dried under streaming nitrogen, before resolved in 100  $\mu$ L DMDS (dimethyl disulfide) with 1.3 mg/mL I<sub>2</sub>. After 30 min incubation at 37 °C, 1 mL saturated Na<sub>2</sub>S<sub>2</sub>O<sub>3</sub> solution (in water) was added to remove I<sub>2</sub>. The mixture was stirred until the brown color completely disappeared. DMDS-derivatives were extracted from the solution



by adding 3 mL hexane, centrifugation and transferring the upper phase to a new vial. All 20 reactions were then combined in one vial, dried under streaming nitrogen and resolved in 2  $\mu$ L acetonitrile.

#### 2.2.7.4. Analysis of DMDS-FAMEs via GC-MS

Combined DMDS-derivatives of FAME extracts were brought onto the GC-MS system via direct infusion of 2  $\mu$ L sample. The system used was a 7890D GC System (Agilent Technologies, Santa Clara, USA) with a HP-5MS column (30 m length, 0.25 mm diameter, 0.25  $\mu$ m film), connected to a 5977B MSD mass detector (Agilent Technologies, Santa Clara, USA).

The GC method used included the following parameters: 37.417 min run time, 70 °C initial temperature, increasing to 220 °C at 8 °C/min, increasing to 320 °C at 15 °C/min, holding at 320 °C for 10 min. Column flow was set to 2 mL/min. MS spectra were acquired for a mass range of 70-900. MS source temperature was set to 230 °C, MS Quad temperature to 150 °C.

24:1;1 DMDS-FAME from a genuine ceramide standard was used to verify derivatization in GC-MS. Double bond position of DMDS-FAMEs was determined by their MS/MS spectra.

### 2.2.8. Fatty acid profile analysis

#### 2.2.8.1. MTBE lipid extraction (after Matyash (Matyash, Liebisch et al. 2008))

For extracting lipids, 1 mL preheated 2-propanole (75 °C) was added to 10 mg lyophilized and homogenized plant material. For fatty acid quantification, standard substances were added (5  $\mu$ L tri-17:0 triglyceride [1 mg/mL in  $\text{CHCl}_3$ ], 20  $\mu$ L di-17:0-MGDG [1 mg/mL in  $\text{CHCl}_3$ /methanol (85:15, v/v)], 10  $\mu$ L di-17:0-PC [1 mg/mL in  $\text{CHCl}_3$ /methanol (1:2, v/v)]). The mixture was heated for 15 min at 75 °C. Afterwards, solvents were evaporated under streaming nitrogen. The sample was resolved in ice-cold methanol and 2.5 mL MTBE (methyl *tert*-butyl ether) and shaken for 1 h at 4 °C. The solution was treated with ultrasound for 10 minutes. Afterwards, 0.6 mL water was added and the sample was incubated at room temperature for 10 min. For stronger phase differentiation, sample was centrifuged at 800  $\times$  g for 15 min. The upper MTBE phase was transferred to a new vial. 0.7 mL methanol/water (3:2.5, v/v) and 1.3 mL MTBE were added to the lower phase. After 10 min incubation at room temperature, the sample was centrifuged at 800  $\times$  g for 15 min and the upper phase combined with the first MTBE phase. The extraction was dried under streaming nitrogen and resolved in  $\text{CHCl}_3$  for further treatment.

#### 2.2.8.2. Solid-phase extraction of lipid classes (after Reich (Reich, Göbel et al. 2009))

SPE-cartridges (Strata SI-1 Silica, 500 mg/6 mL, Phenomenex, Aschaffenburg, Germany) were used for this extraction method. Prior to first use, the cartridges were cleaned by adding consecutively each 2 mL  $\text{CHCl}_3$ , acetone:2-propanol (9:1, v/v), Methanol/acidic acid (9:1, v/v) and acetone and drying the columns overnight.

For extraction, the cartridges were conditioned with 1 mL CHCl<sub>3</sub> and the sample was added dissolved in 1 mL CHCl<sub>3</sub>. For the elution of neutral lipids, 14 mL of CHCl<sub>3</sub> were added on the column, for glycolipids 15 mL acetone:2-propanol (9:1, v/v) and for phospholipids 15 mL Methanol/acidic acid (9:1, v/v). Each lipid class was collected in different fractions and dried under streaming nitrogen. For GC measurements, the sample was resolved in 20-100 µL acetonitrile.

After extraction, the cartridges were washed with 15 mL acetone and dried.

### 2.2.8.3. Acidic methylation (from Miquel (Miquel 1992))

For the conversion of fatty acyl residues to fatty acid methyl esters (FAMES), dry lipid extract was dissolved in 1 mL solution containing 2.5 % (v/v) H<sub>2</sub>SO<sub>4</sub> and 2 % (v/v) dimethoxypropane in Methanol/toluol (2:1, v/v), then incubated at 80 °C for 60 min. Afterwards, 1.5 mL saturated NaCl solution and 1.2 mL *n*-hexane were added. After centrifuging at 450 x *g* for 10 min, the upper phase was transferred to a new vial and dried under streaming nitrogen. The dry residue was resolved in 100 µL acetonitrile.

### 2.2.8.4. Gas chromatography (GC)

FAMES were analyzed using an Agilent 6890 gas chromatograph (Agilent Technologies, Waldbronn, Germany) with a capillary DB-23 column (30 m x 0.25 mm; 0.25 µm coating thickness; J&W Scientific, Agilent Technologies, Waldbronn, Germany). As carrier gas, helium was used at a flow rate of 1 mL/min. The temperature gradient was as follows: 150 °C for 1 min, 150-200 °C at 4 K/min, 200-250 °C at 5 K/min, 250 °C for 6 min. Analysis of gas chromatography data was performed using the Agilent ChemStation data analysis software. Quantification was calculated via the standard substance (see 2.2.8.1.) and the following formula:

$$\frac{FA[AU] * IS[\mu g]}{IS[AU] * MWFA[\mu g/\mu mol] * FW[g]} = \mu mol/g$$

*AU* = Area unit

*FA* = Fatty acid

*IS* = Internal standard

*MWFA* = molecular weight of FA

*FW* = fresh weight of sample

### 2.2.9. Chlorophyll content analysis

This method was adapted from Dunn (Dunn, Turnbull et al. 2004).

Moss plate cultures were harvested after 3 months of growth by scraping off plant material with forceps and freezing in liquid nitrogen. Moss tissue was afterwards lyophilized so the dryness of the different cultivation methods and mutant lines did not interfere with the measurements. For each mutant line and growth condition, 2 plate cultures were grown. About 8 mg homogenized lyophilized material was weighed in for each sample, if possible. Samples of the same line and growth condition with insufficient amounts were combined (applied for all plate cultures grown without tartrate).

Chlorophyll was extracted from samples by adding 600  $\mu\text{L}$  ethyl acetate/acetone (6:4, v/v) and homogenized. Then, 500  $\mu\text{L}$  water was added and the mixture centrifuged. The supernatant was taken off and mixed with 800  $\mu\text{L}$  acetone. This extract was then either directly analyzed or diluted again 1:5.

Chl *a* & *b* were analyzed in extracts by measuring absorption at 646, 664 and 750 nm on a UV/VIS spectrometer (Ultrospec 1100 pro, GE Health Care Life Sciences, Buckinghamshire, England) and calculating chlorophyll content from following formula (from Porra (Porra, Thompson et al. 1989)):

$$\text{Chls } a + b = 19.54 * A^{646} + 8.29 * A^{664}$$

Absorption at 750 nm was subtracted from absorption at other wavelength before calculation.

## 3. Results

---

Lipids are in all organisms essential for maintaining the barrier between the cell's interior and the environment. Lipid properties like length and straightness of FA moieties as well as the shape and charge of the head group have impact on membrane thickness, fluidity and curvature. These are again features that can be modified depending on physical conditions the membrane is exposed to, e.g. temperature, salt concentration, or hydration level. Plants, unlike animals, are mostly exposed to these conditions and therefore rely more heavily on lipid modifications to maintain membrane functionality. A variety of different lipid classes can be affected in plants when exposed to abiotic stresses, including the complex class of sphingolipids. A significant role in sphingolipid modification at cold stress conditions plays the enzyme class of desaturases, which catalyze the formation of double bonds in many lipids.

In this work, the non-vascular model organism *P. patens* is analyzed in detail on how its lipid composition changes at cold stress conditions. This required the design of an analytic LC-MS method that is suited to detect as many lipids as possible in this organism. A special focus was hereby set on the complex class of sphingolipids and the activity of a novel enzyme responsible for modifying them. This enzyme, named PpSFD, is furthermore compared to an enzyme with similar function known from *A. thaliana*, AtADS2, with regards to its *in-vivo* functions for phenotype and lipid composition in *P. patens* and *A. thaliana* mutant and complementation lines.

### 3.1. Lipid composition in *P. patens*

Unlike many vascular model organism plants, *P. patens* has not been described in much detail regarding its lipid composition. Most publications covering this topic are today more than 30 years old and/or focused on a limited number of lipid classes and lipid species (Grimsley, Grimsley et al. 1981, Girke, Schmidt et al. 1998, Morikawa, Saga et al. 2009). Especially sphingolipids in *P. patens* are very scarcely described in the literature. A first aim of this work was therefore to characterize the lipid composition in *P. patens* as extensively as possible.

Analyzing lipids in *P. patens* also provides the opportunity to track changes in lipid composition caused by environmental stresses or mutations. Observing effects of knock-out mutations on an organism can only be sufficiently done when as many possible targets of the gene of interest can be measured. Establishing a reliable method for lipid analysis in *P. patens* therefore also helps in understanding the function of lipid modifying enzymes, like desaturases.

### 3.1.1. Fatty acid composition of *P. patens*

Vascular and non-vascular plants are different in a variety of ways, including the composition of their lipids. This starts already at the composition of FA in these lipids. The FA profile of *P. patens* is quite different to that of vascular plants and was in part described before (Girke, Schmidt et al. 1998, Zank, Zähringer et al. 2002, Kaewsuwan, Cahoon et al. 2006, Beike, Jaeger et al. 2014). These studies usually dealt with moss from plate cultures, grown mostly as leaf-like gametophyte tissue. In this work, moss cultures used for lipid analysis were cultivated exclusively as liquid cultures supplied with 1 % CO<sub>2</sub>-containing air. The growth conditions were set to promote the formation of the fast-growing root-like protonema tissue. As described by Beike (Beike 2013) gametophore and protonema tissues are expected to have mostly similar composition of FAs.

As a starting point for analysis of lipids in *P. patens* the FA composition was analyzed for the given growth conditions. The FA profile of glycolipids, phospholipids and neutral lipids was analyzed using solid phase extraction and GC. To compare lipids from moss with vascular plants, lyophilized wild type plant material of *P. patens* and *A. thaliana* were analyzed in parallel. The direct comparison between FA profiles in *A. thaliana* and *P. patens* is shown in Figure 3.1.

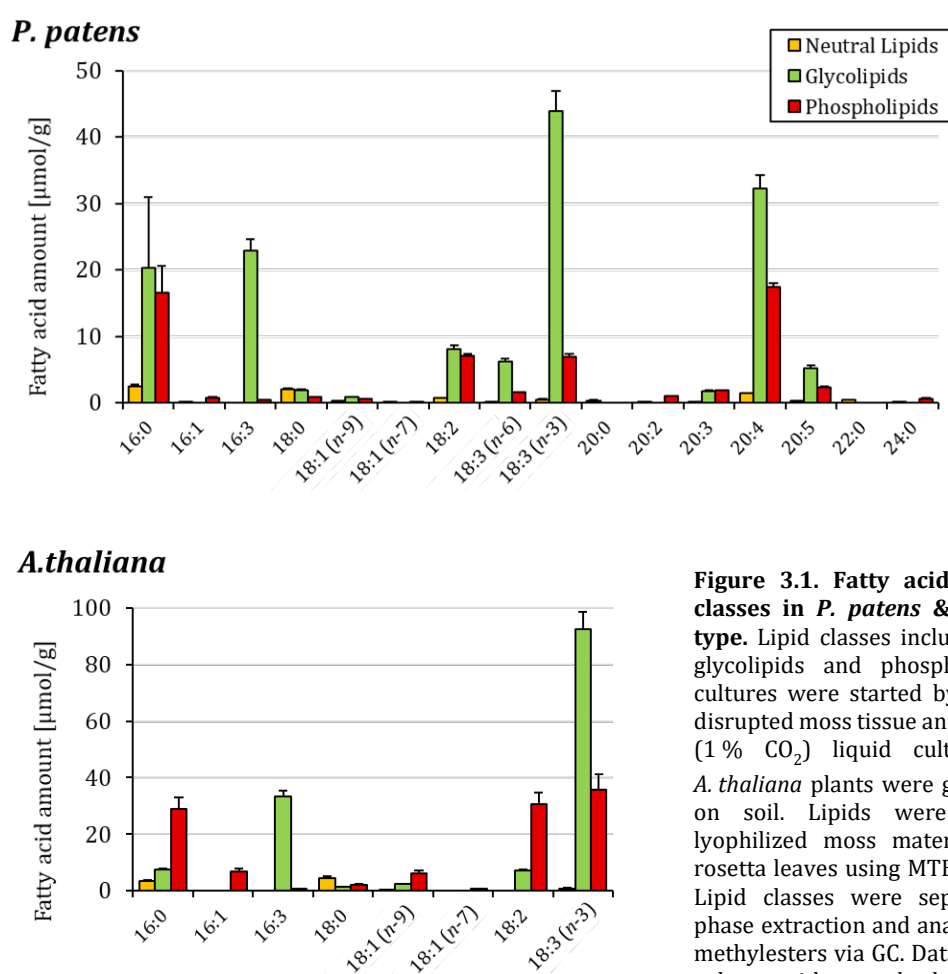


**Figure 3.1. Fatty acid profile of lipid classes in *P. patens* & *A. thaliana* wild type.** Lipid classes include: Neutral lipids, glycolipids and phospholipids. *P. patens* cultures were started by inoculation with disrupted moss tissue and grown in aerated (1 % CO<sub>2</sub>) liquid cultures for 7 days. *A. thaliana* plants were grown for 3 weeks on soil. Lipids were extracted from lyophilized moss material or *A. thaliana* rosetta leaves using MTBE lipid extraction. Lipid classes were separated via solid-phase extraction and analyzed as fatty acid methyl esters via GC. Data represents mean values with standard deviations of 3 biological replicates.

FAs in *A. thaliana* contain either 16 or 18 carbons, longer FAs were not detected in significant amounts. The most common FAs found in *A. thaliana* are 16:0, 16:1, 18:1, 18:2 and 18:3 in phospholipids; 16:0, 16:3, 18:2 and 18:3 in glycolipids; and 16:0 and 18:0 in neutral lipids. Glycolipids are the most abundant lipid class; neutral lipids are detected at comparably low amounts.

*P. patens* contains a much larger variety of FAs than *A. thaliana*. FAs with 20 carbons were found in high abundance in all lipid classes. Phospholipids are mostly composed of 16:0, 16:1, 18:2, 18:3, 20:3, 20:4 and 20:5, as well as small amounts of 24:0. In glycolipids, 16:0, 16:3, 18:0, 18:2, 18:3, 20:3, 20:4 and 20:5 can be found. Neutral lipids were detected in very low amounts, with 16:0, 18:0, 18:2 and 20:4 being the most abundant FAs. Overall, glycolipids are present in *P. patens* at the highest abundance of all lipid classes analyzed.

The FA analysis showed that *P. patens* contains high amounts of the very-long-chain polyunsaturated fatty acid (VLC-PUFA) 20:4 (*n*-6), called arachidonic acid. Arachidonic acid is present in all 3 lipid fractions. It represents the second most abundant FA in phospholipids and glycolipids, as well as the third most abundant FA in neutral lipids. This FA is however not present at all in *A. thaliana*.

### 3.1.2. Establishing a MRM-based UPLC-ESI-MS approach for the lipidome analysis of *P. patens*

In 2015, Tarazona (Tarazona, Feussner et al. 2015) developed a multiplexed lipidomics method using a UPLC-ESI-MS/MS setup. The method is described as a targeted method using MRM, which means that for each analyzed molecule, the transitions from a precursor ion to a fragment ion was measured. If several FA moieties are present in one lipid species, an MRM transition is recorded for each FA separately. This method allows for most lipid species not only to be identified by their overall chemical composition, but also by their exact FA moieties, which cannot be determined by the mass of the molecule alone. Simplified, this means lipids in this method are identified with at least two mass fragments (one kind of head group fragment and one kind of acyl chain fragment), more if more than one acyl residue is present in the molecule (as in all diacyl- and triacyl-glycero-lipids). Analysis of lipids in *P. patens* done in this work is based heavily on the approach described by Tarazona. Extraction of lipids was performed using an isopropanol/hexane/water mixture (60:24:12, v/v/v) which was described to resolve all major lipid classes in plants.

The MRM mode of MS analysis used in this approach is commonly more sensitive than other methods of lipid MS analysis. One drawback is however that all possible FA and LCB combinations in lipid species have to be known beforehand or predicted before measurements are done. Identification of unknown lipid species (e.g. those with unknown head groups or unusual FA moieties) is not possible via this approach. Furthermore, the retention time for most lipid species has to be predicted based on the properties of the lipid species. Tarazona (Tarazona, Feussner et al. 2015) developed an algorithm for predicting the retention time of lipid species without the use of standard substances, based on the FA, LCBs and head groups present in the lipid. The algorithm used was based

on measurements done on *A. thaliana* samples and therefore were tailored to the lipid species and FAs present in this organism.

The method from Tarazona (Tarazona, Feussner et al. 2015) was modified in this work for several aspects: A) Inclusion of additional MRM transitions following established rules for lipid fragment prediction by Tarazona (Tarazona, Feussner et al. 2015), B) Improving the existing rule set by adding new MRM transitions, C) Adding a new lipid class (DGTS/A) to the analysis. A) means that VLC-PUFAs were taken into account as FA moieties in potential lipid species, and B) was accomplished by including head group scans for lipid classes that were only detected at low signal intensity (GIPC) or unclear overlap with other lipid classes (SQDG, PS).

One major difference between lipids in *A. thaliana* and *P. patens* is that the moss contains 20:4 as a major FA, which is not present in vascular plants like *A. thaliana* (see 3.1.1). The algorithm used for retention time prediction did not include accurate data on VLC-PUFAs since these FA moieties are not present in *A. thaliana*. During analysis of *P. patens* samples in this work it was observed that having the FA 20:4 in a lipid molecule led to an unexpected impact on retention time, which could not be calculated by the linear prediction algorithm. Retention time had to be corrected manually for all lipid species containing FA moieties with 20 carbon atoms and at least 4 double bonds (20:4 and 20:5). It was determined that all lipid species with 20:4 and 20:5 FA-moieties caused an additional retention time shift of about 0.5-1 min (depending on the LC gradient used) towards the prediction algorithm.

To develop an accurate lipidomics method for *P. patens*, all assumed lipid species of all lipid classes were assembled and the corresponding MRM-lists created. For glycerolipids, combinations of all FA moieties that were detected during GC FA analysis were taken as the basis for this MRM-list (see 3.1.1.). Additionally, the FA moieties 24:0 and 24:1 were included even if they were not detected during GC analysis. For the sphingolipids, the MRM-list included all possible hydroxylated, non-hydroxylated, saturated and mono-unsaturated FA moieties from C16 up to C26, as well as the LCB moieties 18:0;2, 18:0;3, 18:1;2, 18:1;3 and 18:2;2. The MRM-list for acyl-sterol lipids included the steroid core structures cholesterol, sitosterol, campesterol, stigmasterol and brassicasterol, as well as all FA moieties detected in glycerolipids. Free sterols were analyzed using GC-MS, not LC-MS. The full list of analyzed lipid species is shown in Table 3.1. In summary, the MRM-lists contain 3589 transitions for approximately 1500 lipid species.

Lipid extracts of *P. patens* wild type were measured in a survey analysis to determine the lipidome of the moss before analyzing other samples. The extraction was done exclusively on the protonema tissue type of *P. patens* cultures, the fast-growing filaments commonly grown in liquid cultures. Overall, most lipid species were detected in *P. patens* without much trouble once the delay in retention time caused by VLC-PUFAs was taken into account. However, several lipid classes in *P. patens* proved to be difficult to detect with the given analysis method. The molecular masses of PS and SQDG overlapped with the very prominent lipid class PC, which made identification of lipid species difficult. To make clear which MRM transitions could actually be appointed to PS and SQDG a precursor ion scan was done, focusing on specific head group fragments of these lipid classes. These specific head group fragments were identified by measuring SQDG, PS and PC standard substances with a product ion scan and determining fragments that were uniquely appearing in only one of the lipid classes. Correct peaks for SQDG and PS could therefore be identified. PS

was afterwards analyzed like other lipid species. Peaks of SQDG, however, were detected at very low signal intensity and were barely visible above background noise. The head group scans however suggest that some SQDG species might be present in *P. patens*, but not in sufficient amounts for analysis with this method.

**Table 3.1. Survey of all lipid species used for screening the *P. patens* lipidome.** Lipidome analysis is based on a method from Tarazona (Tarazona, Feussner et al. 2015) and includes UPLC separation and MRM-based ESI-MS analysis. 4 biological replicates of *P. patens* wild type were used for screening.

<sup>1</sup> Free sterols were analyzed via GC-MS.

<sup>2</sup> Screened GIPC head groups included: Hex-HexA-IPC, HexNAC-HexA-IPC, Hex-Hex-HexA-IPC, Hex-HexNAC-HexA-IPC

<sup>3</sup> MRM lists of phospholipids, glycolipids and neutral lipids were determined by profiling fatty acid compositions in each lipid class of *P. patens* wild type via solid phase extraction and GC analysis (see 3.1.1.).

<sup>4</sup> MRM lists of sphingolipids included all possible fatty acid and LCB moieties commonly found in plants.

Lipid class	Head group	Fatty acid moiety <sup>3,4</sup>	Sterol/LCB moiety
Phospho-lipids	PA		
	PC		
	PE	16:0, 16:1, 16:3	
	PG	18:0, 18:1, 18:2, 18:3	
	PI	20:2, 20:3, 20:4, 20:5	
	PS	24:0, 24:1	
Glycolipids	MGDG		
	DGDG	16:0, 16:3	
	SQDG	18:0, 18:1, 18:2, 18:3	
	DGTS/A	20:3, 20:4, 20:5 24:0, 24:1	
Neutral lipids	DAG	16:0, 16:3, 18:0, 18:1, 18:2, 18:3	
	TAG	20:0, 20:3, 20:4, 20:5, 22:0, 24:0, 24:1	
Sterol lipids	Sterols <sup>1</sup>		
	SE	16:0, 16:1, 16:2, 16:3	cholesterol
	SG	18:0, 18:1, 18:2, 18:3, 18:4	brassicasterol
	ASG	20:0, 20:1, 20:2, 20:3, 20:4, 20:5 22:0, 22:1, 24:0, 24:1	campesterol stigmasterol sitosterol
Sphingolipids	Cer	16:0;0, 16:0;1, 16:1;0, 16:1;1	18:0;2 18:0;3
	GlcCer	18:0;0, 18:0;1, 18:1;0, 18:1;1 20:0;0, 20:0;1, 20:1;0, 20:1;1	18:1;2 18:1;3
	GIPC <sup>2</sup>	22:0;0, 22:0;1, 22:1;0, 22:1;1 24:0;0, 24:0;1, 24:1;0, 24:1;1	18:2;2
		26:0;0, 26:0;1, 26:1;0, 26:1;1	

**Abbreviations:**  
 Phosphatidic acid (PA),  
 phosphatidyl-choline (PC),  
 phosphatidyl-ethanolamine (PE),  
 phosphatidyl-glycerol (PG),  
 phosphatidyl-inositol (PI),  
 phosphatidyl-serine (PS),  
 monogalactosyl-diacylglycerol (MGDG),  
 digalactosyl-diacylglycerol (DGDG),  
 sulfoquinovosyl-diacylglycerol (SQDG),  
 diacylglycerol-*O*-(*N,N,N*-trimethyl)-homoserine/alanine (DGTS/A),  
 diacylglycerol (DAG),  
 triacylglycerol (TAG),  
 sterol-ester (SE),  
 sterol-glycoside (SG),  
 acylsterolglycoside (ASG), ceramide (Cer),  
 glycosylceramide (GlcCer),  
 glycosylinositolphosphatidylceramide (GIPC),  
 long-chain base (LCB)

The lipid species DGTS/A and GIPC were overall difficult to detect in *P. patens* samples. Initial surveys for these lipid classes produced no identifiable signals for either class. For both lipid classes, no genuine standard substances were commercially available at the time of this work, so finding similar class-specific fragments as for PS and SQDG could not be accomplished. However, for both lipid classes fragmentation patterns are reported in other publications (Welti and Wang 2004). GIPC, the sphingolipid class with the highest abundance in *A. thaliana* (Markham and Jaworski 2007), was detected with specific head group scans, but only marginally. Signal intensity for these compounds was so low during measurements that only some specific ions could be detected when scanning for double-



charged ions ( $m/z$ ). However, these signals were not high enough to be reliably detected against background noise of the measurement (see 3.1.7. for more details on GIPC measurements). The major problem detecting these molecules probably occurred because of the use of a nanoESI-MS device which is not optimized to ionize large molecules above 1000 Da size. GIPC commonly have a mass of at least 1200 Da, depending on the number of sugar moieties in the head group. Analyzing double-charged molecules instead of single-charged molecules (as for all other lipid classes in this method) halved the detected  $m/z$  value, bringing it within reach for a mass spectrometer that is optimized for  $m/z$  values lower than 1200. However, even scanning for these double-charged molecules did not yield high enough peaks to confidently identify the presence of GIPC in *P. patens*.

For DGTS/A, only one lipid species could be confirmed (18:2/18:2, data not shown). The low signal intensity of DGTS/A also prohibited further analysis of the compound to determine which exact head group (DGTS or DGTA) was present in *P. patens*. Both DGTS & DGTA are typically found in marine algae as well (Künzler and Eichenberger 1997). All in all, it was concluded that the lipid classes SQDG, DGTS/A, and GIPC are probably present in *P. patens* protonema tissue, but in such low amounts that they could not be detected in sufficient signal intensity, at least under the experiment conditions given in this work. These lipid classes were consequently not further analyzed in other parts of this work.

Overall, 729 lipid species in 19 lipid classes were reproducibly detected in four independently grown and analyzed *P. patens* wild type samples. This includes 252 species of phospholipids, 77 species of glycolipids, 163 species of neutral glycerolipids, 79 species of sterol lipids, 89 species of sphingolipids, and 69 species of lyso-lipids. The method used does not include standard substances as references to absolute lipid amounts. For MS analysis, the absolute amount of a measured molecule is difficult to determine even with the use of standards, since molecular composition and the overall mass of a molecule all have an impact on the ionization in the mass spectrometer. All data gathered is therefore shown as relative peak area against the total peak area of all molecules measured in one lipid class. The data does not allow to draw conclusions about which lipid class might be the most or least abundant one in *P. patens*.

The complete list of all detected lipid species and the corresponding FA/LCB moieties is shown in Table 3.2.

**Table 3.2. Lipids species detected in *P. patens* wild type.** Moss cultures were started by inoculation with disrupted moss tissue and grown in aerated (1% CO<sub>2</sub>) liquid cultures for 7 days. Lipids were extracted from lyophilized moss material using a one-phase isopropanol/hexane/water extraction. Lipid species were characterized via MRM-based UPLC-QTrap-ESI-MS analysis. Only lipid species detected with a relative peak area of > 0.01 % were included in the dataset. Lipids were measured in 4 biological replicates.

<sup>1</sup>Free sterols were analyzed via GC-MS.

Lipid class	Head group	Lipid fatty acid moiety (Lyso-lipid fatty acid moiety)	Sterol/LCB moiety	No. of detected lipid species	
				Lipid	Lyso-lipid
Phospho-lipids	PA	16:0, 16:1, 16:3, 18:0, 18:1, 18:2, 18:3, 20:2, 20:3, 20:4, 20:5, 24:0 (16:0, 16:1, 18:0, 18:1, 18:2, 18:3, 20:0, 20:3, 20:4, 20:5, 22:0, 24:0)	-	PA 58	LPA 12
	PC	16:0, 16:1, 16:3, 18:0, 18:1, 18:2, 18:3, 20:2, 20:3, 20:4, 20:5, 24:0, 24:1 (16:0, 18:0, 18:1, 18:2, 18:3, 20:0, 20:1, 20:3, 20:4, 20:5, 22:0, 24:0, 24:1)	-	PC 62	LPC 13
	PE	16:0, 16:1, 18:0, 18:1, 18:2, 18:3, 20:2, 20:3, 20:4, 20:5, 24:0, 24:1 (16:0, 18:0, 18:1, 18:2, 18:3, 20:0, 20:1, 20:3, 20:4, 20:5, 22:0, 24:0, 24:1)	-	PE 56	LPE 13
	PG	16:0, 16:1, 16:3, 18:0, 18:1, 18:2, 18:3, 20:2, 20:3, 20:4, 20:5 (16:0, 16:1, 18:1, 18:2, 18:3, 20:4, 24:0)	-	PG 24	LPG 7
	PI	16:0, 16:1, 16:3, 18:0, 18:1, 18:2, 18:3, 20:2, 20:3, 20:4, 20:5 (16:0, 18:2, 18:3, 20:4)	-	PI 26	LPI 4
	PS	16:0, 16:1, 16:3, 18:0, 18:1, 18:2, 18:3, 20:2, 20:3, 20:4, 20:5, 24:0, 24:1 (14:1)	-	PS 26	LPS 1
Glyco-lipids	MGDG	16:0, 16:3, 18:0, 18:1, 18:2, 18:3, 20:3, 20:4, 20:5 (16:0, 16:3, 18:2, 18:3, 20:3, 20:4, 20:5)	-	MGDG 39	LMGDG 7
	DGDG	16:0, 16:3, 18:0, 18:1, 18:2, 18:3, 20:3, 20:4, 20:5 (16:0, 18:0, 18:2, 18:3, 20:3, 20:4, 20:5, 24:0)	-	DGDG 37	LDGDG 8
	SQDG	- (16:0, 18:2)	-	SQDG 0	LSQDG 2
	DGTS/A	18:2	-	DGTS/A 1	-
Neutral lipids	DAG	16:0, 16:3, 18:0, 18:1, 18:2, 18:3, 20:0, 20:3, 20:4, 20:5, 22:0, 24:0, 24:1	-	DAG 88	
	TAG	16:0, 16:3, 18:0, 18:1, 18:2, 18:3, 20:0, 20:3, 20:4, 20:5, 22:0, 24:0, 24:1	-	TAG 75	
Sterol lipids	Sterols <sup>1</sup>	-	sito, camp, stig, isof	Sterols 4	
	SE	16:0, 16:1, 18:0, 18:1, 18:2, 18:3, 18:4, 20:0, 20:3, 20:4, 20:5, 22:0, 24:0, 24:1	chol, bras, camp, stig, sito	SE 32	
	SG	-	chol, sito, camp, stig, isof	SG 5	
	ASG	16:0, 16:1, 16:2, 16:3, 18:0, 18:2, 18:3, 18:4, 20:0, 20:1, 20:2, 20:3, 20:4, 24:0, 24:1	chol, bras, camp, stig, sito	ASG 38	
Sphingolipids	Cer	16:0;0, 16:1;1, 18:0;0, 18:0;1, 18:1;0, 20:0;0, 20:0;1, 20:1;0, 22:0;0, 22:0;1, 22:1;0, 22:1;1, 24:0;0, 24:0;1, 24:1;0, 24:1;1, 26:0;0, 26:0;1, 26:1;0, 26:1;1	18:0;2, 18:0;3, 18:1;2, 18:1;3, 18:2;2	Cer 55	
	GlcCer	16:0;1, 16:1;1, 18:0;0, 18:0;1, 18:1;0, 18:1;1, 20:0;0, 20:0;1, 20:1;0, 20:1;1, 22:0;0, 22:0;1, 22:1;0, 22:1;1, 24:0;0, 24:0;1, 24:1;0, 24:1;1, 26:0;1	18:0;2, 18:0;3, 18:1;2, 18:1;3, 18:2;2	GlcCer 34	free 2 LCBs (18:0;2, 18:0;3)
	GIPC	-	-	GIPC 0	

**Abbreviations:**  
Phosphatidic acid (PA),  
phosphatidyl-choline (PC),  
phosphatidyl-ethanolamine (PE),  
phosphatidyl-glycerol (PG),  
phosphatidyl-inositol (PI),  
phosphatidyl-serine (PS),  
monogalactosyl-diacylglycerol (MGDG),  
digalactosyl-diacylglycerol (DGDG),  
sulfoquinovosyl-diacylglycerol (SQDG),  
diacylglycerol-*O*-(*N,N,N*-trimethyl)-homoserine/alanine (DGTS/A),  
diacylglycerol (DAG),  
triacylglycerol (TAG),  
sterol-ester (SE),  
sterol-glycoside (SG),  
acylsterolglycoside (ASG),  
ceramide (Cer),  
glycosylceramide (GlcCer),  
glycosylinositolphosphate-ceramide (GIPC),  
long-chain base (LCB)

### 3.1.3. Phospholipids in *P. patens*

Phospholipids in *P. patens* were detected as the lipid classes phosphatidic acid (PA), phosphatidyl-choline (PC), phosphatidyl-ethanolamine (PE), phosphatidyl-glycerol (PG), phosphatidyl-inositol (PI), phosphatidyl-serine (PS), and their respective lyso-lipids. The highest number of lipid species was detected in PC (62), the lowest number in PG (24). The most abundant FA moiety detected in these phospholipids is 20:4 in PA, PC and PS, but not in PG and PI. The most abundant lipid species are 16:0/20:4 in PA, PE, PI and PS, 16:0/18:2 in PC, and 16:0/18:3 in PG (see Figure 3.2.). Other main lipid species include: 16:0/18:2, 16:0/18:3, 18:2/20:4, 18:3/20:4, 20:4/20:4, and 20:5/20:4 in PA; 16:0/18:3, 16:0/20:4, 18:2/20:4, 18:3/20:4, and 20:4/20:4 in PC; 16:0/20:3 and 20:4/20:4 in PE; 16:0/16:0, 16:0/18:2 and 16:1/18:3 in PG; 16:0/18:2 and 16:0/18:3 in PI; 16:0/20:5, 20:4/20:4, 20:4/24:0 and 20:4/24:1 in PS.

FAs with a carbon-chain length of 24 were detected in PA, PC, PE, and PS, but not in PI and PG. The mono-unsaturated variant of this FA, 24:1, was only detected in PC, PE and PS. Only in PS are FA with 24 carbons present at significant amounts at about 15 – 25 % relative peak area, all other phospholipid classes contain less than 5 % relative amount of these lipid species.

### 3.1.4. Glycolipids and betaine lipids in *P. patens*

Glycolipids in *P. patens* were detected as the lipid classes monogalactosyl-diacylglycerol (MGDG), digalactosyl-diacylglycerol (DGDG). The betaine lipid class DGTS/A (diacylglycerol-*O*-(*N,N,N*-trimethyl)-homoserine/alanine) was detected consistently only as a single lipid species (18:2/18:2). Since the abundance of this lipid species was very low, it was not possible to analyze the species any further to determine if it was DGTS or DGTA that was present. The lipid class sulfoquinovosyl-diacylglycerol (SQDG) was detected only in precursor scans but could not be measured consistently as MRMs.

The most abundant FA moiety detected in glycolipids is 18:3. The most abundant lipid species for MGDG is 16:3/18:3 at about 50 %, for DGDG it is 18:3/20:4 at about 25 %. Other major lipid species are 18:3/20:4 and 20:4/20:4 in MGDG, as well as 16:0/18:2, 16:0/18:3, 16:3/18:3, 18:2/20:4, 18:3/18:3, 20:4/20:4 and 20:4/20:5 in DGDG. Glycolipids did not contain measurable amounts of C24 FAs (see Figure 3.3.).

### 3.1.5. Neutral glycerolipids in *P. patens*

Neutral glycerolipids in *P. patens* were detected as the lipid classes diacylglycerides (DAG), and triacylglycerides (TAG). Since lipid species with 3 FA moieties are very complex to assign individual FA moieties to, TAG lipids were identified as apparent species only. For easier analysis of the presence of certain FAs in TAG, MRMs of FA were summarized, not individual lipid species. Overall, 88 apparent lipid species were detected in TAG.

The most abundant FA moiety for DAG is 16:0, for TAG it is 20:4. The most abundant lipid species in DAG is 18:2/16:0, (at about 22 %), followed by 18:3/16:0, 20:4/16:0, 20:4/18:2, 20:4/18:3, 20:4/20:4 and 20:4/20:5. Both neutral lipid classes contain FAs with carbon chains longer than 20 carbons, but only DAG contain also the mono-unsaturated FA 24:1 (see Figure 3.4.).

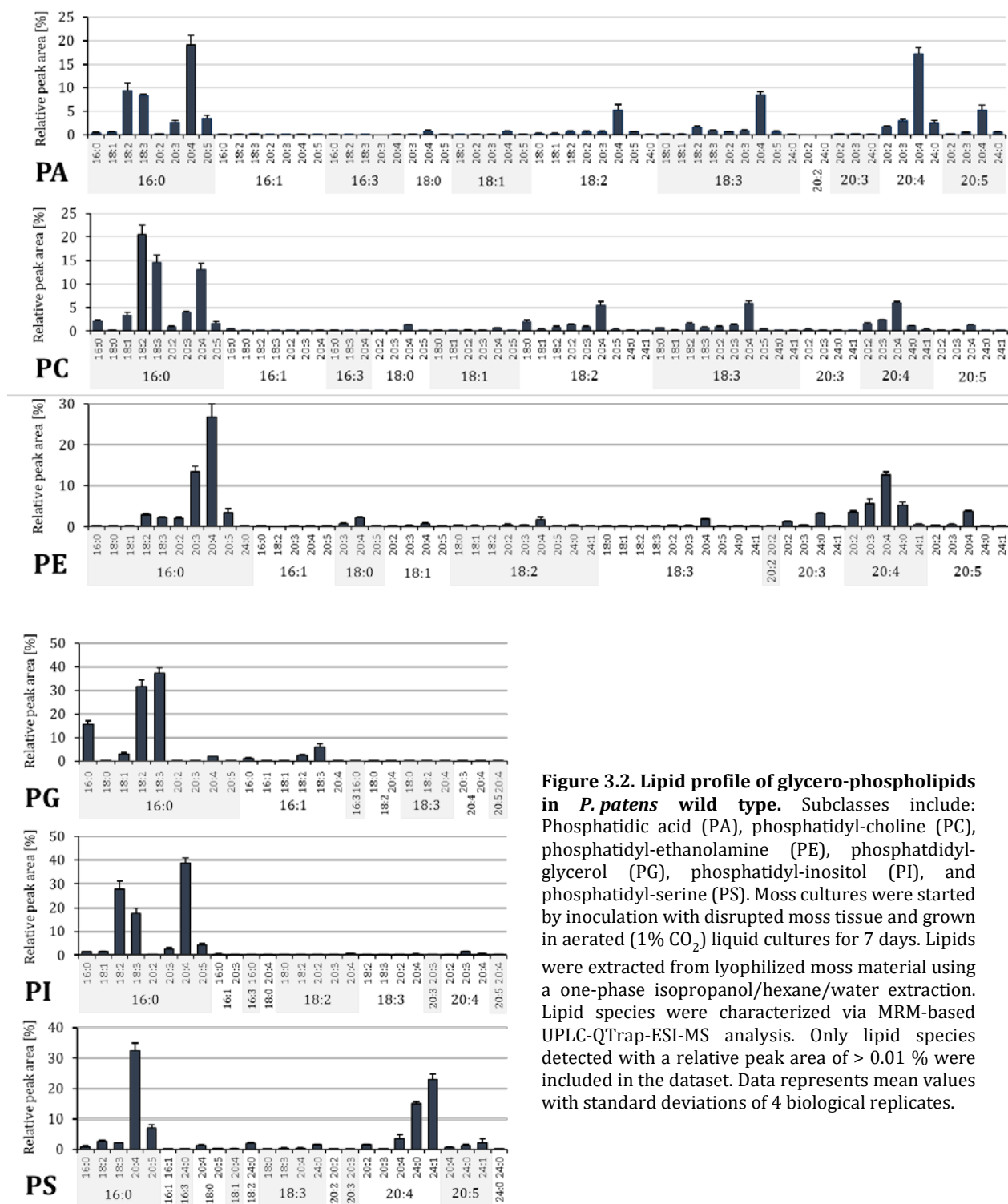


**Figure 3.2. Lipid profile of glycerophospholipids in *P. patens* wild type.** Subclasses include: Phosphatidic acid (PA), phosphatidyl-choline (PC), phosphatidyl-ethanolamine (PE), phosphatidyl-glycerol (PG), phosphatidyl-inositol (PI), and phosphatidyl-serine (PS). Moss cultures were started by inoculation with disrupted moss tissue and grown in aerated (1% CO<sub>2</sub>) liquid cultures for 7 days. Lipids were extracted from lyophilized moss material using a one-phase isopropanol/hexane/water extraction. Lipid species were characterized via MRM-based UPLC-QTrap-ESI-MS analysis. Only lipid species detected with a relative peak area of > 0.01 % were included in the dataset. Data represents mean values with standard deviations of 4 biological replicates.

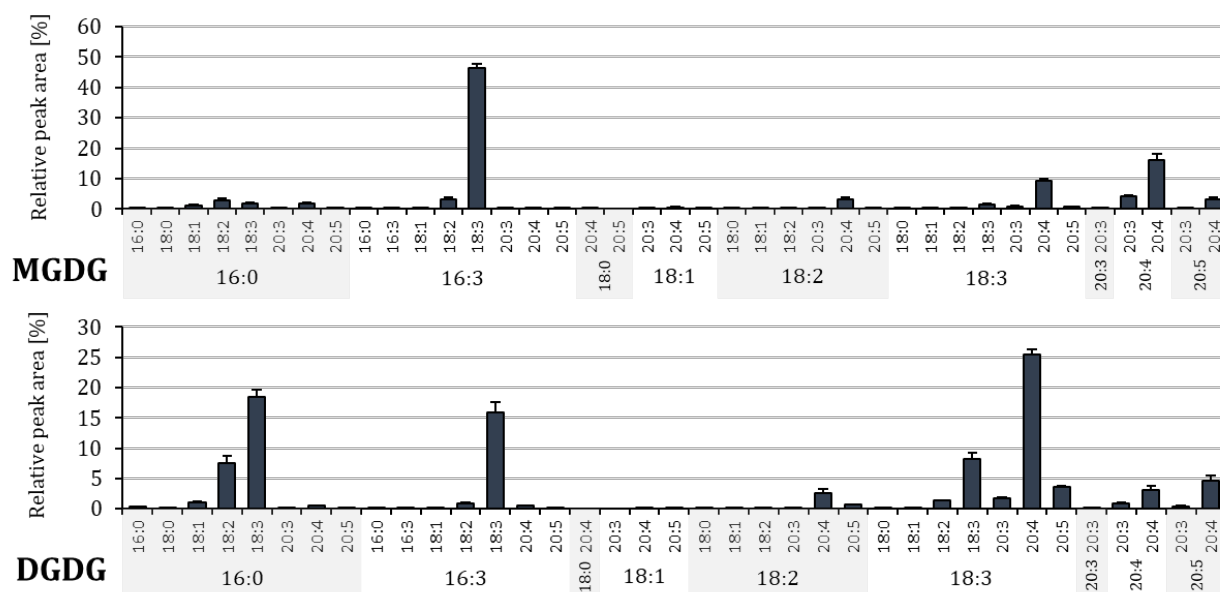


**Figure 3.3. Lipid profile of glycerol-glycolipids in *P. patens* wild type.** Subclasses include: Monogalactosyl-diacylglyceride (MGDG), digalactosyl-diacylglyceride (DGDG). Moss cultures were started by inoculation with disrupted moss tissue and grown in aerated (1% CO<sub>2</sub>) liquid cultures for 7 days. Lipids were extracted from lyophilized moss material using a one-phase isopropanol/hexane/water extraction. Lipid species were characterized via MRM-based UPLC-QTrap-ESI-MS analysis. Only lipid species detected with a relative peak area of > 0.01 % were included in the dataset. Data represents mean values with standard deviations of 4 biological replicates.

### 3.1.6. Sterol lipids in *P. patens*

Sterol lipids in *P. patens* were detected as the lipid classes sterolesters (SE), free sterols, acylsterylglucosides (ASG), and sterylglucosides (SG). Free sterols were measured using GC-MS, not UPLC-ESI-MS. Free sterols were detected in about equal parts as the sterols sitosterol, campesterol and stigmasterol, as well as minor amounts of isofucosterol. The most common steroid core structures found in all other sterol lipids are sitosterol and campesterol, which are present in these lipids in about equal relative amounts. The steroid core structure cholesterol was detected in SG in only very low relative amounts, but it was not detected in free sterols. The sterol esters SE and ASG however contain cholesteryl esters, even though in lower amounts compared to sitosteryl and campesteryl esters. Brassicasteryl esters were detected in very minor amounts in SE and ASG, but brassicasterol was not detected in SG or free sterols.

Distribution of FA moieties was very broad in SE, no single SE species was detected at relative amounts higher than 15 %. In ASG, the lipid species profile is dominated by a few molecules, the FA moiety 16:0 being the most abundant (with sitosterol and campesterol), followed by 16:3 and 20:4. Overall, the highest abundant lipid species in sterol lipids are sitosteryl/20:4 in SE, sitosteryl/16:0 in ASG, and about equal amounts of campesterol and sitosterol in SG (see Figure 3.5.). Other main lipid species in SE include 16:0, 18:2, 18:3, 20:4 and 20:5 with both sitosterol and campesterol as core structures.

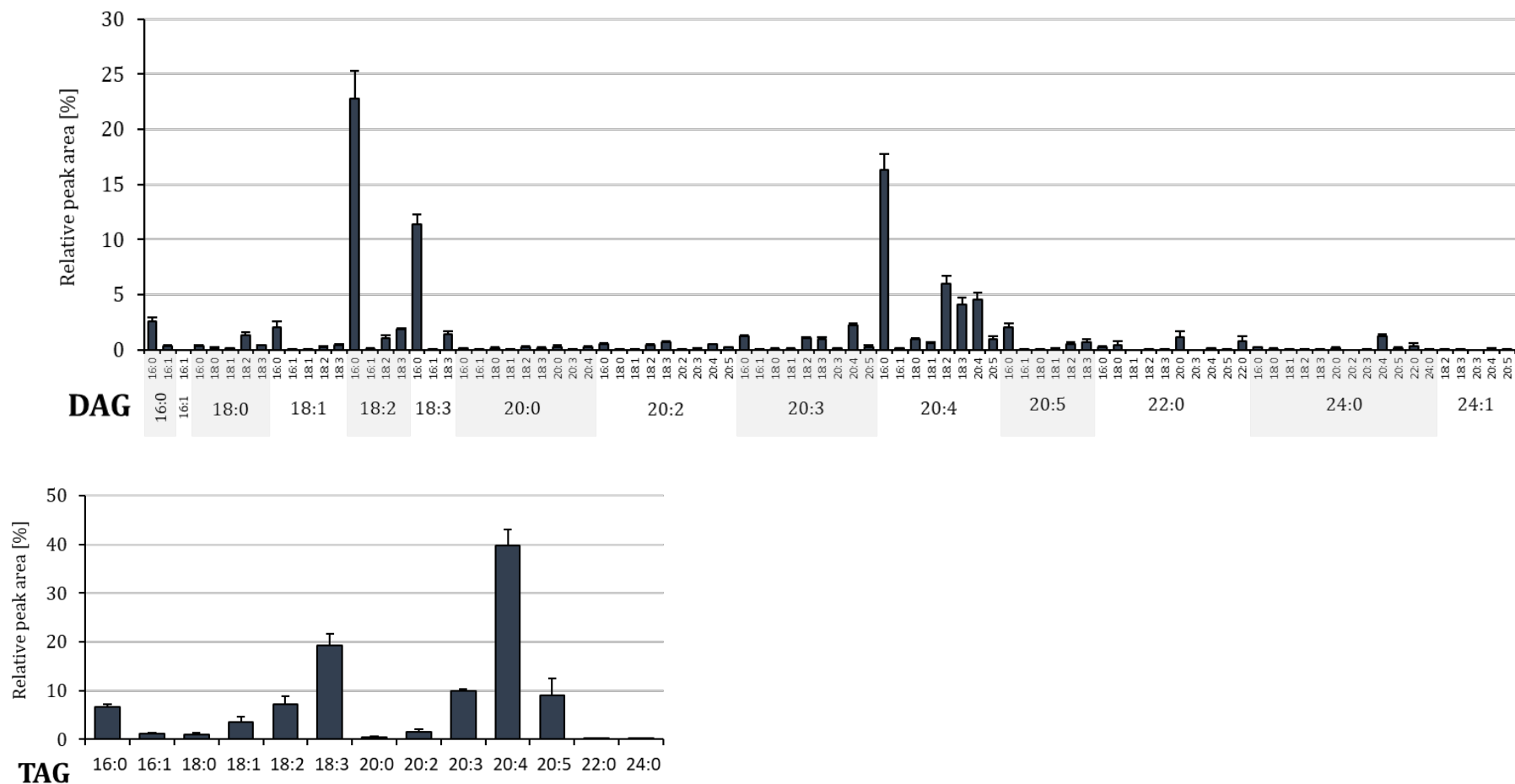


**Figure 3.4. Lipid composition of neutral glycerolipids in *P. patens* wild type.** Subclasses include: Diacylglycerides (DAG), and triacylglycerides (TAG). For TAG, only the FA composition is shown. Moss cultures were started by inoculation with disrupted moss tissue and grown in aerated (1% CO<sub>2</sub>) liquid cultures for 7 days. Lipids were extracted from lyophilized moss material using a one-phase isopropanol/hexane/water extraction. Lipid species were characterized via MRM-based UPLC-QTrap-ESI-MS analysis. Only lipid species detected with a relative peak area of > 0.01 % were included in the dataset. Data represents mean values with standard deviations of 4 biological replicates.

## Results

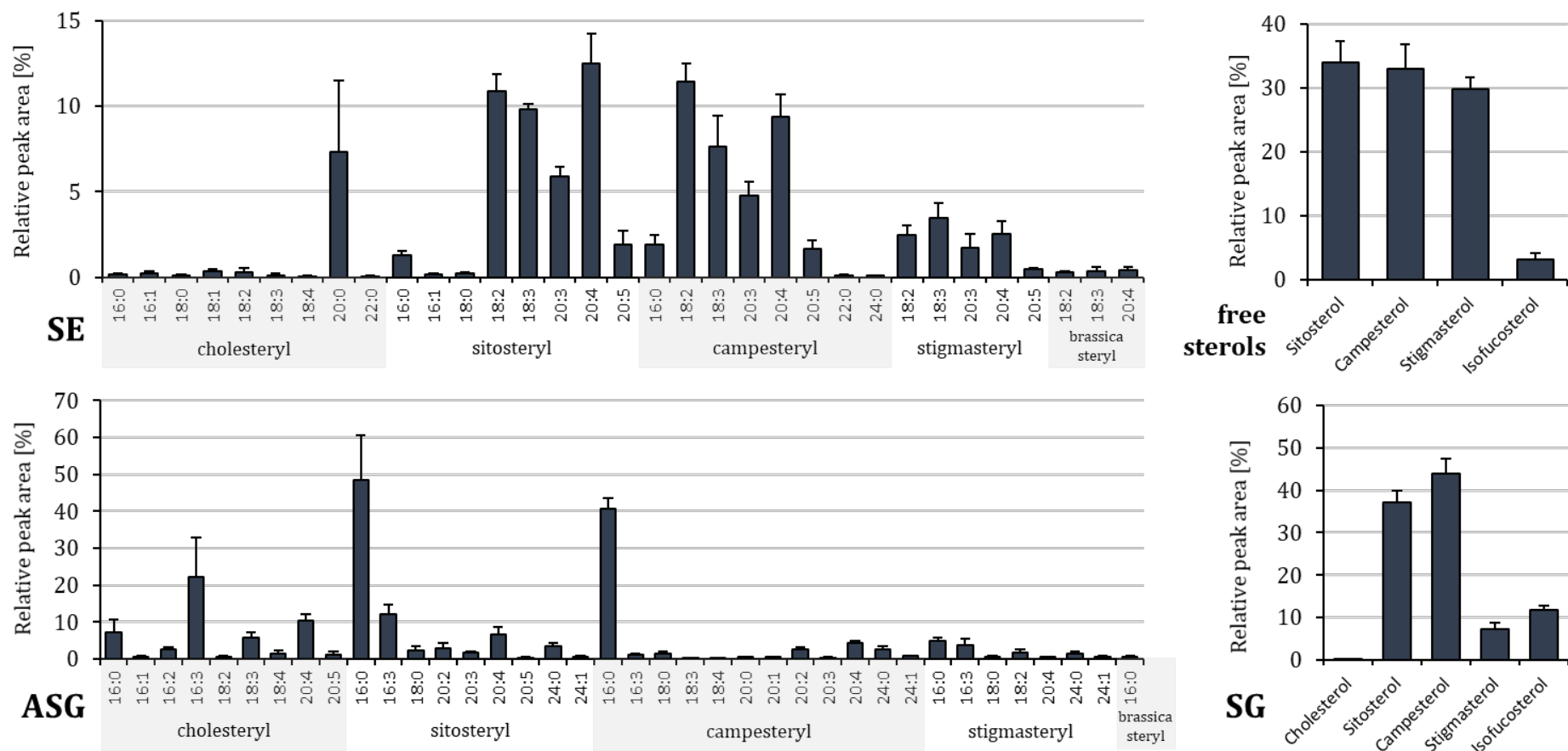


**Figure 3.5. Lipid composition of sterol lipids in *P. patens* wild type.** Subclasses include: Sterolesters (SE), free sterols, acylsteryl-glucosides (ASG), and sterylglucosides (SG). Moss cultures were started by inoculation with disrupted moss tissue and grown in aerated (1% CO<sub>2</sub>) liquid cultures for 7 days. Lipids were extracted from lyophilized moss material using a one-phase isopropanol/hexane/water extraction. Lipid species were characterized via MRM-based UPLC-QTrap-ESI-MS analysis. Only lipid species detected with a relative peak area of > 0.01 % were included in the dataset. Free sterols were measured via GC-MS. Data represents mean values with standard deviations of 4 biological replicates.

### 3.1.7. Sphingolipids in *P. patens*

Sphingolipids in *P. patens* are mainly composed of ceramides (Cer) and glycosylceramides (GlcCer). Cer lipid species are present mainly with the LCB 18:0;3 as a backbone, with only minor amounts of other LCBs present. GlcCer are dominated by the LCB 18:2;2, with more than 95 % of all GlcCer being present with this LCB.

In both sphingolipid classes, hydroxylated FA moieties are by far more abundant than non-hydroxylated ones. The most abundant FA moieties present in Cer are those with 24 carbon length, 18:0;3/24:0;1 being the most abundant Cer species, followed by its mono-unsaturated variant 18:0;3/24:1;1. Contrary to Cer, a single lipid species makes up more than 95 % of GlcCer: 18:2;2/20:0;1. All other FA moieties in GlcCer are present in very low relative amounts, though 24:0;1 and 24:1;1 can also be found (see Figure 3.6.).

Precursor ion scans also suggest a very low amount of glycosyl-inositol-phosphorylceramide (GIPC) to be present in *P. patens* when scanning for double-charged molecules. These molecules could not be detected consistently in all samples, because their signals were not confidently detected against background noise. The precursor ion scans suggest these GIPC species to be mostly consisting of the LCB 18:0;3 and the FA 24:0;1, similar to ceramides. Measured were head groups with 2 and 3 sugar moieties, consisting of glucose, glucuronic acid or N-acetylglucosamin as sugars. The head group containing the two sugar residues HexNAc and HexA appears to be the most abundant head group (data not shown). Nevertheless, the presence of GIPC in *P. patens* could ultimately not be verified.

Free LCBs were only detected for 18:0;3 and 18:0;2 (see Appendix 2).

### 3.1.8. Lyso-lipids in *P. patens*

Lyso-lipids are variants of diacyl-lipids that only contain one FA moiety instead of two. For all glycerolipid classes, lyso-lipids were detected as well. The highest number of lysolipids was detected for PC, while for DGTS/A none were detected. Lyso-lipids mostly reflect the relative lipid profiles of their corresponding diacyl-lipid classes but were overall detected at very low signal intensity. For lyso-PS, a lipid species was detected that did not appear in any diacyl-lipid class: 14:0 (see Appendix 3). It is not clear whether this might be a measurement error, since signal intensity for this molecule was just above background level.

Overall, lyso-lipids were detected at very low signal intensities and were not analyzed further for other experiments.



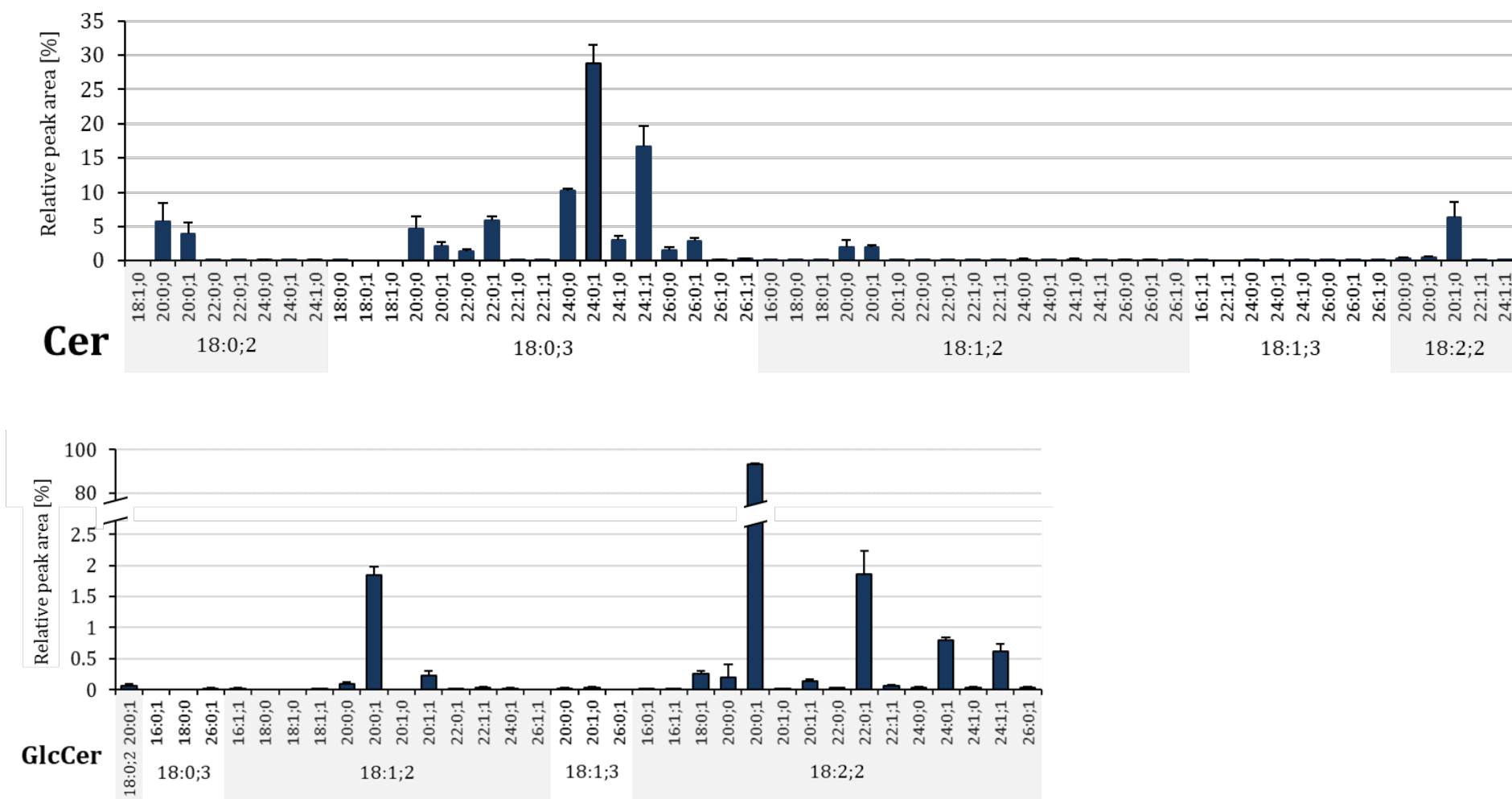


**Figure 3.6. Spingolipid composition in *P. patens* wild type.** Subclasses include: Ceramides (Cer), and glycosyl-ceramides (GlcCer). Moss cultures were started by inoculation with disrupted moss tissue and grown in aerated (1% CO<sub>2</sub>) liquid cultures for 7 days. Lipids were extracted from lyophilized moss material using a one-phase isopropanol/hexane/water extraction. Lipid species were characterized via MRM-based UPLC-QTrap-ESI-MS analysis. Only lipid species detected with a relative peak area of > 0.01 % were included in the dataset. Data represents mean values with standard deviations of 4 biological replicates.

### 3.2. *PpSFD* - a *P. patens* sphingolipid fatty acid desaturase

Establishing a method for lipidome analysis in *P. patens* and having an extensive overview about the lipid composition in *P. patens* was the basis necessary for analyzing the influence of lipid modifying enzymes in this organism. Under cold conditions, plants modify lipids in a variety of different ways. Desaturation of sphingolipids, may it be at the LCB backbone or the FA moiety, has been described of being involved in cold stress adaptations in *A. thaliana* (Chen, Markham et al. 2012, Chen and Thelen 2013). Anna Beike (Beike 2013) discovered a gene of a putative desaturase in *P. patens* that was upregulated at cold stress conditions. The enzyme was predicted by to be involved in modifying sphingolipids. Sequence comparison on a peptide level predicted a structural relationship between this protein and sphingolipid LCB desaturases. *P. patens* KO lines of this gene (originally designated *gko*) did not show any visible phenotype at normal growth conditions or after short-term cold stress treatment for 24 h.

When this desaturase was expressed heterologously in *Saccharomyces cerevisiae* strains *ole1* lacking the only fatty acid desaturase, accumulation of mono-unsaturated C24 and C26 hydroxy-FAs in ceramides was detected (done by Dr. Kirstin Feußner and Dr. Ellen Hornung, University of Göttingen, data not shown). The desaturase gene was therefore considered to be a sphingolipid fatty acid desaturase and the gene named *PpSFD* (*P. patens* sphingolipid fatty acid desaturase). The *P. patens* KO-lines were re-named *Ppsfd*, or short: *sfd*. In this work, *PpSFD* was analyzed in regards to peptide structure, relationship to other desaturases, and activity on lipid composition in *P. patens*.

#### 3.2.1. *PpSFD* is a bifunctional cytochrome-*b5* fusion protein related to front-end desaturases

In order to classify the putative sphingolipid FA desaturase *PpSFD*, an *in-silico* characterization at the peptide sequence level was done. The peptide sequence was retrieved from NCBI with the designation XP\_024359978. The protein is classified as a hypothetical protein in NCBI. The peptide is 469 amino acids (aa) long and encoded on the gene PHYPADRAFT\_171332 from the genomic region NW\_001865542.1. The gene is 1913 bp long without introns, the transcript measures 1410 bp. Other genes in the same genomic region are all considered hypothetical proteins. Two of these genes have estimated functions: XP\_001780766 is predicted to contain several DNA- and ubiquitin-interacting domains, XP\_001780786 has a predicted P-loop-NTPase (via NCBI conserved domain prediction tool (Marchler-Bauer, Derbyshire et al. 2014)). Another protein with high sequence identity to *PpSFD* (78.2 %) is present in *P. patens* designated PNR35346. This gene homologue was shown by Anna Beike (Beike 2013) to not be transcribed at any condition, classifying it as a pseudogene. The two proteins with the highest overall peptide similarity to *PpSFD* from other organisms are a hypothetical protein from the bryophyte *Marchantia polymorpha* subsp. *ruderalis* (OAE24732, 55.4 % peptide identity) and a hypothetical protein from the diatom *Thalassiosira pseudonana* (XP\_002290058, 44.0 % peptide identity).

Analysis of the PpSFD peptide sequence with the NCBI conserved domain prediction tool (Marchler-Bauer, Derbyshire et al. 2014) identified two domains. The first one is a cytochrome-*b5* domain near the N-terminus from aa 32-78, the second a fatty acid desaturase-like (FADS-like) domain from aa 189-439 (see Figure 3.7.). The FADS-like domain contains 3 conserved His-boxes at aa 197-204, 227-237, and 409-416. The third His-box contains a glutamine (Q) instead of a histidine (H) at the first position, which is typical for bi-functional fusion desaturases (Alonso, Garcia-Maroto et al. 2003).

To understand the relationship between PpSFD and other bi-functional fusion desaturases from *P. patens* and *A. thaliana*, a direct sequence comparison was performed. Using the online tools ClustalW (Thompson, Gibson et al. 2003) and ExpASY boxshade (Artimo, Jonnalagedda et al. 2012) PpSFD was matched against the sphingolipid LCB  $\Delta 8$  desaturases AtSLD1 (AAM64895) & AtSLD2 (OAP10850, both Chen (Chen, Markham et al. 2012)), the putative sphingolipid LCB desaturase PpSLD (XP\_024364920), as well as the front-end desaturases Pp $\Delta 5$ FADS (XP\_024396886, (Kaewsuwan, Cahoon et al. 2006)) and Pp $\Delta 6$ FADS (XP\_024379482, (Girke, Schmidt et al. 1998)). All desaturases contained a cytochrome-*b5* domain and a FADS-like domain (see Figure 3.7.). The comparison also showed that all 6 desaturases contained the conserved 3 His-boxes with a Q instead of an H at position 1 of the third His-box.

Furthermore, a phylogenetic tree was designed to compare PpSFD with desaturases from a variety of different organisms from vascular and non-vascular plants, microalgae, fungi and other eukaryotes (see Figure 3.7.). All matches found via NCBI's Blast tool (Johnson, Zaretskaya et al. 2008) were predicted to be bi-functional desaturases, but not for all proteins enzymatic activity was proven. The phylogenetic tree was calculated with Geneious 8.1.8 Tree Builder tool using pairwise alignment (global alignment), Jukes-Cantor genetic distance model and Neighbor-Joining tree build method. Gap open penalty was set to 12, gap extension penalty to 3 (see Figure 3.8.).

The closest to PpSFD related desaturases can be ordered into 4 groups. Highest sequence similarity within desaturases of known functions are  $\Delta 5$  front-end desaturases (Figure 3.8, blue background). These proteins were described in bryophytes (including *P. patens* itself), microalgae and some fungi, but not in vascular plants. Another group of front-end desaturases related to PpSFD are  $\Delta 6$ -desaturases, described in non-vascular plants and microalgae (Figure 3.8, red background). Both front-end desaturase groups are necessary for the synthesis of VLC-PUFAs, which are present in *P. patens* (see 3.1.1.). The third group of desaturases related to PpSFD with known function are the  $\Delta 8$ -desaturases which desaturate LCBs (Figure 3.8, yellow background). This is the only class of desaturases in this phylogenetic tree that includes enzymes found in vascular plants. The fourth group of desaturases, however, include only proteins with unverified or assumed function. These proteins have the closest relation to PpSFD of all desaturases tested (Figure 3.8, grey background). They originate from microalgae, fungi, non-vascular plants and choanoflagellates, but not vascular plants. PpSFD would be the first desaturase of this group to be analyzed. Even though PpSFD is considered to be a sphingolipid fatty acid desaturase, its sequence does not seem to be strongly related to known desaturases of the same function of higher plants. The desaturase AtADS2, which desaturates FAs in sphingolipids in *A. thaliana*, is not closely related at all to PpSFD, groups outside all other analyzed desaturases of the phylogenetic tree (see Figure 3.8., blue text). The relationship between AtADS2 and PpSFD is further analyzed in segment 3.4. of the results.

At_d8-SLD1	1	-----MAEETEKRYITNEDLKMHNKSGDL
At_d8-SLD2	1	-----MADQTKRYVTSGLKMKHNKPGDL
Pp_d8-SLD	1	-----MGPLAAEDELGSPQELKVDHLRSPSITSGELSRHNKFDL
Pp_d6-FADS	1	MVSSGGGLQQGSLEENIDVEHLASMPLLGDFVNVIIGSVRSWSFSGVQGLKRLTSRKRVSDFSVCMSSTEVQKNSNSQEAATVVLAEVVKPVRRRSRVSRKRSYLTETVSRHTTRPMD
Pp_d5-FADS	1	-----MAPHSADTAGLVPSEDLRLRTSNKSGPEQEQTLTKKYTLLEDVSRHNTPAD
Pp_SFD	1	-----MATSEAVRNHIKPGIVGRPNIVLPPISDFSTAS-KPTRL
consensus	1	.....
At_d8-SLD1	25	WIAIQGKVVNVSQDWIKTHPGGDTVILNLVQGDVTDAFIAFHPGTAWHHLDLHFTGYHIRDFQVSS-----EVSRYDYYRMAAEFRKLGLENK-----GHVTLMTLAFVA
At_d8-SLD2	25	WISIQGKVVYDSDWIKSHPGCEAAILNLACQDVTDAFIAVHPCTAWHHLKLLHNGYHVRDHHVS-----DVSRYDYYRMAAEFRKLRCLFDKK-----GHVTLMTLTCVQ
Pp_d8-SLD	44	WISIQGKVVNVTGWLKPKHPCGCEIPDLHLACQDVTDAFLAFHPGTAWHHLDPFLVCTLS-DYDVP-----LVAAEHRRLLRERFKAAGLTKNP-----LNVYALYACWVV
Pp_d6-FADS	121	WIVIKNKVYDSDFAAQHPGC-SVITTYFCRDGTDAPSSPHAGTAKKILQEFYIGDVDNVEPTP-----ELLNDYRDLRALFLREQLFRSS-----KLYYVFKLTNI
Pp_d5-FADS	51	WVIVIKGVYDVTSWIPNHPGC-SLHVVKAGQDSTQLFDSYHPLYVRKMLAKYICGLVPSAGDDKFKKATLEY-----ADAENEDFYLVVKQVRESYFKSNKINPQIHPHMIKSLPILG
Pp_SFD	38	LTKIHGKWDLTKEERHPCGFVALGLARCRDVTVMFESHHPFNRRKILDAILMKYIEDASDSKHLQTLQLHGVPESHFEWPSAFGEALKQVKEYEAGE--SKRRNISLREATKASPS
consensus	121	.....
At_d8-SLD1	123	AMFLGVLYGVLACTSVFAHQIAAALGLLWQOSAYIG---HDSGHYVIMSNSKSYNRFAQLLSGNCLIGISAWKKWTHNAHHLACNS---LDYDPLDQHIPVFAVSTKFFNSLTSR
At_d8-SLD2	123	VMLAAVLYGVLACTSIWAHLHSAVLLGLLWQOSAYVG---HDSGHYVITSTKPCNKLIQLLSGNCLIGISAWKKWTHNAHHLACNS---LDHOPDLQHIPVFAVSTKFFNSMTSR
Pp_d8-SLD	141	PLLALSVLGVLMSQSPFVHMLSAAMLGVVNWSQGVVG---HDGCHCCMFKNPNIDRFVAILVGDCLSGISAWKKRHNNAHHLACNS---IEYDPLDQYIPVFAVSTKFFNSLTSR
Pp_d6-FADS	218	SIFSSASIAIYCSKSYMAVLSACMMALCFQCCGWLSS---HDFLHNCVFETRWLNEVVGYLIGNSVVGFSICWKKRHNNAHHLAHPNCECDQLYQPIDDDIDTLPITAMSKDILATVENK
Pp_d5-FADS	165	GYPASYLLAFVWSSVLSLFFALWNGFFAAEVGVSI---QHDGNHCSYTKWRGFGYIMGALDLVGLASSFMWRQHVVGHSFTNVDN---YDPIRVDKDPVRRVATQPRQWY
Pp_SFD	156	RWVEIATLAVLFLSTPHGFFRGRDWRFLLLPLTANLGLVNI---DATFAFSDNWRWNALPYAFP--YFSSPFSWYHQNIGRHSYPPNVS---DRDPLVLDHYWMMKREHRDVKWLPFH
consensus	241	.....
At_d8-SLD1	233	FYDRKLTDFPVARFLVSYQHTFYFVPMCFGRINLFIQTELLLFSKREVPDRALN--FACILVFWNTWFFLLV--SCLPNWQERFFVFTSFTVTALQHQFTLNHFAADVVGPFPGSDWF
At_d8-SLD2	233	FYGRKLTDFPLARFLISYQHTFYFVPMCVGRINLFIQTELLLFSKRHVDRALN--IACILVFWNTWFFLLV--SFLPNWQERFFVFTSFAVTAHQVQFCLNHFAADVVGPFPGNDWF
Pp_d8-SLD	251	FYDRVMPFDGLARSLIAYQHTFYFPHMAVARVNLVQSLWLTSSKHVDRWLE--LGAGFFFLWFFLLV--SYLP-SSERFVFLVSVFVTCIQHVQFCLNHFSVYQCGEKSRAWV
Pp_d6-FADS	333	TFLE---VLCYQHLFFETALLFFARGSWLFWQSWRYTSTAKLAAVALL--EKTLILHYEWFELGQVWYLLPQKPLVNMVVFELMCGMLLGFVFLSHNGMVEVYN--KSKFEV
Pp_d5-FADS	275	HAYQHIYLAVYGTALKSIFLDDFLAYFTGSGIPVVKAKMTPLEFNIFQGRLL--LYAFYMPVLPVSVYGVHSGGTFLALYVASQLITGWMMLAFVQVAVHVVDDVAFPTPECGKVKGGWA
Pp_SFD	269	KNQSTWVFMFLFWWSVSVFGLTMTQDLWMLQTNLNEVVPMAISGSRRLRHILGRVLTIGIHAWPPFVWVETWGKAFASFLIPYLPFVFLFMNTQINHLPHPTTH-----AADADWY
consensus	361	.....
At_d8-SLD1	349	EQQAACHTDISCR-SYMDWFFGGLQFOLEHHLFFELPRCHLRKVSFVQVELCKKENLPYRSMSWNEANVLTINTLTKAAYOARDVANPVVKN--LVWEALNTHG
At_d8-SLD2	349	EQTACTLDISCR-SYMDWFFGGLQFOLEHHLFFELPRCHLRVTSFVVKELCKKENLPYRSLSWNEANVWTRTLKNAALOARDATNPVLKN--LLWEAVNTHG
Pp_d8-SLD	366	EQSARCTLNESTP-AYMDWFFGGLQFOIEHHLFFELPRHMLRKYKFKVRFPCCKEGLPYESVSWNEANRMIRTLRTAALOARDFTKAPALSESLLWEAVNSKG
Pp_d6-FADS	438	NAQIVTTRDIKAN-LFNDWFFGGLNRQIEHHLFFELPRHMLNKAAPQVEALCLKHLGVYEDVTIAAGTCKVLRKALKEVAEAEHQYAAASQQT-----
Pp_d5-FADS	393	AMQVATTDSPRSWFVGHVSGGLNNQIEHHLFFGVCHVHYPAIQIPEVKTCKEFDVVPVAYPTFWTALRAHFAHLKKVGLTEFLRDG-----
Pp_SFD	383	KHQVITAQDFGVGSKFCHLFGGLNLYQVI---LFFVNHCHLPQLQPIVAVLCEYDVGTTARCYVHAIQLHHQHSRLATKIEHAD-----
consensus	481	.....



Figure 3.7. Peptide sequence comparison between PpSFD (XP\_024359978) and the most closely related desaturases in *A. thaliana* and *P. patens* (PpD5-FADS, PpD6-FADS, PpD8-SLD, AtD8-SLD1 & AtD8-SLD2). Peptide sequences were obtained from NCBI. Sequences were aligned using online tools ClustalW & ExPASy boxshade. Black boxes indicate identical and grey boxes similar amino acid residues. Conserved domains are highlighted with green (Cytochrome *b5*) or purple (FADS-like domain) bars as predicted by NCBI Conserved Domain tool on the *PpSFD* peptide sequence. Three conserved His-Boxes are highlighted with red boxes and red bars.

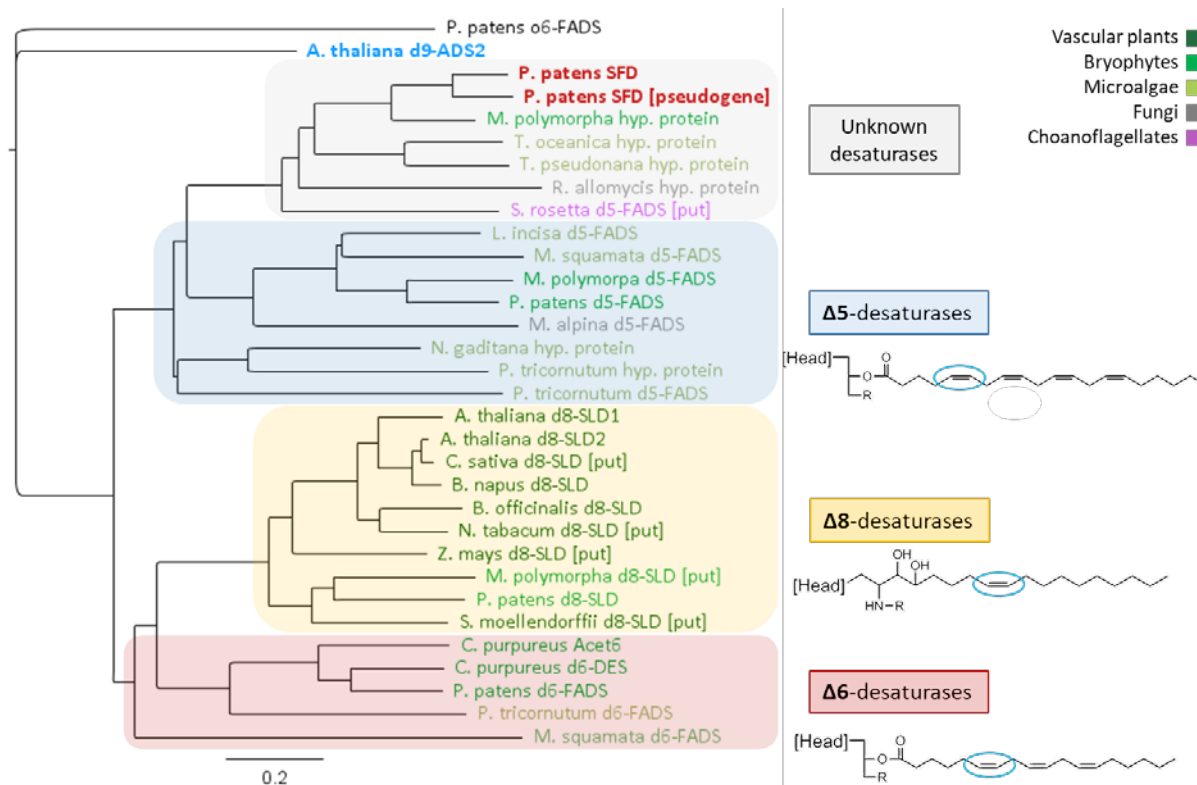


**Figure 3.8. Phylogeny of PpSFD compared with closely related desaturases from other organisms.** Compared were peptide sequences of 32 proteins. As outgroup, the putative *P. patens*  $\omega$ 6-desaturase was chosen. PpSFD and its homologue pseudogene are highlighted in red. The *A. thaliana*  $\omega$ 9-desaturase AtADS2 is highlighted in blue. Putative protein functions based on conserved sequence identity are marked with [put]. The tree was calculated with Geneious 8.1.8, Geneious Tree Builder tool, and built from pairwise alignment using global alignment, Jukes-Cantor genetic distance model and Neighbor-Joining tree build method. Gap open penalty was set to 12, gap extension penalty to 3. Protein identities can be found in Appendix 8.

### 3.2.2. *Ppsfd* knock-out lines do not contain any mono-unsaturated C24 fatty acids in sphingolipids and some phospholipids, except for phosphatidyl-serine

The three *PpSFD* KO-lines that were created by Anna Beike (Beike 2013) were analyzed at the lipid level to determine the exact activity of this desaturase on all lipids in *P. patens*. Anna Beike showed in her work that KO-lines of *PpSFD* are stable and did not produce *PpSFD* transcript (Beike 2013). For analyzing the mutant chemotype in this work a newly established lipidomics method was used (as described in 3.1.2.). This method is capable of covering over 700 lipid species in *P. patens* and is therefore well suited to observe effects of this mutation on all lipid classes in the moss. For analysis, wild type and *sfd* lines were grown in aerated liquid cultures (air containing 1 % CO<sub>2</sub>) for 7 days with growth conditions optimized for the formation of fast-growing protonema tissue, therefore yielding a high amount of biomass. During preliminary LC-MS analyses it was observed that all three KO-lines *sfd3*, *sfd10* and *sfd11* had similar general lipid composition (data not shown), so *sfd10* was used as mutant line for all further analyses (in the following referred to as *sfd* or *Ppsfd*).

Preliminary analysis of *S. cerevisiae ole1* lines transformed with *PpSFD* suggested that *PpSFD* is a desaturase that acts on FA moieties in sphingolipids (work done by Dr. Kristin Feußner and Dr. Ellen Hornung, University of Göttingen, data not shown). Therefore, the first class of lipids analyzed in *sfd* were the sphingolipids. In ceramides, the FA 24:1;1 is the second most abundant FA moiety found (mostly with the LCB 18:0;3), while its saturated variant 24:0;1 represents the most abundant one (see Figure 3.6.). In *sfd*, the amount of 24:1;1 and 24:1;0 is reduced drastically in comparison to wild type, almost down to detection limit (see Figure 3.9.). The saturated FAs 24:0;1 and 24:0;0, however, accumulate in *sfd* significantly. The same effect is also detectable for C26 FA moieties, but these species are present in much lower amounts to begin with (see Appendix 4). The effect of the mutation is not only detectable in ceramides, but also in glycosyl-ceramides, where overall amount of C24 FAs is much lower compared to ceramides. The by far most abundant GlcCer species 18:2;2/20:0;1, is not affected at all by the mutation. Nevertheless, the comparatively low amounts of 24:1;1 and 24:1;0 FA moieties are also drastically reduced in this lipid class, similar to ceramides (see Figure 3.9.). The FA 24:0;1 accumulates in this lipid class as well. *PpSFD* therefore has an influence on FA moieties of both sphingolipid classes in *P. patens*, but only on those with 24 or 26 carbons length.

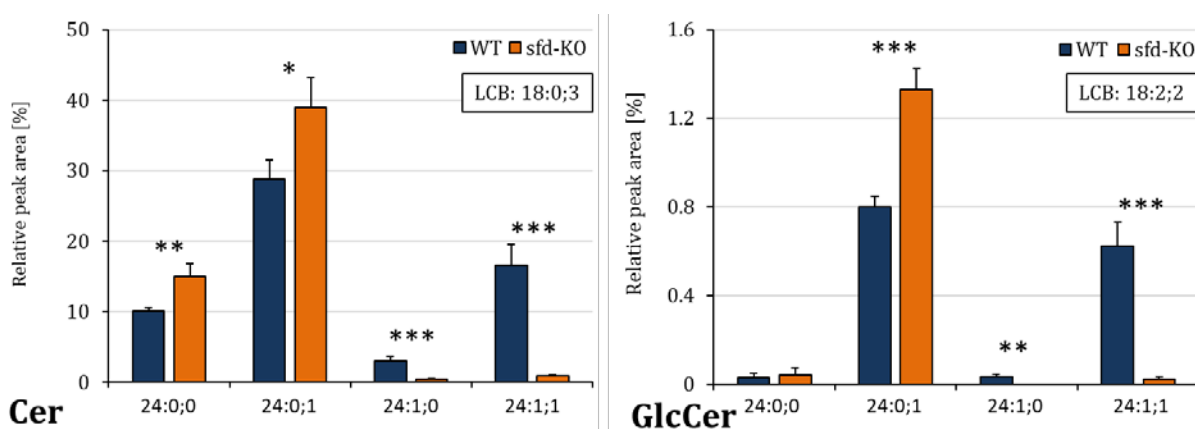


**Figure 3.9. Comparison of sphingolipids that contain C24-fatty acid moieties in *P. patens* wild type & *sfd*-KO line.** Subclasses include: Ceramides (Cer), glycosyl-ceramides (GlcCer). Moss cultures were started by inoculation with disrupted moss tissue and grown in aerated (1% CO<sub>2</sub>) liquid cultures for 7 days. Lipids were extracted from lyophilized moss material using a one-phase isopropanol/hexane/water extraction. Lipid species were characterized via MRM-based UPLC-QTrap-ESI-MS analysis. Only lipid species detected with a relative peak area of > 0.01 % were included in the dataset. Displayed are data for lipid species containing LCB 18:0;3 (ceramides) or LCB 18:2;2 (glycosyl-ceramides). Data represent mean values with standard deviations of 4 biological replicates. Asterisks represent results of student t-test performed for the difference in relative peak area between wild type & KO-line. \* =  $p < 0.05$ , \*\* =  $p < 0.01$ , \*\*\* =  $p < 0.001$ .

Since sphingolipids are not the only lipid class that contains 24:1 FA moieties, *sfd* was also analyzed for effects in some phospholipid classes. Phospholipids that contain 24:1 FAs in *P. patens* are PC, PE and PS (see Figure 3.2.). In PC and PE, the relative amount of 24:1-containing lipid species is strongly reduced (see Figure 3.10.). In wild type moss, these 24:1 lipid species make up combined less than 1 % of all lipid species in these lipid classes and are therefore far less abundant than compared with ceramides. PS, however, contains high relative amounts (up to 20 %) of desaturated C24 FAs in wild type (see Figure 3.2.). In *sfd*, 24:1 levels in PS are not affected (see Figure 3.10.). Drastic effects on lipid species not containing any C24 FAs were not observed in *sfd* lines for any lipid class.

Overall, it could be shown that *sfd* KO-lines have strongly reduced amounts of most lipid species that contain monounsaturated C24 FA moieties. This effect was most strongly seen in ceramides, where these FAs are most common in *P. patens*, but also in glycosylceramides, PC and PE. PS, which contains relatively high amounts of 24:1 compared to other phospholipids in *P. patens*, was not affected by the mutation.

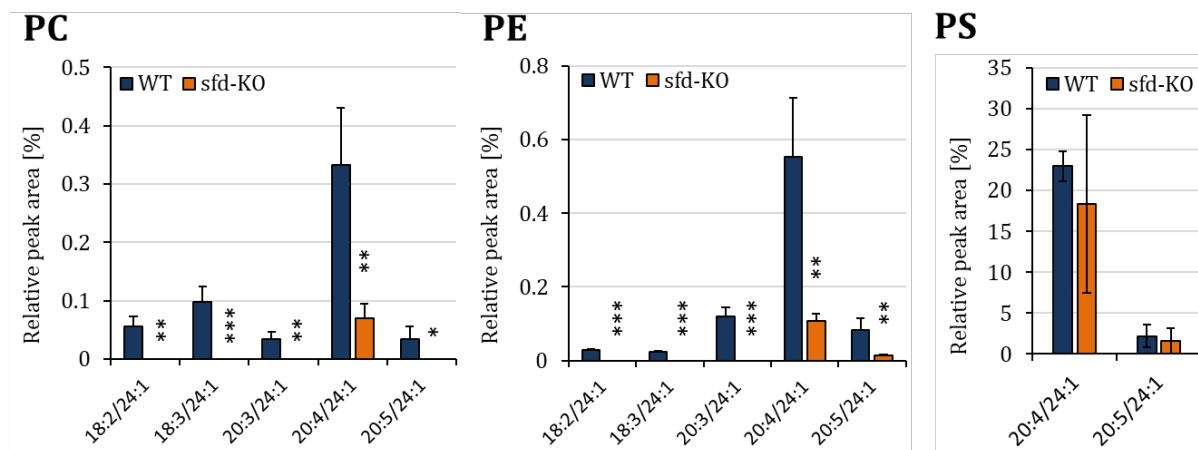


**Figure 3.10. Comparison of phospholipids that contain the fatty acid 24:1 in *P. patens* WT & *sfd*-KO line.** Subclasses include: Phosphatidyl-choline (PC), phosphatidyl-ethanolamine (PE), phosphatidyl-serine (PS). Moss cultures were started by inoculation with disrupted moss tissue and grown in aerated (1% CO<sub>2</sub>) liquid cultures for 7 days. Lipids were extracted from lyophilized moss material using a one-phase isopropanol/hexane/water extraction. Lipid species were characterized via MRM-based UPLC-QTrap-ESI-MS analysis. Only lipid species detected with a relative peak area of > 0.01 % were included in the dataset. PC, PE & PS lipid species containing the FA 24:1 are displayed. Data represent mean values with standard deviations of 4 biological replicates. Asterisk represent results of student t-test performed for the difference in relative peak area between wild type & KO-line. \* =  $p < 0.05$ , \*\* =  $p < 0.01$ , \*\*\* =  $p < 0.001$ .

### 3.3. Effects of cold stress on *P. patens* wild type and *Ppsfd*

Cold stress has severe effects on the lipid composition of membranes in all kinds of organisms. From studies about different plants (Buchanan 2015) it is known that cold stress adaptation of lipids include a higher degree of FA desaturation and the preference of shorter FAs over longer ones. This is done to maintain the fluidity of membranes at lower temperatures. In *A. thaliana*, desaturation of sphingolipids has been shown to be important to deal with cold stress, be it on the LCB or on the FA moiety of the lipid (Chen, Markham et al. 2012, Chen and Thelen 2013). The sphingolipid FA desaturase PpSFD in *P. patens* is upregulated at cold stress conditions (Beike 2013) which suggests a similar importance for dealing with cold stress as in *A. thaliana*. In order to analyze cold stress effects on lipid chemotype and phenotype in *P. patens* wild type and *Ppsfd*, an experiment was designed to apply such low temperature conditions on moss liquid cultures. Normally grown *P. patens* aerated glass tube liquid cultures (7 days at long-day conditions, 1 % CO<sub>2</sub>-containing air) were exposed to temperatures at about 4 °C by submerging the glass tubes in crushed ice for 24 h. The glass tube culture was then harvested and analyzed for its lipid

composition. Additionally, agar plate cultures of *P. patens* were grown at 6 °C and continuous light for 3 months and the effects on the phenotype were observed.

### 3.3.1. Cold stressed *P. patens* wild type significantly adjust FA composition of most glycerolipids, *sfd* does not

In general, it was observed that cold stress affects phospholipids, glycolipids and neutral glycerolipids differently, but not significantly on a single lipid species level (see Figure 3.11.). Lipid profiles of PC, MGDG and TAG (representative of phospholipids, glycolipids and neutral glycerolipids) show slight accumulation or decrease of some lipid species after cold stress, but most lipid species are not significantly different compared to wild type (see Figure 3.11.). It was assumed that stronger effects might only be visible for combined lipid species instead of single lipid species. Therefore, lipid species were summarized in three categories that divide a lipid class into two distinct fractions without overlap. These categories were based on: a) the length of fatty acids in the lipid species, b) the combined number of double bonds in the lipid species, and c) the presence of the FA 20:4 in the lipid species.

Regarding FA length, lipid species were divided into “Long” and “Very Long” lipids. “Long” lipids include those which contain only C16 and C18 FA moieties. “Very Long” lipids are lipids that contain at least one FA species with 20 or more carbons. Several phospholipid classes showed a significant decrease in length after cold stress. Accumulation of shorter FAs is significant in PC and PS, and similar trends can be observed for the remaining phospholipid classes except PG. PG shows a different trend than the rest of phospholipids, significantly accumulating longer FAs after cold stress. In neutral glycerolipids, a trend similar to phospholipids is observed. DAG and TAG accumulate shorter lipid species, which is more pronounced in DAG (see Appendix 5). Contrary to phospholipids and neutral glycerolipids, glycolipids show opposite effects. At cold stress, both MGDG and DGDG significantly accumulate lipid species with increased chain length (see Appendix 5). A direct comparison of FA length between PC and MGDG is shown in Figure 3.12.

Another way to divide lipids is by the number of double bonds in the whole lipid molecule. Phospholipids and DAG were ordered into lipids with 0-3 and lipids with 4-9 double bonds. Glycolipids were ordered into 0-6 and 7-9 double bonds. TAGs were ordered into 0-8 and 9-15 double bonds. When ordered into one group with few double bonds and one with many double bonds, phospholipids and neutral lipids again show similar trends (see Appendix 6). At cold stress, the number of double bonds in PC, PS and TAG goes significantly down, with similar trends observable in PI, PE, PA and DAG. In PG, number of double bonds does not appear to be affected by cold stress. In glycolipids, the effects of cold stress are again reversed compared to other lipid classes (see Appendix 6). In both MGDG and DGDG, the number of double bond goes significantly up after cold treatment. Double bond numbers in PC and MGDG are compared in Figure 3.13.

The content of arachidonic acid (20:4), which is present in high abundance in most lipid classes of *P. patens*, is also strongly affected by cold stress in most lipid classes (see Appendix 7). In PC, PI, PS and DAG, lipids that contain 20:4 significantly decrease after cold



stress. Similar trends are also visible for PE, PA and TAG, while PG is not affected. Similar to double bond amount and FA length, cold stress effects are the opposite for glycolipids. MGDG and DGDG lipid species containing 20:4 accumulate after cold stress (see Appendix 7). A comparison between 20:4-containing lipids in PC and MGDG is shown in Figure 3.14.

The significant changes in lipid composition observed after cold stress in wild type *P. patens* are not observable in *sfd* moss. Except for TAG (and PG regarding 20:4 content), no lipid class shows significant changes of lipid composition after cold stress regarding number of double bonds, FA length or the presence of 20:4. In TAG, however, changes in lipid composition become more pronounced after cold stress compared to normal growth regarding all 3 categories (see Appendix 5, 6, 7.).

Overall, cold stress in *P. patens* affects the composition of phospholipids & neutral lipids differently than glycolipids. While PC accumulate shorter lipids with less double bonds and lower 20:4 content, MGDG accumulate longer lipids with more double bonds and higher 20:4 content. In *sfd*, these effects are less pronounced and not significant, except for TAG.

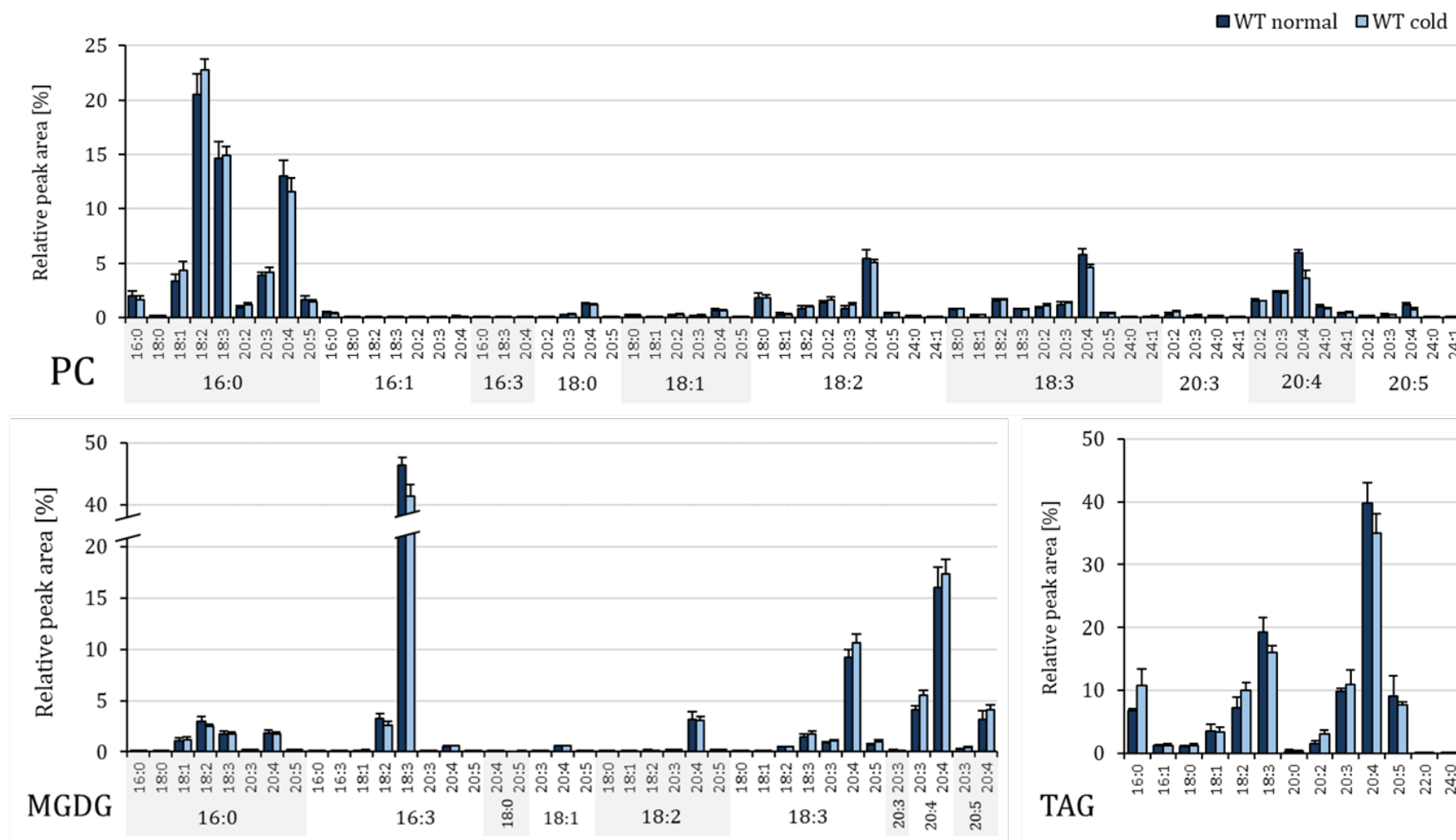


**Figure 3.11. Lipid composition changes in *P. patens* wild type after cold stress treatment.** Lipid subclasses include: Phosphatidyl-choline (PC), monogalactosyl-diacylglyceride (MGDG) and triacylglyceride (TAG). Moss cultures were started by inoculation with disrupted moss tissue and grown in aerated (1% CO<sub>2</sub>) liquid cultures for 7 days. Cold treated samples were grown 1 additional day at ~ 4 °C. Lipids were extracted from lyophilized moss material using a one-phase isopropanol/hexane/water extraction. Lipid species were characterized via MRM-based UPLC-QTrap-ESI-MS analysis. Only lipid species detected with a relative peak area of > 0.01 % were included in the dataset. Data represent mean values with standard deviations of 4 biological replicates.

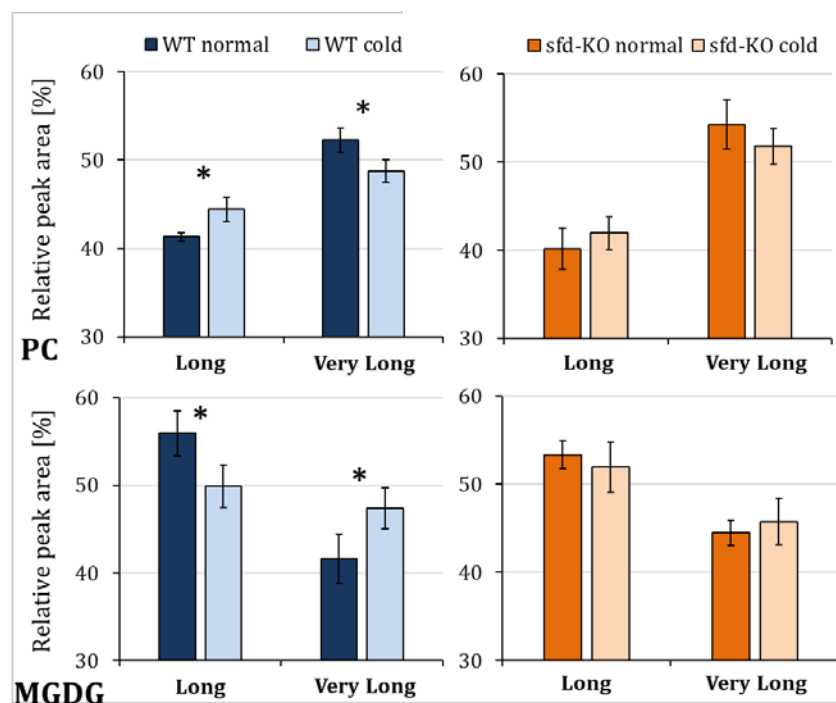


**Figure 3.12. Effects of cold stress on FAs chain length in combined lipid species of PC and MGDG.** Samples were taken from *P. patens* wild type & *sfd*-KO plants, grown at normal conditions or treated with cold stress. Moss cultures were started by inoculation with disrupted moss tissue and grown in aerated (1% CO<sub>2</sub>) liquid cultures for 7 days. Cold treated samples were grown 1 additional day at 4 °C. Lipids were extracted from lyophilized moss material using a one-phase isopropanol/hexane/water extraction. Lipid species were characterized via MRM-based UPLC-QTrap-ESI-MS analysis. Only lipid species detected with a relative peak area of > 0.01 % were included in the dataset. Data represent mean values with standard deviations of 4 biological replicates. “Long” lipids include all lipid species that contain only C16 & C18 fatty acids, but no C20 or longer fatty acids; “Very Long” lipids contain at least one C20-24 fatty acid moiety. Asterisks represent results of student *t*-test. \* = *p* < 0.05.

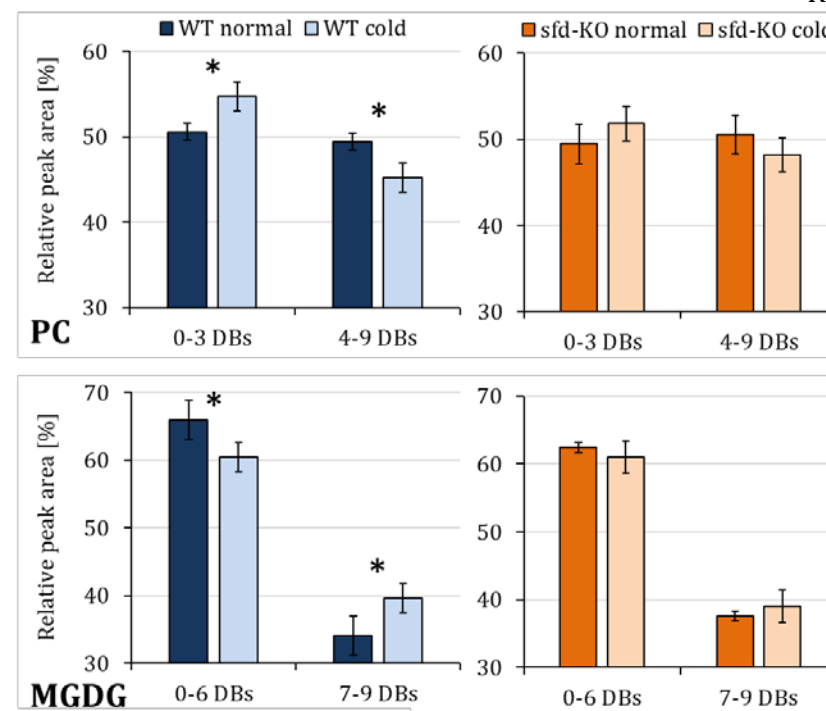


**Figure 3.13. Effects of cold stress on total number of double bonds in combined lipid species of PC and MGDG.** Samples were taken from *P. patens* wild type & *sfd*-KO plants, grown at normal conditions or treated with cold stress. Moss cultures were started by inoculation with disrupted moss tissue and grown in aerated (1% CO<sub>2</sub>) liquid cultures for 7 days. Cold treated samples were grown 1 additional day at 4 °C. Lipids were extracted from lyophilized moss material using a one-phase isopropanol/hexane/water extraction. Lipid species were characterized via MRM-based UPLC-QTrap-ESI-MS analysis. Only lipid species detected with a relative peak area of > 0.01 % were included in the dataset. Data represent mean values with standard deviations of 4 biological replicates. Asterisks represent results of student *t*-test. \* = *p* < 0.05.

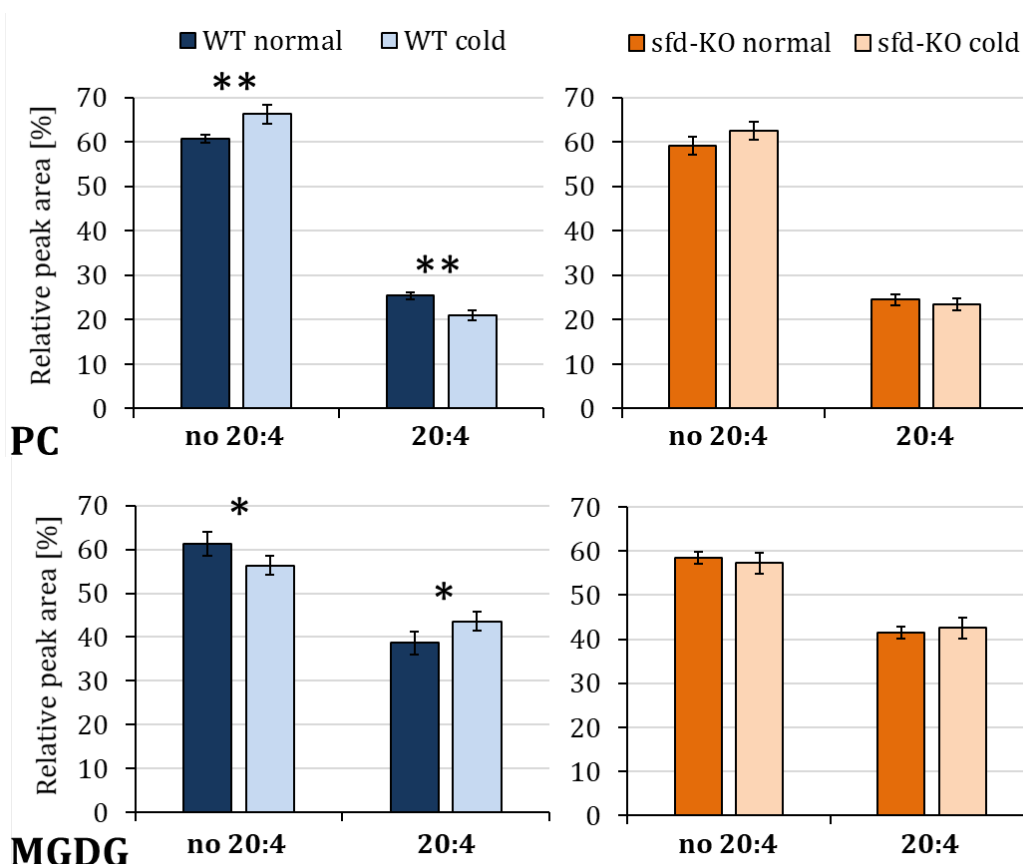


**Figure 3.14. Effects of cold stress on the amount of the FA 20:4 in combined lipid species of PC and MGDG.** Samples were taken from *P. patens* wild type & *sfd*-KO plants, grown at normal conditions or treated with cold stress. Moss cultures were started by inoculation with disrupted moss tissue and grown in aerated (1% CO<sub>2</sub>) liquid cultures for 7 days. Cold treated samples were grown 1 additional day at 4 °C. Lipids were extracted from lyophilized moss material using a one-phase isopropanol/hexane/water extraction. Lipid species were characterized via MRM-based UPLC-QTrap-ESI-MS analysis. Only lipid species detected with a relative peak area of > 0.01 % were included in the dataset. Data represent mean values with standard deviations of 4 biological replicates. Asterisks represent results of a student *t*-test. \* =  $p < 0.05$ , \*\* =  $p < 0.01$ .

### 3.3.2. Ceramides in *P. patens* accumulate more C24 FAs at cold stress while glycosyl-ceramides are not affected

It was already shown in 3.1.7. that sphingolipids in *P. patens* are dominated by relatively few lipid species. The most abundant ceramides contain FAs with 24 carbons and are hydroxylated. Upon cold stress, the amount of C24 FAs in ceramides accumulated, except for the FA 24:0;0. Ceramide species with other FAs and those that do not contain the predominant LCB 18:0;3 decrease in relative amount after cold stress treatment (see Appendix 8.). Glycosyl-ceramides are not significantly affected by cold stress treatment.

In *sfd*, ceramides do not contain mono-unsaturated FAs, but instead elevated levels of saturated C24 FAs (see 3.2.2.). At cold stress, the FA 24:0;1 accumulates even more compared to unstressed moss. Similar to wild type, the amount of 24:0;0 goes down after

cold stress, but to a smaller degree (see Figure 3.15.). Glycosyl-ceramides are not affected by cold stress in *sfd* as well (see Appendix 8).

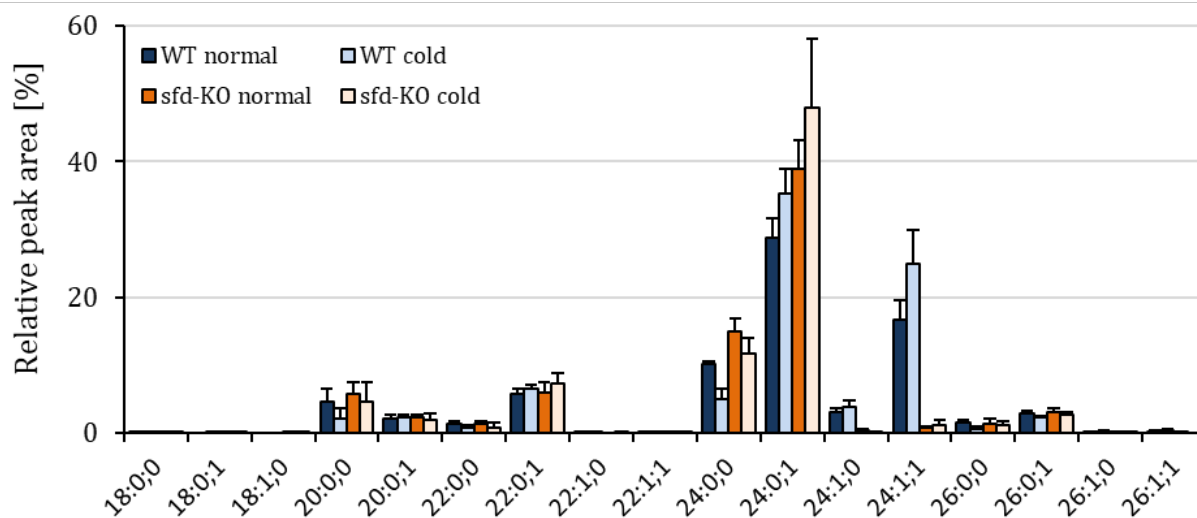


**Figure 3.15. Ceramide composition changes in *P. patens* wild type & *sfd-KO* after cold stress treatment.** Only ceramides with the LCB 18:0;3 are depicted. Moss cultures were started by inoculation with disrupted moss tissue and grown in aerated (1% CO<sub>2</sub>) liquid cultures for 7 days. Cold treated samples were grown 1 additional day at 4 °C. Lipids were extracted from lyophilized moss material using a one-phase isopropanol/hexane/water extraction. Lipid species were characterized via MRM-based UPLC-QTrap-ESI-MS analysis. Only lipid species detected with a relative peak area of > 0.01 % were included in the dataset. Data represent mean values with standard deviations of 4 biological replicates.

### 3.3.3. Total amount of 5 major lipid groups is not affected in cold stressed *P. patens* wild type, but in *sfd*

All measured 19 lipid classes can be ordered into 5 major groups (see Table 3.1.): sphingolipids, phospholipids, glycolipids, neutral lipids, and sterol lipids. The different lipid classes in these groups were detected at varying signal intensities. This is related to the overall amount of these lipids, but signal intensity is also affected by how well the different molecules ionize in the LC-MS measurements. Therefore, it is not possible to consider the lipid class with the highest detected signal intensity to be the one with the highest abundance. For the purpose of relative comparison, however, measured peak areas of lipid classes can be combined to observe the relative changes happening to the 5 major lipid groups in *P. patens*. To observe effects on the 5 lipid groups at cold stress, the total peak area of each lipid class within these groups were combined and compared between wild type and *sfd*.

In wild type *P. patens*, cold stress does not cause significant changes to the total amount of the combined lipid groups. There are however significant changes detectable between cold-stressed wild type and cold-stressed *sfd*. Phospholipids and sterol lipids significantly

decrease in *sfd* compared to wild type at cold stress, while glycolipids and neutral lipids accumulate (see Figure 3.16.).

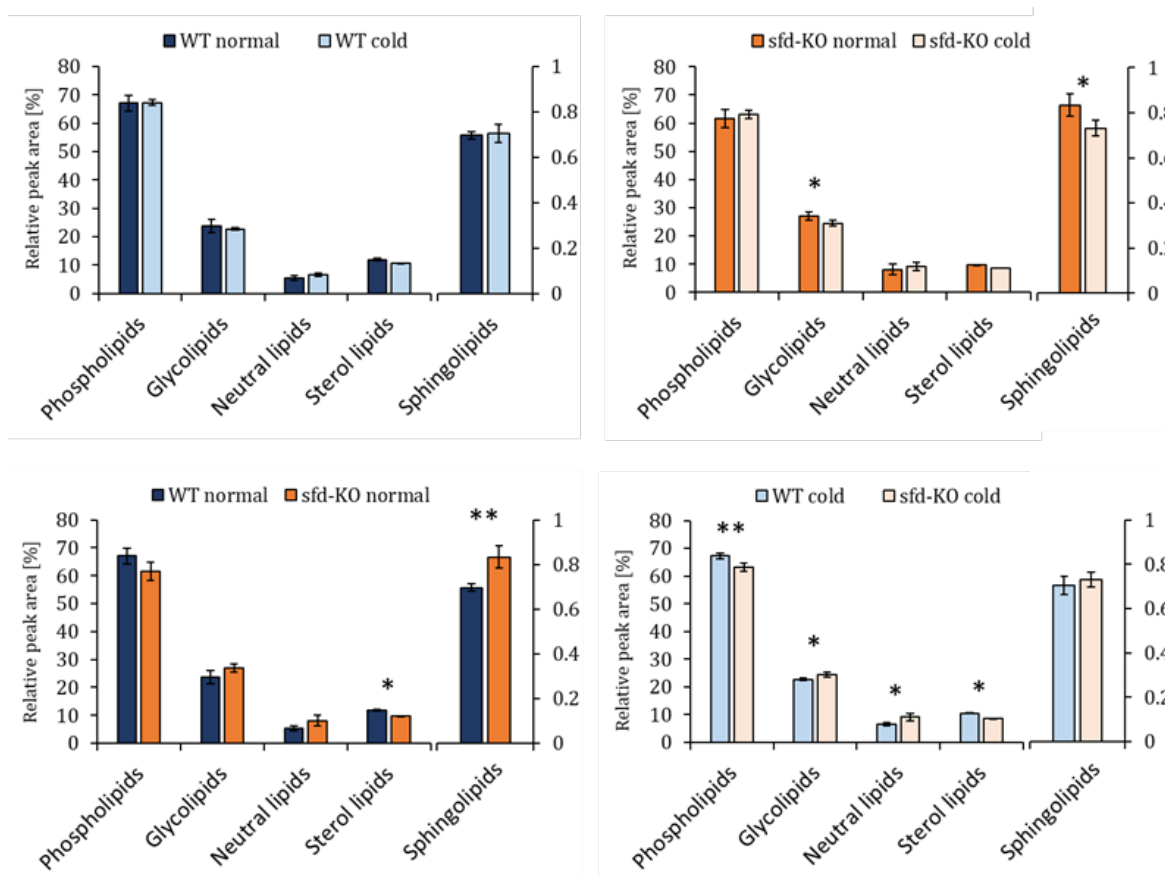


**Figure 3.16. Relative peak area of combined detected lipid species in *P. patens* wild type & *sfd-KO* at normal & cold stress conditions ordered into 5 major lipid groups.** Each lipid group contains the combined total peak area of all included lipid classes of that group (see Table 3.1.). Samples were taken from *P. patens* wild type & *sfd-KO* plants, grown at normal conditions or treated with cold stress. Moss cultures were started by inoculation with disrupted moss tissue and grown in aerated (1% CO<sub>2</sub>) liquid cultures for 7 days. Cold treated samples were grown 1 additional day at 4 °C. Lipids were extracted from lyophilized moss material using a one-phase isopropanol/hexane/water extraction. Lipid species were characterized via MRM-based UPLC-QTrap-ESI-MS analysis. Only lipid species detected with a relative peak area of > 0.01 % were included in the dataset. Data represent mean values with standard deviations of 4 biological replicates. Asterisks represent results of student *t*-test performed for the difference in combined relative peak area. \* =  $p < 0.05$ , \*\* =  $p < 0.01$ .

Neutral lipids accumulate significantly between cold stressed wild type and cold stress *sfd*. When looking only at total TAG amount, *sfd* contains more than double the relative amount compared to wild type, both at cold stress and normal conditions (see Figure 3.17.).

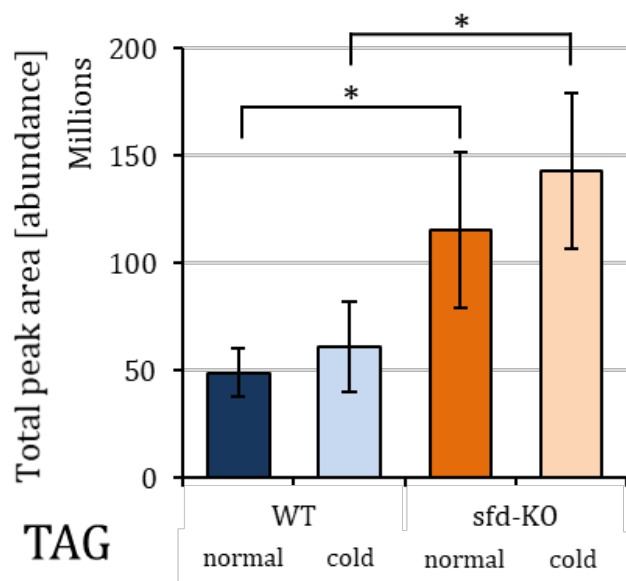


**Figure 3.17. Total peak area of all detected TAG lipid species in *P. patens* wild type & *sfd*-KO at normal & cold stress conditions.** Samples were taken from *P. patens* wild type & *sfd*-KO plants, grown at normal conditions or treated with cold stress. Moss cultures were started by inoculation with disrupted moss tissue and grown in aerated (1% CO<sub>2</sub>) liquid cultures for 7 days. Cold treated samples were grown 1 additional day at 4 °C. Lipids were extracted from lyophilized moss material using a one-phase isopropanol/hexane/water extraction. Lipid species were characterized via MRM-based UPLC-QTrap-ESI-MS analysis. Only lipid species detected with a relative peak area of > 0.01 % were included in the dataset. Data represent mean values with standard deviations of 4 biological replicates. Asterisks represent results of student *t*-test performed for the difference in relative peak area between wild type & KO-line. \* = *p* < 0.05.

### 3.3.4. Long time exposure to cold stress and continuous light shows enhanced chlorophyll degradation of *Ppsfd*

Anna Beike tested cold stress conditions on *sfd* plate cultures (Beike 2013), but under the tested conditions (4 °C, 4 days, 16 h light/8 h dark cycle) no difference was detected between wild type and *sfd*. Exposure of moss cultures to cold stress for longer time periods was not analyzed in that study. Therefore, *P. patens* wild type and 3 *sfd* KO-lines were grown for a prolonged time (3 months) under continuous light and low temperature (6 °C) for phenotype analysis. As a control, the same lines were grown similarly, but at normal temperature (24 °C). Additionally, 2 lines of the FA-elongase KO-mutant *elo* (PSE1, (Zank, Zähringer et al. 2002)), which is necessary for the synthesis of the FA 20:4, were analyzed as well to verify if the presence of the FA 20:4 has an impact on growth in *P. patens*. Chemotypes of all KO-lines were also verified via LC-MS analysis (data not shown).

At normal temperature, plate cultures of wild type and *sfd* grown at gametophore inducing conditions (without tartrate) look similar for all lines. Gametophores develop normally, tissue remains green and no signs of chlorotic or dried out tissue was detected (see Appendix 8).

When grown at medium containing tartrate (causing *P. patens* cultures to grow predominantly as protonema), wild type and *sfd* moss cultures show browning of tissues after 3 months of growth (see Figures 3.18. & 3.19.). The moss colonies form sponge-like structures which seem to dry out, especially when compared to gametophore-induced cultures (Appendix 9 & Appendix 10). At normal growth conditions, tissue of *sfd* lines appears to dry out stronger compared to wild type. The mutant lines have overall browner colonies and some cultures show a straw-like coloration of protonema tissue. The intensity of this phenotype is however not consistent for all plate cultures, some *sfd* colonies appear to be less dehydrated than others, even when from the same line. Lines *sfd10* and *sfd11* appear to show the most drying of the *PpSFD* KO-lines at normal temperature (see Figure 3.18.).

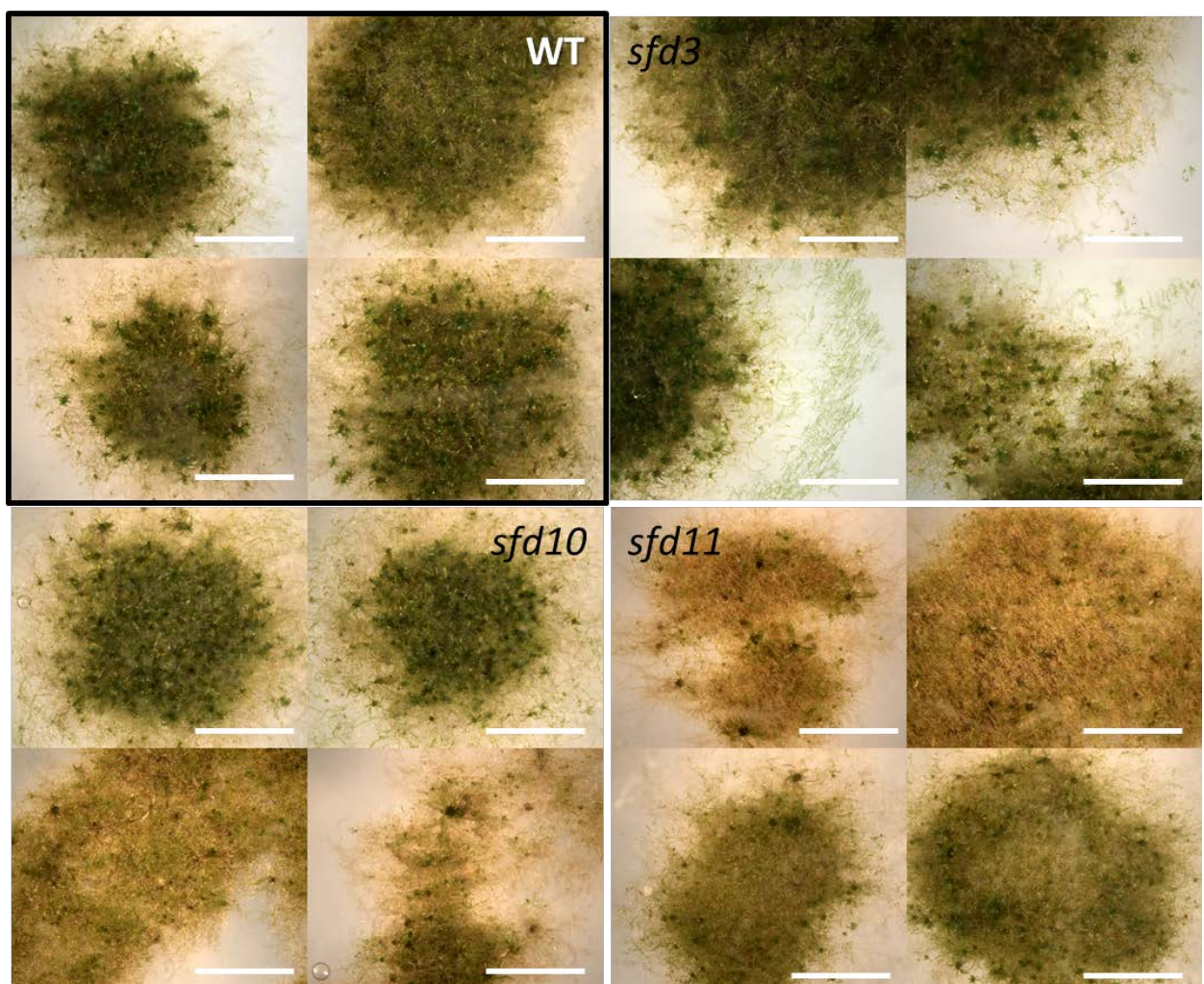


**Figure 3.18. Moss plate cultures at normal temperature (24 °C) and protonema-inducing growth conditions (with tartrate).** *P. patens* strains used are wild type (WT) and *PpSFD* KO-lines *sfd3*, *sfd10* and *sfd11*. Agar plate cultures were grown for 3 months at continuous light. Pictures were taken from two independent plate cultures for each strain. Scale bar = 0.5 cm

Cold-stressed (6 °C) wild type plate cultures with tartrate look overall more healthy than those grown at room temperature, generally being greener and developing larger gametophytes (see Figure 3.19.). The *sfd* KO-lines are again drier and show stronger



browning of tissue and straw-like colorations compared to wild type. Lines *sfd3* and *sfd11* appear to be stronger affected by the growth conditions than *sfd10*.

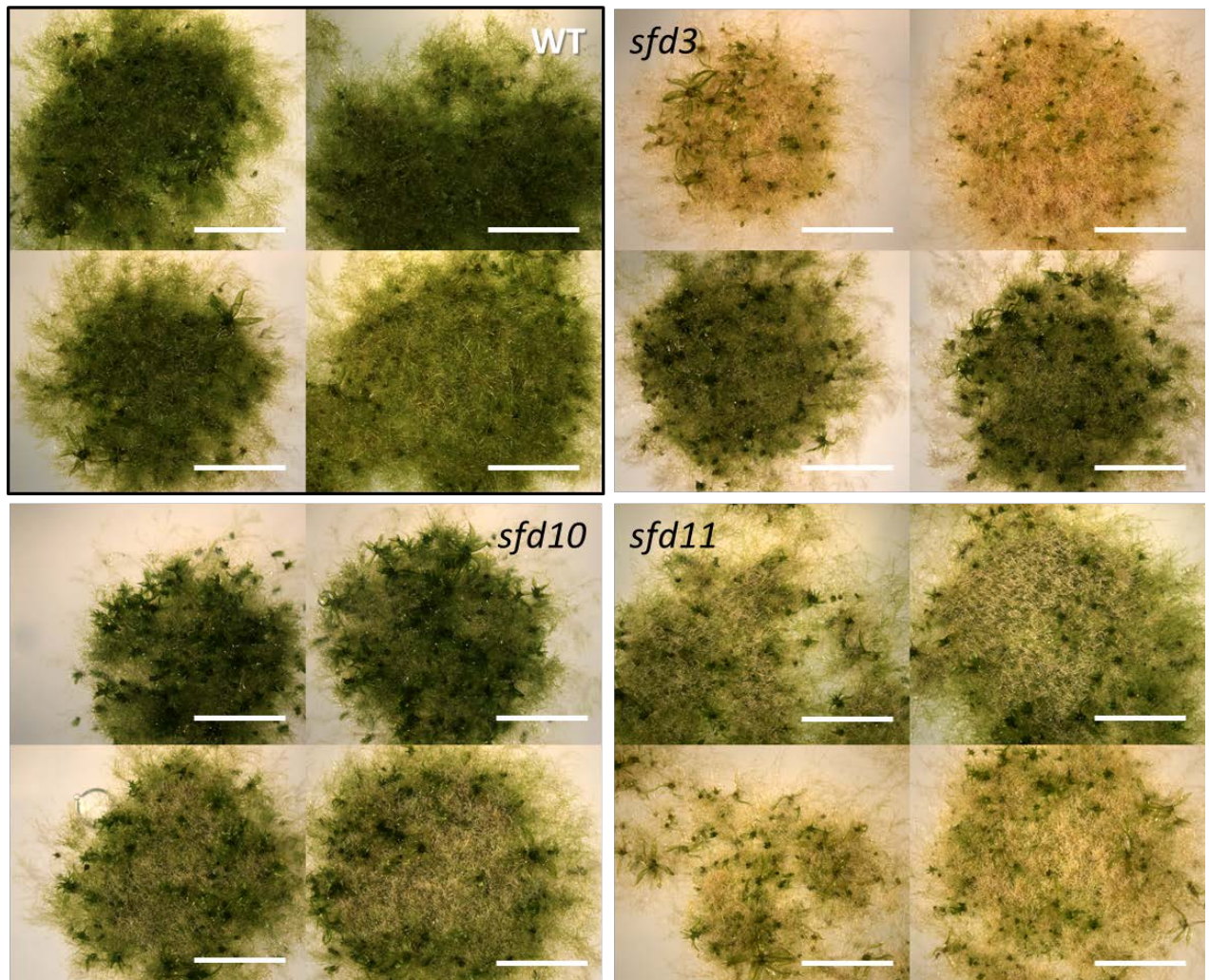


**Figure 3.19. Moss plate cultures at cold stress temperature (6°C) and protonema-inducing growth conditions (with tartrate).** *P. patens* strains used are wild type (WT) and *PpSFD* KO-lines *sfd3*, *sfd10* and *sfd11*. Agar plate cultures were grown for 3 months at continuous light. Pictures were taken from two independent plate cultures for each strain. Scale bar = 0.5 cm

In gametophore-inducing growth conditions (without tartrate) moss cultures look overall healthier than those with tartrate. All lines form colonies with large gametophores and no visible sponge-like tissue. At normal temperatures, wild type and *sfd* KO-lines are visually indistinguishable (see Appendix 9). At cold stress, some *sfd* show a slight brown coloration, but overall tissue formation seems to be similar to wild type (see Appendix 10).

KO lines of *PpELO* look mostly similar to wild type, be it without tartrate (Appendix 11) or with tartrate (Appendix 12). The line *elo35* shows slightly more browning of tissue when grown at cold stress without tartrate compared to wild type. Both *elo35* and *elo131* produced a lot more protonema on medium with tartrate compared to wild type, forming dome-like colonies.

To verify the observed phenotypes, moss tissue from tartrate-containing plate cultures was furthermore scraped off the plate cultures, lyophilized and analyzed for its chlorophyll content. Chlorophyll was extracted using an acetic acetate/acetone mixture and the light absorption was measured at 646 and 664 nm (see Figure 3.20.).

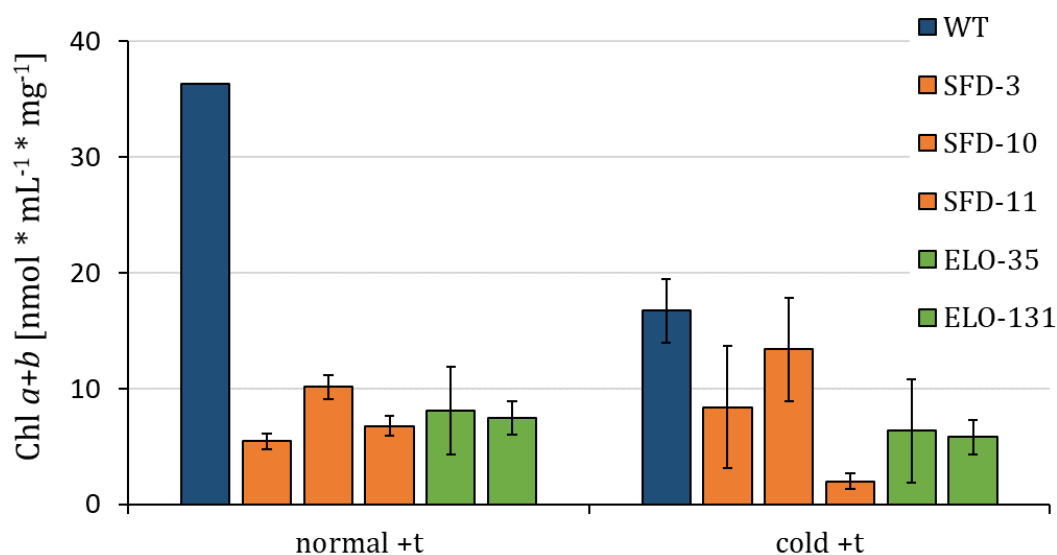


**Figure 3.20. Chlorophyll content of normal grown (24°C) and cold stressed (6°C) of *P. patens* wild type and KO-lines from protonema-inducing growth conditions (with tartrate).** *P. patens* strains used are wild type (WT), *PpSFD* KO-lines *sfd3*, *sfd10*, *sfd11*, and *PpELO* KO-lines *elo35* & *elo131*. Agar plate cultures were grown for 3 months at continuous light. Chlorophyll was extracted from lyophilized moss tissue with acetic acetate/acetone. Absorption of wavelengths 646 & 664 nm was measured with a photometer. Data represent average and standard deviations of 2 extractions except for normally grown wild type (1 extraction) for a single experiment.

At normal temperatures, protonema-induced plants of wild type *P. patens* have a much higher chlorophyll content compared to *sfd* and *elo* KO-lines. At cold stress conditions wild type contains less chlorophyll than at normal temperatures. On average, both *sfd* and *elo* lines have still less chlorophyll content than wild type, even though not by much. Cold stress in general does not have a strong impact on the chlorophyll content of *sfd* and *elo* lines, which remains equally low for both conditions. Wild type, however, reduces its chlorophyll content at cold stress.

For gametophore-induced plate cultures, it was not possible to harvest sufficient amounts of plant material for chlorophyll analysis.

### 3.4. Complementation of *A. thaliana ads2.1* KO-mutant with *PpSFD*

AtADS2 (Acyl-CoA desaturase-like 2) is a mono-functional desaturase that introduces double bonds in FAs that are bound to sphingolipids in *A. thaliana* (Smith, Dauk et al. 2013). The KO-mutant line *ads2.1* was described to be sensitive to cold stress conditions (Chen and Thelen 2013). When grown at 6 °C and continuous light for extended periods (up to 6 months), *ads2* KO-lines developed much slower, built less biomass and were incapable of producing functional flowers. Sphingolipids and some phospholipid classes (PC, PE, and PS) were affected by the mutation and did not contain desaturated FAs with 24 or 26 carbons length. Since AtADS2 and PpSFD seem to catalyze very similar reactions (introducing double bonds into C24-26 FA moieties in sphingolipids and phospholipids) it was considered if PpSFD could substitute for AtADS2 in *A. thaliana*. PpSFD was heterologously expressed in *ads2.1* to observe if the moss enzyme can fulfill the same function as AtADS2 in *A. thaliana*.

The *A. thaliana* KO-line *ads2.1* was transformed via *Agrobacterium tumefaciens* mediated transformation using two different plasmid constructs. Both constructs contained the 35S promoter from the cauliflower-mosaic-virus (CaMV-35S) which acts as an overexpression promoter in plants. One of the constructs contained the gene for AtADS2, the other one PpSFD. Transformation for both types of constructs was performed successfully.

#### 3.4.1. Establishment of a rapid method for identifying transformed *A. thaliana* lines by chemotype analysis via LC-MS

Since *Agrobacterium*-mediated gene transfer was used for transformation resulting in random integration of the genes, it was expected that the expression levels could be drastically different from line to line. The ultimate quality that was looked for in good transformation lines was the ability of producing the desired metabolic product of the enzyme, not just high expression levels of the gene. Since in *ads2* levels of monounsaturated C24 FAs are virtually absent, any transformation line with higher relative amounts of these compounds could be considered functional. To screen these high-performing transformation lines with as little effort and time as possible, a new rapid screening method for chemotype identification was developed.

The method used is in essence based on the same method used for lipidomic analysis (see 3.1.), but adjusted for high throughput rather than accuracy. Plant material was harvested from T1 transformation lines that were grown for seed harvest under normal conditions. Of these plants (whose seeds were later collected as separate lines), one leaf was plucked after about 1 month of growth. Lipids were then extracted from the whole leaf (not lyophilized) via the same isopropanol/hexane/water based extraction described in 3.1.2. without weighing or tissue disruption of the plant material. This ensured that extraction could be performed rapidly. The extracts were then analyzed for ceramides and glycosyl-

ceramides with a reduced set of MRMs, only including major sphingolipid species known from *A. thaliana*. For data analysis, the relative peak height of the compounds of interest (in this case Cer(18:1;3/24:1;1)) were compared to similar compounds which should not directly be affected by the mutation (in this case Cer(18:1;3/16:0;1)). This comparison ensured that the total amount of the target lipid in question was actually high in the transformation line compared to the knock-out lines, regardless of varying extraction efficiency caused by the use of whole leaves. A schematic representation of the workflow for this method is shown in Figure 3.21.

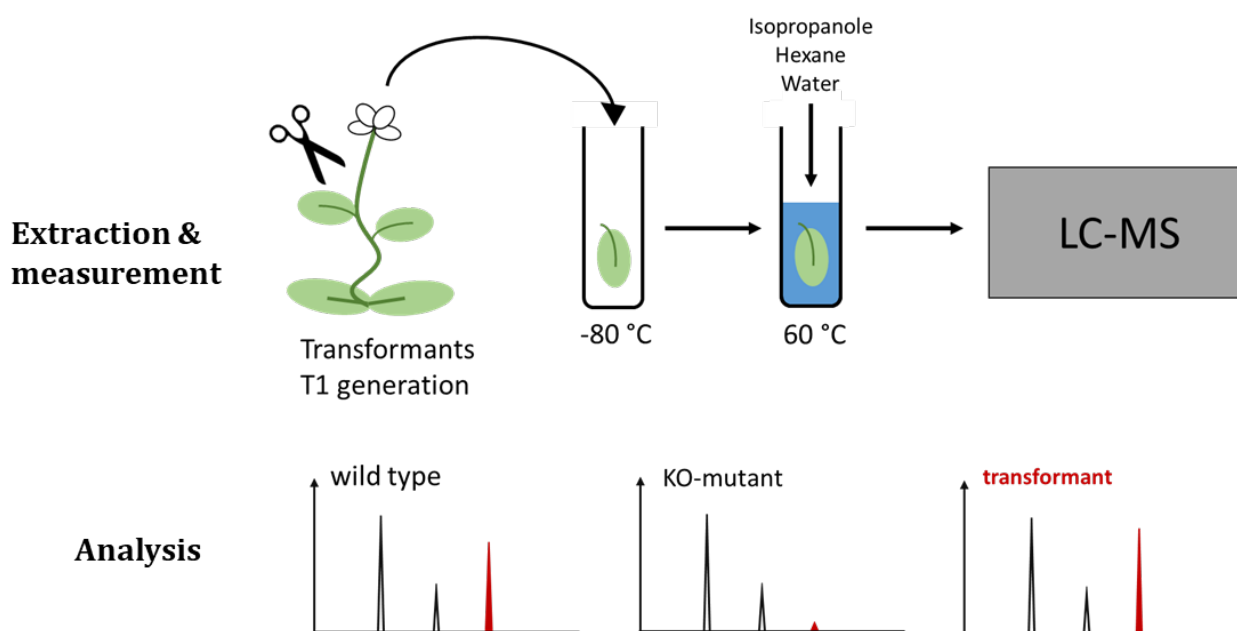


**Figure 3.21. Scheme for rapid chemotype analysis of transformation lines.**

By using this “quick and dirty” approach on the *AtADS2* and *PpSFD* complementation lines several high-producing lines were recovered for each construct. For *ads2.1/35S::AtADS2*, three lines were chosen for analysis (F01, F03, F09). For *ads2.1/35S::PpSFD*, also three lines were chosen (C05, C10, C11). These lines were grown together with *A. thaliana* wild type and *ads2.1* both at normal and cold stress conditions. Normal growth conditions include: 24 °C, 16 h light/8 h dark cycle. Cold stress conditions include: 24 °C, 16 h light/8 h dark cycle for 15 days, than transfer to 6 °C, continuous light for 59 days. Cold stressed plants from wild type, *ads2.1* and lines F03, F09, C05 and C11 were harvested at the end of the experiment (all plant parts above soil levels) and analyzed for transcript levels (see 3.4.2.), phenotype (3.4.3.) and lipid composition (3.4.4.). Lines F01 and C10 were not analyzed further due to time restrictions.

### 3.4.2. Lines of *ads2.1* complemented with *PpSFD* have strongly elevated transcript levels of *PpSFD*

It could be shown via qRT-PCR that the genes *AtADS2* in F03 & F09 as well as *PpSFD* in C05 & C11 are transcribed in high amounts. Fold over reference values of gene transcripts against actin transcripts (as reference gene) show 5-fold higher transcript levels of *AtADS2* in F03 and 15-fold higher transcript levels of *AtADS2* in F09 compared to wild type *A. thaliana* plants. In C05 & C11, *AtADS2* transcript levels remained very low, comparable to the KO mutant *ads2.1*. In wild type, *ads2.1*, F03 and F09, no significant transcript levels of the moss gene *PpSFD* were detected. In C05 and C11, transcript levels of *PpSFD* were detected in high amounts, comparable to transcript levels of *AtADS2* in F03 (see Figure 3.22.).

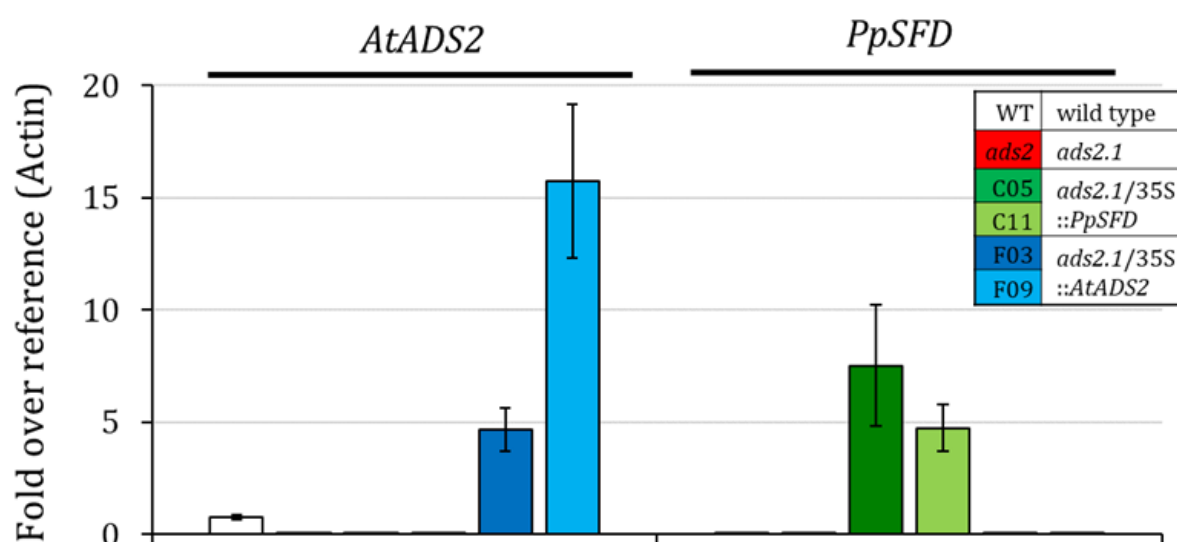


**Figure 3.22. Relative transcript levels of genes *AtADS2* & *PpSFD* in different cold-stressed *A. thaliana* complementation lines.** Complementation lines were transformed with *AtADS2* (lines F03 & F09) or *PpSFD* (lines C05 & C11) under control of the CaMV 35S promoter via agrobacterium-mediated transformation of the *A. thaliana* *ADS2*-KO line *ads2.1*. Measurements were done via RT-PCR. Shown are fold over transcript levels against the reference gene (actin). Plants were grown at long-day conditions (16 h day/8 h night, 24 °C) for 15 days before being transferred to cold stress conditions (continuous light, 6 °C) for 59 days. Bar diagrams represent mean values with standard deviations for either 3 (wild type, *ads2.1*, C05) or 4 (C11, F03, F09) biological replicates.

Overall, both the homologous complementation (with *AtADS2*) and the heterologous complementation (with *PpSFD*) in *Atads2.1* was successful. Transcript levels of all tested lines were 5 – 15 times higher compared to wild type *AtADS2* transcript.

### 3.4.3. Transgenic *ads2.1/35S::PpSFD* lines show recovered phenotype at cold stress growth, similar to *ads2.1/35S::AtADS2*

When grown at normal conditions (24 °C, 16 h light/8 h dark cycle), all *A. thaliana* lines (wild type, *ads2.1*, F03, F09, C05, C11) grew similar without differences in phenotype (data not shown). At cold stress conditions (6 °C, continuous light), *ads2.1* showed a strong phenotype compared to wild type *A. thaliana* plants. Wild type plants grew steadily during the experiment, developing normal-sized leaves and deep green color. Plants of *ads2.1* showed a severe phenotype after the transfer to cold stress conditions. They remain roughly the size they had before the transfer to cold stress, with only very small new dark green leaves forming under these conditions. These newer leaves remain in size smaller than the first leaf pairs, which dried out and lost color completely after the cold treatment. The weight of *ads2.1* plants after cold stress of 59 days is at least 5-fold lower than wild type plants after similar growth conditions (see Figure 3.23).

All analyzed complementation lines grew significantly better at cold stress than *ads2.1*. All lines developed dark green leaves with normal leaf sizes. Overall plants size and weight, however, does not reach the level of wild type plants. C05 plants have about 40 % weight of wild type plants, C11, F03 and F09 about 60 %. All complementation lines have significantly higher plant weight compared to *ads2.1* at cold stress conditions. There was no visual difference observed between *PpSFD* and *AtADS2* complementation lines (see Figure 3.23.). The cold stress growth experiment showed that *PpSFD* can complement the cold sensitive phenotype of *ads2.1* just as well as the homologue enzyme in *A. thaliana*, *AtADS2*.

### 3.4.4. Levels of unsaturated C24 FA moieties in cold stressed complementation lines is similar to cold stressed *A. thaliana* wild type

Complementation lines and control lines were analyzed for lipid composition regarding the presence of monounsaturated C24 and C26 FAs using the lipidomic method described in 3.1. Analyzed lipid classes include the sphingolipid classes Cer and GlcCer, as well as the phospholipid classes PC, PE and PS, which are known to contain C24 and C26 FAs in *A. thaliana*. In our measurement, sphingolipids in cold-stressed *A. thaliana* were dominated by the LCB 18:1;3 and the FA 24:1;1, making up about 60 % of both ceramides and glycosyl-ceramides. Unsaturated FAs were also found in minor amounts in C26 FAs. The sphingolipid class of GIPC, which is present in *A. thaliana* (Markham and Jaworski 2007), was not analyzed in this work, as the analysis of ceramides and glycosyl-ceramides was deemed sufficient for describing sphingolipids.

In *ads2.1*, relative amounts of monounsaturated FAs in sphingolipids are strongly reduced, down to 1.3 % of the wild type amount. In contrast to that, the saturated FA moieties are present in much higher amounts, up to 60 % of 24:0;1 in glycosyl-ceramides of cold stressed *ads2.1* (see Figure 3.24.). Sphingolipid composition in all complementation lines was similar to wild type plants.

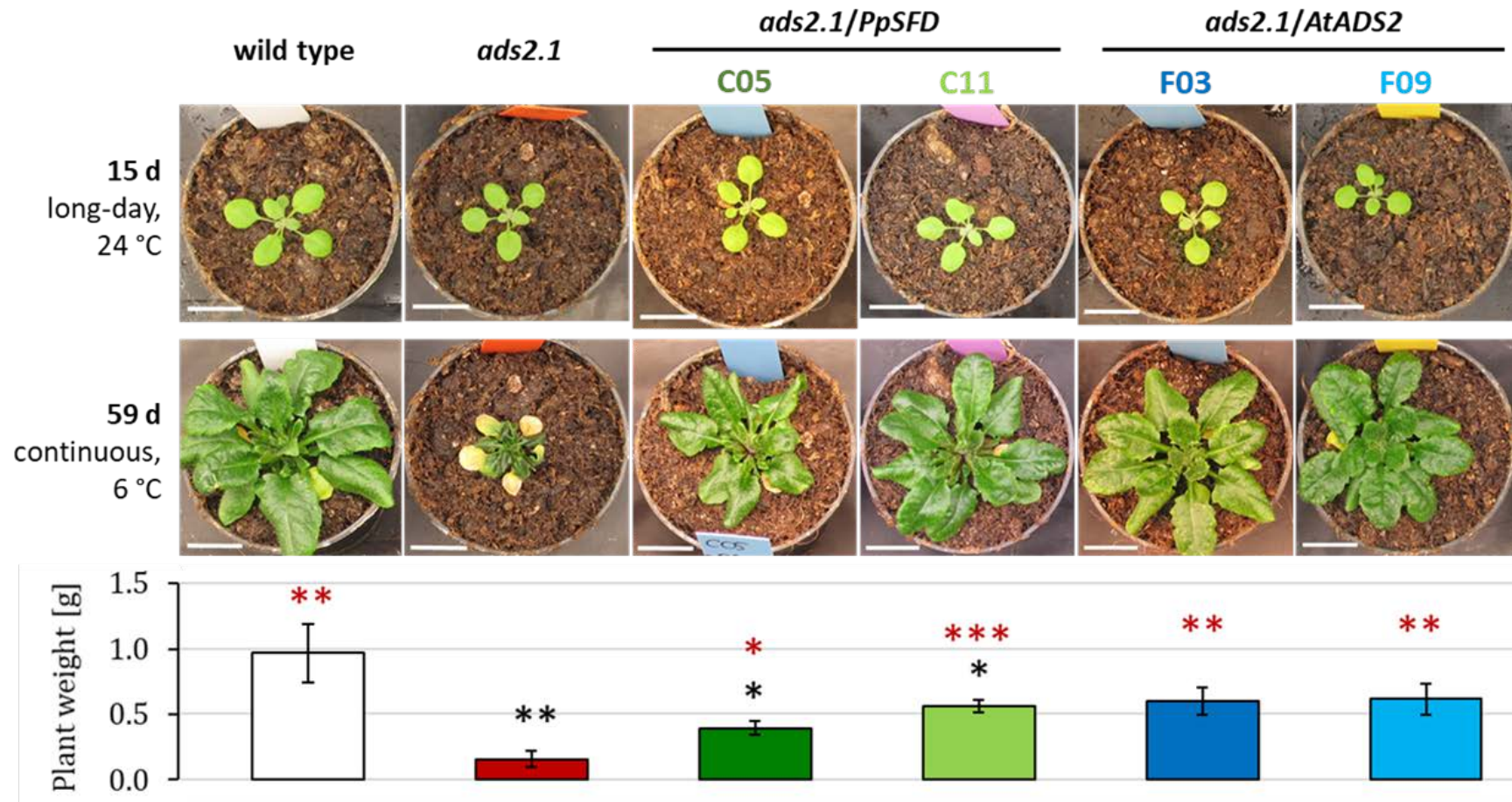


**Figure 3.23. Cold stress experiment with *A. thaliana* complementation lines.** Complementation lines were transformed with *AtADS2* (lines F03 & F09) or *PpSFD* (lines C05 & C11) under control of the CaMV 35S promoter via *Agrobacterium*-mediated transformation of the *A. thaliana* *ADS2*-KO line *ads2.1*. Plants were grown at long-day conditions (16 h day/8 h night, 24 °C) for 15 days before being transferred to cold stress conditions (continuous light, 6 °C) for 59 days. Images of plants were taken directly before transfer to cold stress conditions, as well as at the end of the experiment. All plant parts above soil level were harvested & weighed. Bar diagrams represent mean values with standard deviations for either 3 (wild type, *ads2.1*, C05) or 4 (C11, F03, F09) biological replicates. Student *t*-test was performed analyzing weight differences between wild type (black asterisks) or *ads2.1* (red asterisks) with the other lines. \* =  $p < 0.05$ , \*\* =  $p < 0.01$ , \*\*\* =  $p < 0.001$ . The images shown are representative of 3 – 4 plants for each plant lines. An independent experiment with the same lines (except C05) was performed under identical conditions and produced similar results.

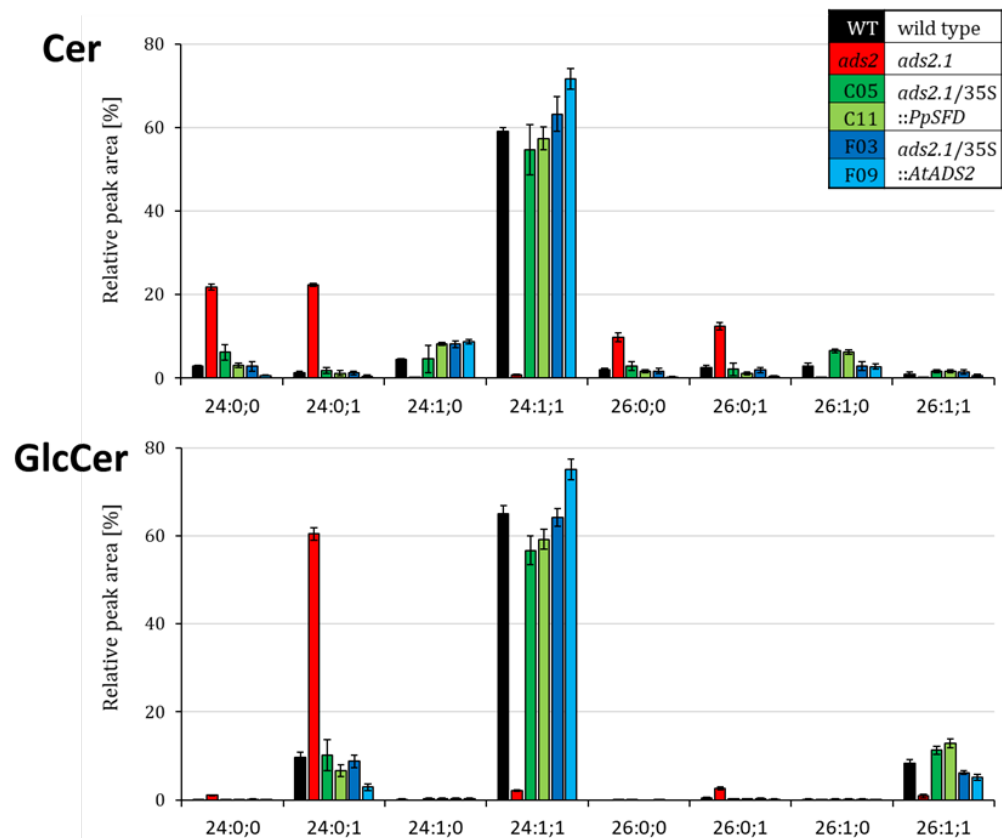


**Figure 3.24. C24 and C26 containing sphingolipids in *A. thaliana* mutant *ads2.1* and its complementation lines with *AtADS2* and *PpSFD*.** Complementation lines were transformed with *AtADS2* (lines F03 & F09) or *PpSFD* (lines C05 & C11) under control of the CaMV 35S promoter via *Agrobacterium*-mediated transformation of the *A. thaliana* *ADS2*-KO line *ads2.1*. Plants were grown at long-day conditions (16 h day/8 h night, 24 °C) for 15 days before being transferred to cold stress conditions (continuous light, 6 °C) for 59 days. Lipids were extracted from lyophilized samples using a one-phase isopropanol/hexane/water extraction protocol. Lipid species were separated by UPLC with a C18-RP-column and measured via MRM-based QTrap-ESI-MS analysis. Bar diagrams represent mean values with standard deviations for either 3 (wild type, *ads2.1*, C05) or 4 (C11, F03, F09) biological replicates. Displayed are sphingolipid species with the LCB 18:1/3 and C24-26 fatty acids.

Cold stressed *A. thaliana* wild type also contains 24:1 FA moieties in PC, PE and PS, similar to *P. patens* wild type (Smith, Dauk et al. 2013). 24:1 is most abundant in PS with up to 20 % relative amount for PS(18:3/24:1) and are more abundant than 24:0 FAs. In *ads2.1*, the amount of 24:1-containing phospholipids is strongly reduced in all three phospholipid classes, while 24:0 FA moieties become more abundant as a response (see Figure 3.25.). Regarding saturated C24 phospholipids, complementation lines show very similar lipid profiles to wild type. Levels of unsaturated FAs in phospholipids are similar in *PpSFD* complementation lines and wild type. In *AtADS2* complementation lines, however, 24:1-levels seem to not only match wild type levels, but exceed them even. In F09 and F03, 24:0-PE levels are significantly lower than wild type, while PE levels of 24:1 FA moieties are in contrast 2-fold increased over wild type. Levels of PS are similar to wild type in all complementation lines.

Overall, *AtADS2* complementation lines contain more 24:1 phospholipids than wild type, while *PpSFD* complementation lines have similar levels of 24:1 phospholipids to wild type *A. thaliana*. Sphingolipid composition in both *AtADS2* and *PpSFD* complementation lines matches that of wild type plants.



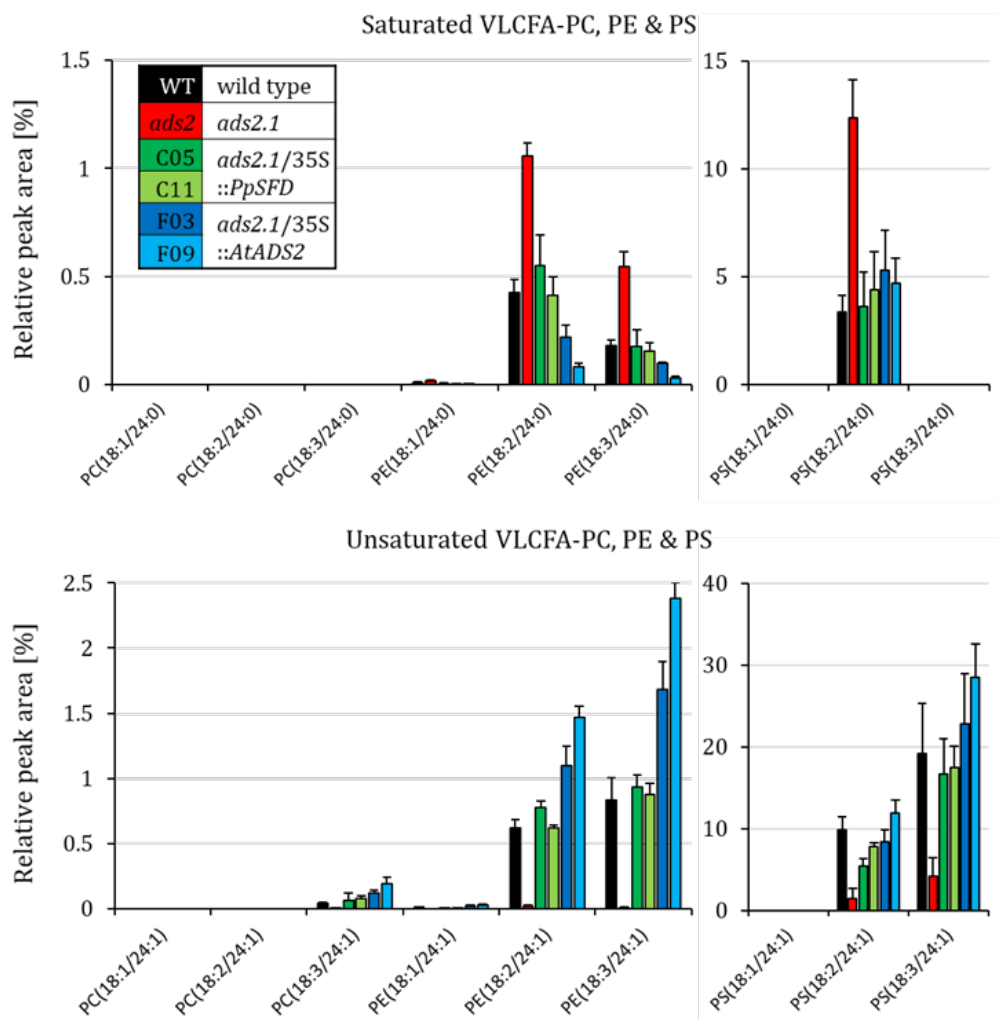


**Figure 3.25. Relative peak area of C24 fatty acid PC, PE & PS in *A. thaliana* complementation lines.** Complementation lines were transformed with *Atads2* (lines F03 & F09) or *Ppsfd* (lines C05 & C11) under control of the CaMV 35S promoter via *Agrobacterium*-mediated transformation of *Atads2.1*. Plants were grown at long-day conditions (16 h day/8 h night, 24 °C) for 15 days before being transferred to cold stress conditions (continuous light, 6 °C) for 59 days. Lipids were extracted from lyophilized samples using a one-phase isopropanol/hexane/water extraction protocol. Lipid species were separated by UPLC with a C18-RP-column and measured via MRM-based QTrap-ESI-MS analysis. Bar diagrams represent mean values with standard deviations for either 3 (wild type, *ads2.1*, C05) or 4 (C11, F03, F09) biological replicates.

### 3.4.5. AtADS2 desaturates at *n*-9 position, while *PpSFD* (in the *ads2.1* background) desaturates at both *n*-8 and *n*-9 position

It was shown in 3.4.4. that both AtADS2 and PpSFD catalyze the insertion of a double bond into C24 FAs in ceramides. It remained however unclear if the two enzymes have different positional preferences towards the double bond insertion. Smith (Smith, Dauk et al. 2013) reported AtADS2 to catalyze double bond formation in C24 and C26 FAs at the *n*-9 position of the FA. In order to analyze the double bond position preference of PpSFD, an experimental assay was designed to extract as much 24:1;1 FAs as possible from lyophilized plant samples, to purify trans-methylated FAs and to derivatize the FA to make

the double bond position detectable by GC-MS analysis. Focusing analysis on hydroxylated FAs hereby made sure that only FA moieties from sphingolipids were analyzed. Viability of the method was tested with genuine ceramide standard (18:1;2/24:1;1) with *n*-9 position of double bond in the FA moiety. Lines that were analyzed include *A. thaliana* and *P. patens* wild type, *Atads2.1*, *Ppsfd*, and the *ads2.1/PpSFD* complementation line C11. Each line was analyzed twice. The line C11 is here of special interest since it could be observed if PpSFD retains its preference for double bond insertion when expressed in a foreign organism.

Extraction of lipids for this method was done via a one-phase isopropanol/hexane/water extraction, similar to what was used for LC-MS analysis of the lipidome (see 3.1.). Since sphingolipids are present in relatively small amounts in plants, a high amount of plant material was used for extraction: 20 x 10 mg lyophilized material (for both *A. thaliana* and *P. patens* samples). The lipid extract was then treated with highly acidic conditions at 100 °C in methanol for 20 h to ensure the hydrolysis of all FA residues from all lipid classes (including peptide bonds of sphingolipids) into fatty acid methyl esters (FAMES). FAMES were then separated on HPLC and treated with DMDS to derivatize double bonds into di-thiomethyl-ethyl groups, which fragmentize in a characteristic manner in GC-MS analysis (Francis and Veland 1987). Overall yields of derivatized 24:1;1 FAMES created via this method were generally very low and were detected at weak signal intensities. When combining 20 extractions into one analysis, it was possible to measure signals that were high enough to be detected against background noise.

DMDS derivatization and GC-MS analysis confirmed that in *A. thaliana* wild type the double bond in the 24:1;1 FA moiety of sphingolipids is present exclusively at *n*-9 position. Double bond position was determined by the presence of three characteristic fragments:  $m/z = 173$  (methyl end up to the thiomethylated C16 of FA carbon chain),  $m/z = 317$  (carboxyl-ester end up to the thiomethylated C15 of FA carbon chain) and  $m/z = 269$  (carboxyl-ester end up to the C15 of FA carbon chain without thiomethyl group). In *P. patens*, 24:1;1 is present predominantly as *n*-8, identified by the fragments  $m/z = 159$  (methyl end up to the thiomethylated C17 of FA carbon chain),  $m/z = 331$  (carboxyl-ester end up to the thiomethylated C16 of FA carbon chain) and  $m/z = 283$  (carboxyl-ester end up to the C16 of FA carbon chain without thiomethyl group). Fragment patterns are shown in Figure 3.26. B. In *P. patens* wild type, lower amounts of *n*-9 specific fragments were also detected at the same retention time of the GC separation, suggesting that 24:1;1 is present with two different double bond positions which are not separated on the GC (see Figure 3.26. A). Content of *n*-8 was about 4-fold higher in *P. patens* compared to *n*-9. The KO lines *Atads2.1* and *Ppsfd* both did not contain any detectable amounts of 24:1;1 (data not shown).

In the *ads2.1/PpSFD* C11 complementation line, both *n*-8 and *n*-9 double bonds were detected in 24:1;1, with *n*-8 being present in about 2-fold higher abundance. The double bond position in this line is therefore distributed similar to *P. patens* wild type, but with slightly higher relative content of *n*-9 (see Figure 3.26. A). In *A. thaliana*, AtADS2 inserts double bonds in C24 and C26 FAs both at the *n*-9 position (Smith, Dauk et al. 2013). As stated above, the method used in this work did not produce high amounts of 24:1;1 DMDS-FAMES, even when combining many samples. In 3.4.4., it was observed that *A. thaliana* also contains 26:1;1 FA moieties in sphingolipids, yet in much lower relative amounts. However, the very low sensitivity of this method prevented the analysis of 26:1;1 FAMES in this work. Since only the double bond position in 24:1;1 was analyzed, it could not be

determined if PpSFD counts from the carboxyl end or the methyl end of a FA for double bond insertion.

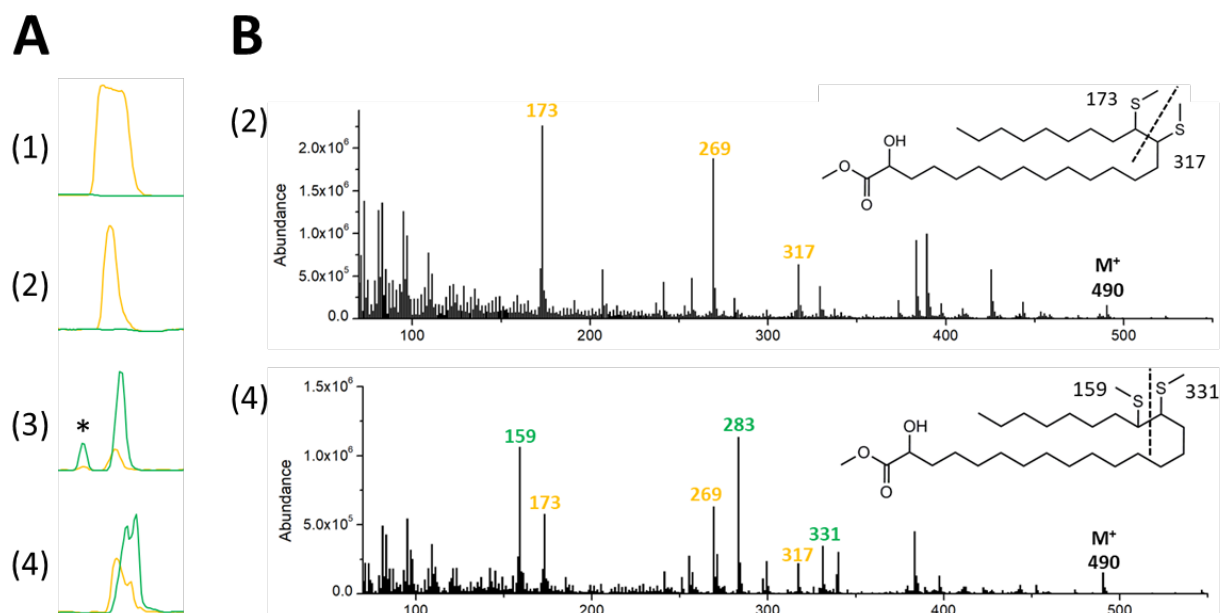


**Figure 3.26. Analysis of double bond position in 24:1;1 in *A. thaliana* wild type, *P. patens* wild type & *A. thaliana ads2.1/35S::PpSFD* (C11).** Measurements were done via GC-MS. A: A: Extracted ion chromatogram of the analytical fragments for *n*-9 (*m/z* 269, orange line) or *n*-8 (*m/z* 283, green line) double bond positions of 24:1;1 DMDS-FAMES, shown for: (1) 24:1;1 ceramide standard (*n*-9), (2) *A. thaliana* wild type, (3) *P. patens* wild type (Asterisk marks an unknown substance), (4) *ads2.1/35S::PpSFD* complementation line C11. B: Mass spectra of *n*-9 24:1;1 DMDS-FAMES in (2) *A. thaliana* wild type and (4) *ads2.1/35S::PpSFD* complementation line C11. Position of double bonds in 24:1;1 DMDS-FAMES is shown in chemical formulas. Measurements depicted are representative for 2 independent measurements each.

All in all, a novel approach for analyzing the double bond position in FAs of sphingolipids was developed and used in this work. PpSFD was shown to be a desaturase with a main regional specificity towards *n*-8 position and minor specificity towards *n*-9 position in 24:1;1. This is in contrast to AtADS2, which inserts double bonds exclusively at the *n*-9 position. PpSFD retains its double bond specificity also when expressed heterologously in *A. thaliana*.

## 4. Discussion

---

In this work, the bryophyte *P. patens* was analyzed for its lipid composition and its response to cold stress on a lipid and phenotype level. Furthermore, the putative sphingolipid desaturase PpSFD was analyzed on a peptide level, how lipid composition and phenotype are affected in *Ppsfd* KO-mutants, and how a desaturase with similar function from *A. thaliana* - AtADS2 - compares to this desaturase on a peptide and functional level.

### 4.1. Lipid composition in *P. patens* is far more diverse compared to *A. thaliana* due to higher FA variety

#### 4.1.1. *P. patens* does not require the fatty acid 20:4 for survival at normal and cold conditions

Prior to analyzing the complete lipidome of *P. patens*, the FA composition of neutral lipids, glycolipids and phospholipids was analyzed in this work. The FA profile of *P. patens* differs slightly from what was observed for *P. patens* in other works, e.g. Beike (Beike, Jaeger et al. 2014), where 16:0 was measured as the most prominent FA, whereas here the FA 18:3 was far more abundant (see Figure 3.1.). This could, however, also be caused by the slightly different growth conditions and lighting conditions. Overall, the profile is similar in this work.

The FA profile of *P. patens* was also compared to that of *A. thaliana*. It was observed that the FA profile in *P. patens* contains far more different FA species than *A. thaliana*, as also described before by other authors (Grimsley, Grimsley et al. 1981, Beike, Jaeger et al. 2014). The main difference between the two species is the presence of VLC-PUFAs in the FA profile, which are not present at all in *A. thaliana* (see Figure 3.1.). VLC-PUFAs do not appear in significant amounts in any vascular plant species (Alonso, Garcia-Maroto et al. 2003), but vascular plants can be genetically engineered to obtain desaturase and elongase genes from non-vascular plants and microalgae, as done for *Camelina sativa* (Ruiz-Lopez, Haslam et al. 2014). In this work, it was reconfirmed that in *P. patens*, the VLC-PUFA arachidonic acid (20:4) is a major FA moiety found in all lipid classes. In phospholipids, it is even the most abundant FA moiety, in glycolipids the second most abundant. Even though 20:4 plays such a prominent role in the FA profile, it apparently is not required for survival for *P. patens*, since KO-mutants that lack this FA grow normally under standard growth conditions (Zank, Zähringer et al. 2002, Kaewsuwan, Cahoon et al. 2006). Analysis of *elo* KO-lines (that do not produce 20:4) in this work also showed no significant difference in phenotype or chlorophyll content compared to wild type. This was observed in all tested conditions, be it at normal and cold temperatures or with and

without tartrate in the medium (see Appendix 11 & 12). This raises the question why *P. patens* synthesizes this FA and if other FAs are capable of fulfilling the same function.

In *A. thaliana*, it was shown that polyunsaturated FAs are necessary to maintain photosynthesis at high and low temperatures (Buchanan 2015). *P. patens elo* lines still contain the polyunsaturated FAs 18:3 and 16:3 despite lacking 20:4, so the functionality of the photosynthesis apparatus might still be maintained in these mutants. However, analysis of chlorophyll content shows that chlorophyll content in *elo* lines may be lower compared to wild type *P. patens* (see Figure 3.20.), which would suggest some discrepancy in plastid viability. For the chlorophyll content test only a limited number of replicates could be analyzed, so this result stays up for debate. The *elo* cultures did otherwise look equally healthy to wild type.

20:4 is also present in high relative amounts in *P. patens* neutral lipids, while other polyunsaturated FAs are lower in this lipid class and the saturated FAs 16:0 and 18:0 are present in higher amounts. This is comparable to how the microalgae *L. incisa* accumulates VLC-PUFAs under stress (Bigogno, Khozin-Goldberg et al. 2002). For microalgae, it was theorized that these VLC-PUFAs are important precursors for other lipids that are available for the organism immediately as soon as normal conditions are met again (Khozin-Goldberg, Yu et al. 2000). It is however unclear if for *P. patens* a similar function can be assumed for 20:4. VLC-PUFAs could also act as precursors for phytohormones like oxylipins (Andreou, Brodhun et al. 2009), but in mosses, this topic is only preliminarily researched. It is known from *P. patens* that it does not contain the full pathway of synthesizing the defense and development hormone jasmonic acid, which is commonly found in vascular plants (Stumpe, Göbel et al. 2010, Scholz, Brodhun et al. 2012). It is still unknown if there are alternative oxylipins present in *P. patens* that might rely on 20:4 as precursor. However, since no phenotype was observed for *elo* lines under any tested conditions, a developmental role of such oxylipins seems unlikely at this point.

It is noteworthy that during lipid analysis in this work, 20:4-containing lipids eluted from UPLC at unexpected retention times, slightly later than a linear algorithm for the number of double bonds in a FA would expect it. The fourth double bond in a FA has apparently a different effect on the hydrophobicity of the molecule than the first individual three double bonds had on the lipid. A study analyzing the VLC-PUFAs 20:5 and 22:6 in human cells showed an increase in plasma membrane fluidity in cells that contain more of these VLC-PUFAs (Hashimoto, Hossain et al. 1999). Nevertheless, no study is known to the author that compares PUFAs and VLC-PUFAs regarding their physical properties in a membrane of plants. The exact function of 20:4 and other VLC-PUFAs can therefore still not be predicted for the plant organisms that do contain them. It is possible that in the context of living on land, VLC-PUFAs did not have the same importance for plants as they did for microalgae. Further evolution of land plants included apparently the loss of the genes responsible for VLC-PUFA synthesis, since these genes are not present anymore in vascular plants (Meesapyodsuk and Qiu 2012). It can be assumed that this gene loss would only have happened if VLC-PUFAs were not necessary for surviving on land. Another possibility is that in the case of bryophytes, the presence of VLC-PUFAs is actually important for survival at arid land conditions, but these conditions are not efficiently replicated in a lab environment.

#### 4.1.2. Lipid species in *P. patens* are far more diverse than in *A. thaliana*, largely due to the additional FA moiety 20:4

In this work, an extensive lipidomic workflow (originally developed by Pablo Tarazona (Tarazona, Feussner et al. 2015)) was used to determine the presence and individual composition of 19 different lipid classes in *P. patens* (see Table 3.2.). Of the tested lipid classes, traces were found for all of them, but the exact composition of SQDG, DGTS/A and GIPC could not be further determined. Even though exact quantification of lipid molecules with the used analysis techniques is not possible, it was assumed that these three lipid classes are present in only very low amounts in *P. patens*. Earlier lipid analyses by different authors suggest that in bryophytes the lipid classes SQDG and DGTS are present, though *P. patens* was not analyzed (Dembitsky 1993). Unpublished data cited by Buré (Buré, Cacas et al. 2014) also suggests a presence of GIPC in *P. patens*, but no molecular species could be named. It is also noteworthy that even though Tarazona (Tarazona, Feussner et al. 2015) could analyze some GIPC species in *A. thaliana* with a similar setup, the method used was not optimized for analyzing GIPC, which only insufficiently ionize in nanoESI devices due to their high mass. However, the fact that GIPC were only detected with low signal intensity in *P. patens* leads to the conclusion that they are indeed present in very low amounts compared to *A. thaliana*. This is somewhat surprising since GIPC are the most abundant class of sphingolipids in most vascular plants, including *A. thaliana*, where GIPC make up more than half of the sphingolipid content in leaves (Markham and Jaworski 2007). Peptide sequence comparison with *A. thaliana* genes suggests the presence of IPC synthase genes in *P. patens* (Phypa\_135744, Phypa\_59752, Phypa\_143973, according to NCBI (Coordinators 2016)), but it is not known if they are active.

SQDG are also present in vascular plants and commonly make up the smallest portion of glycolipids, but they are still present in detectable amounts (Buchanan 2015). DGTS/A however are not present in vascular plants, making it a remnant compound from marine plants and other non-vascular plants that contain higher amounts of this betaine (Vogel and Eichenberger 1992). Betaines were reported for bryophytes to be present, but *P. patens* was not analyzed (Dembitsky 1993). It is possible that under the given growth conditions for *P. patens* cultures in this work the formation of DGTS was not preferred. It was suggested for algae (Künzler and Eichenberger 1997) that DGTS has similar properties than PC and is formed mainly at phosphate-limited growth conditions, which were not present in our experiment. All in all, the absence of significant amounts of SQDG and GIPC represents one of the strongest differences of *P. patens* compared to vascular plants, indicating that the synthesis of these lipid classes might have a bigger role for the survival of more complex plants. The relative low presence of betaine lipids compared to other mosses might be a special property of *P. patens* as an organism that was grown continuously at lab conditions for decades. The synthesis of these lipids are however an indicator the close relationship to marine organisms and represents a feature that was lost in later plant development. For both SQDG and betaine synthesis, necessary genes appear to be present in *P. patens* (*A. thaliana* SQD2-like XP\_024385518, *A. thaliana* SQD1-like XP\_024386550, *C. reinhardtii* betaine-synthase-like XP\_024358925, according to NCBI blastp (Johnson, Zaretskaya et al. 2008)).

Judging from the FA profile (see Figure 3.1.), the main group of lipids that were found in *P. patens* are glycolipids, present as MGDG and DGDG. This is in line with what is known from vascular plants, where glycolipids are also a major lipid class in photosynthetic tissues

(Buchanan 2015). A high amount of glycolipids was therefore also expected for *P. patens* since as a photosynthetic organism, chloroplasts probably make up the majority of membranes inside their cells, and plastid membranes contain mainly glycolipids (Buchanan 2015). It was however surprising that only traces of the sulfolipid SQDG were detected in *P. patens*, which is common in all photosynthetic organisms (Buchanan 2015). The medium in which *P. patens* was grown contained several components that serve as sulfur source, so unavailability of sulfur should not be an issue here. *A. thaliana* KO-lines that do not produce SQDG any more show impaired growth only under phosphate-limited conditions (Yu, Xu et al. 2002), suggesting that SQDG is present in plastid membranes only to limit the use of phosphate in nature. It is possible that in the context of this work *P. patens* did not produce SQDG because phosphate was present in high abundance in the growth medium. FA composition in the other glycolipids contain mostly the FAs 16:3 and 18:3 similar to *A. thaliana*, but also with high amounts of 20:4 (see Figure 3.3.). It is not clear if 20:4 plays an important role for the functionality of glycolipids in *P. patens*, especially since there is no known phenotype for KO-lines that lack this FA in *P. patens* (Girke, Schmidt et al. 1998, Zank, Zähringer et al. 2002, Kaewsuwan, Cahoon et al. 2006).

Judging from the signal intensity of the ESI-MS analysis of lipids, the phospholipid composition in *P. patens* seems to be dominated mostly by PC and PE, though absolute amounts of these lipids can of course not be determined from the MS data. All phospholipid classes have as main lipid species mostly those that contain 16:0, together with 18:2, 18:3 or 20:4 (see Figure 3.2.). Interestingly, the phospholipid class PG contains almost no 20:4. In plants, PG is commonly the most abundant phospholipid class in plastids (Buchanan 2015). Since 20:4-containing plant organisms are not very thoroughly analyzed on lipid levels, it remains unclear what reason the absence of 20:4 in PG might have. A similarity between *P. patens* and *A. thaliana* phospholipids is that in PS higher amounts of FAs with 24 carbons can be found (either as 24:0 or 24:1, (Smith, Dauk et al. 2013). This seems to be a conserved feature of PS in plants since these long FAs are otherwise only found in sphingolipids in higher amounts (Markham, Molino et al. 2011).

In *P. patens* neutral lipids, there is a relatively high amount of polyunsaturated FAs found, mostly as 18:2, 18:3 and 20:4, often in combination with the saturated FA 16:0. Both DAG and TAG contained mostly lipid species that also contained 20:4 (see Figure 3.4.). In seed plants like *A. thaliana*, neutral lipids are mostly present in a similar composition, with 18:2 being the most abundant FA in *A. thaliana* seeds (O'Neill, Gill et al. 2003). Only the presence of 20:4 is different in *P. patens*. It is noteworthy that unlike seed plants, *P. patens* does not produce oil-accumulating tissue types like seeds and does not produce large amounts of lipid oil bodies under stress like microalgae (as far as we observed). However, it was stated before that mosses might contain higher amounts of neutral lipids in leaf-like tissues than seed plants (Dembitsky 1993) with up to 70 % of lipids being present as neutral lipids. This observation, however, could not be made in this work for *P. patens* with neutral lipids making up only a very small portion of lipids in a total FA profile (see Figure 3.1.). It is unclear if this is a special feature of *P. patens* or if under the given growth conditions in the laboratory, bryophytes in general produce less neutral lipids. The study by Dembitsky (Dembitsky 1993) was performed predominantly from bryophyte samples collected in the wild. Similar to *L. incisa*, the neutral lipids in *P. patens* contained high amounts of 20:4 (Bigogno, Khozin-Goldberg et al. 2002).

Sterol composition in *P. patens* showed some differences to what is known from *A. thaliana*. In *A. thaliana*, sterol composition is largely dominated by the steroid core

structure sitosterol (Schaeffer, Bronner et al. 2001), while other sterols are only present in minor amounts. In *P. patens*, however, we found about equal amounts of sterol lipids containing sitosterol and campesterol, while in free sterols stigmasterol was also present in high amounts (see Figure 3.5.). In earlier analysis of *P. patens* sterols (Morikawa, Saga et al. 2009) the sterol profile was dominated however by stigmasterol, with less campesterol and minor amounts of sitosterol. It is unclear why the sterol analysis in this work and in the previous work differ so much, but it could be caused by the difference in growth conditions for the moss cultures. In the work by Morikawa, *P. patens* plate cultures were analyzed and the medium also contained 5 % sucrose, while in this work aerated liquid cultures were analyzed with no carbon source added to the medium.

#### 4.1.3. Sphingolipids in *P. patens* differ strongly from *A. thaliana*

Apart from the presence of the FA 20:4, the biggest difference in lipid composition between *P. patens* and *A. thaliana* can be seen at the level of sphingolipids. A major difference between the two organisms is that only trace amounts of GIPC were detected in *P. patens*. In *A. thaliana*, GIPC make up the majority of sphingolipids with more than 50 % relative content (Markham and Jaworski 2007). They are also very prominent and diverse in all other kinds of plants (Buré, Cacas et al. 2014). Mosses, however, have only been marginally analyzed for sphingolipid composition up to now, so it remains unclear if the low amount of GIPC in this study is an anomaly for this specific organism, the growth conditions applied, or if this is a feature found in all bryophytes or mosses. It is possible that GIPC represent a more complex class of sphingolipids that was more important in the further development of flowering plants, but not for early land colonizing bryophytes. However, it is not clear which exact function the GIPC have in this context. Due to the limitations of the analysis technique it is not clear which one of the other two sphingolipid classes, ceramides or glycosyl-ceramides, is present in a higher amount in *P. patens*. It was however observed that ceramides in *P. patens* are far more diverse compared to glycosyl-ceramides, containing a greater variety of FA and LCB moieties (see Figure 3.6.). The major FA moieties in *P. patens* ceramides are C24 FAs, with hydroxylated FAs being more prominent than non-hydroxylated ones. FA moieties with less than 20 carbons were only barely detected in any sphingolipid species in *P. patens*. This is in stark contrast to what is known for *A. thaliana*, where C16 FAs are present in ceramides and glycosyl-ceramides in significant amounts (Markham and Jaworski 2007).

Glycosyl-ceramides are dominated in *P. patens* by a single lipid species, 18:2;2/20:0;1 (see Figure 3.6.). This FA/LCB combination is only a very minor compound in ceramides. It is highly unusual for glycosyl-ceramides in plants to be present as mostly only one species and this was not reported for any other plant to the knowledge of the author. The FA of this dominant compound, 20:0;1, is not present in high amounts in *A. thaliana* glycosyl-ceramides (Markham and Jaworski 2007), but it is the dominant FA species in rice glycosyl-ceramides (Ishikawa, Ito et al. 2016). The dominant LCB in *P. patens* glycosyl-ceramides, 18:2;2, is however similar to that found in most vascular plants as major LCB, like tomato and soybean (Markham, Li et al. 2006) or rice (Ishikawa, Ito et al. 2016). The in plants very common LCB in glycol-ceramides 18:1;3, which in *A. thaliana* is the main LCB in all sphingolipids (Markham and Jaworski 2007), is in *P. patens* barely detectable. In rice, 18:1;3 is also a major LCB of glycosyl-ceramides besides 18:2;2 (Ishikawa, Ito et al.



2016). It might be possible that in *P. patens* mono-unsaturated LCBs are synthesized as an intermediate and immediately further desaturated to 18:2;2, therefore appearing only in minor amounts in sphingolipid profiles.

Interestingly, the two main sphingolipid classes in *P. patens* seem to be distinctly different from each other in their LCB and FA compositions, which would support a theory that the different lipid classes fulfill different functions in *P. patens*. To support this theory, further analyses would have to be made on the difference of sphingolipids in *P. patens*, possible by creating KO-lines for genes required for glycosyl-ceramide synthesis in *P. patens* and monitoring changes in phenotype. Studies on *A. thaliana* would support this theory on divided functionality, since here KO-lines affecting mostly glycosyl-ceramides are strongly impaired in development (Chen, Markham et al. 2008) or pathogen response (König, Feussner et al. 2012).

## 4.2. Cold stress in *P. patens* affects lipid composition differently depending on the lipid class

Lipid composition in plants plays a major role in adjusting to environmental stresses. For vascular plants, it has been largely reported that polyunsaturated FAs, mostly 18:2 and 18:3, are crucial in this regard for the plant to retain photosynthesis activity (Buchanan 2015). In *P. patens*, the VLC-PUFA 20:4 also has to be taken into account in this regard, serving as an even further unsaturated FA moiety in lipids. However, photosynthetic organisms containing 20:4 are rarely analyzed in detail, since they only include bryophytes and marine plants and microalgae. In this work it was observed that in cold-treated *P. patens* plants, the grade of desaturation and the length of the FAs were both significantly affected, though in opposite ways when comparing phospholipids & neutral lipids with glycolipids (see Figures 3.12., 3.13., 3.14.). While in phospholipids, FA moieties in general were shorter and contained less double bonds after cold stress, while in glycolipids longer and stronger desaturated FA moieties accumulated at cold stress. This could also be linked directly to the presence of the FA 20:4, which was reduced in phospholipids and accumulated in glycolipids after cold stress. The classical accumulation of more unsaturated C18 FAs however was not observed, which is the response reported for *A. thaliana* (Uemura, Joseph et al. 1995). However, organisms that do contain 20:4, like *L. incisa*, also accumulate 20:4 at stress conditions (Bigogno, Khozin-Goldberg et al. 2002). Apparently, in *P. patens* cold affects lipids that are present in plastids (glycolipids) very differently than lipids in other types of membranes. This theory would also be supported by the fact that PG, the most prominent phospholipid in plastids (Buchanan 2015) is the only phospholipid class with similar pattern as glycolipids (though not as strongly affected as glycolipids). However, since all analyzed lipids in this work were extracted from complete *P. patens* plants and not from separate membrane fractions, it can only be assumed how the different lipid classes are distributed among different cellular membranes. For the sake of discussion it is assumed that most lipid classes in *P. patens* will be broadly similar distributed as in *A. thaliana*.

Since *P. patens* accumulates 20:4 in glycolipids at cold stress, it could be assumed that this FA is essential for photosynthesis activity at low temperatures in *P. patens*. This is however negated by the fact that *P. patens elo* plate cultures, which do not produce 20:4, grow normally even after months of cold stress treatment. Apparently, *P. patens* is capable of compensating the loss of 20:4 FAs in some way, but it remains unclear how. It is possible that the presence of C18 PUFAs is sufficient for the plant to retain photosynthesis activity at cold conditions, like other plants do (Buchanan 2015). However, analysis of *elo* mutant lines in this work showed a decrease in chlorophyll content compared to wild type at normal conditions, even though the plants looked normal on a phenotype level. There has to this point no other phenotype been reported for *P. patens elo* mutants, at normal or other growth conditions (Zank, Zähringer et al. 2002). It therefore has to be assumed that 20:4 might not fulfill an essential function in *P. patens*, at least under laboratory conditions. In the wild, *P. patens* might be more dependent on 20:4 being present in its lipids to deal with certain environmental conditions, but this has not been studied yet. Since 20:4 and other VLC-PUFAs are present throughout bryophytes (Dembitsky 1993) it might be possible that 20:4 plays a bigger role in other moss species. Since many moss species thrive in very cold climates, there could also be a benefit of 20:4 in dealing with freezing stress instead of cold stress, meaning temperatures below 0 °C. This kind of stress was not analyzed in this work. Also, *P. patens* is generally considered to not be a moss species with high adaptation to very cold climates (Beike 2013), so cold-stress adaptation for this organism might not be as developed as in other bryophytes.

Cold stress had no significant effects on the overall relative amounts of lipid groups in wild type *P. patens* (see Figure 3.16.). This was unexpected since in *A. thaliana*, cold acclimatization lead to the accumulation of PC and ceramides and decrease of MGDG (Degenkolbe, Giavalisco et al. 2012). Decrease in MGDG was also reported by Tarazona 2015 (Tarazona, Feussner et al. 2015), together with a decrease of TAG. In *P. patens*, neutral lipids did not accumulate, which would be a common response to stress in vascular plants and microalgae (Volkman, Jeffrey et al. 1989, Welti, Li et al. 2002). However, it has to be mentioned that for lipid analysis in this work, the applied cold stress on *P. patens* liquid cultures was only 24 h long, which might not be enough time to change the overall amounts of lipids in the plant. Instead, they were perhaps adjusted only on a FA level.

In sphingolipids it was observed that glycosyl-ceramides were not affected at all by cold stress conditions, while ceramides were modified towards accumulating more of the most common species 18:0;3/24:0;1 and 18:0;3/24:1;1. In *A. thaliana* it was shown that at cold stress mostly sphingolipids with unsaturated FA residues accumulate after cold stress (Tarazona, Feussner et al. 2015). It is however not clear what exact function sphingolipids play in the response to cold stress. Both LCB and FA desaturases acting on sphingolipids were shown to be involved in the response to cold stress (Chen, Markham et al. 2012, Chen and Thelen 2013, Smith, Dauk et al. 2013). It was speculated that the sphingolipids hereby might be important for the organism to maintain plasma membrane characteristics at low temperatures (Markham, Lynch et al. 2013). This could also be the case for *P. patens* where ceramides represent the sphingolipid class with higher variability and therefore greater potential for modifications. It could also be possible that these sphingolipids are necessary for the formation of membrane microdomains (Bhat and Panstruga 2005) that might in return be responsible for starting signaling cascades in response to temperature changes. Shifting the ceramide profile towards the most prominent lipid molecules might improve the capability of the membrane to form these microdomains.

### 4.3. PpSFD is a sphingolipid FA desaturase acting on ceramides and some phospholipids

It was shown in this work that the putative cold-induced desaturase Phypha\_171332, discovered by Anna Beike (Beike 2013), is indeed a FA desaturase catalyzing the formation of mono-unsaturated FAs of 24 and 26 carbons length which are predominantly found in ceramides of *P. patens* (see Figure 3.9.). PpSFD may have also additional activity on FA moieties in PC and PE, but not on PS, which is the only phospholipid class in *P. patens* that contains high relative amounts of 24:0 and 24:1 FA moieties (see Figure 3.10.). PpSFD was identified as a bi-functional membrane desaturase, containing a cytochrome-*b5* domain and the specific His-box motif typical for this class of desaturases (Alonso, Garcia-Maroto et al. 2003). Since it takes FAs as substrate and not LCBs, it should be assumed that PpSFD is a front-end desaturase (Meesapyodsuk and Qiu 2012). PpSFD might have a very unique function compared to other desaturases since at the date of writing this work, no other plant front-end desaturase is known that inserts the first double bond into a very long saturated FA moiety.

Analysis via DMDS-derivatization of hydroxylated FAMES from *P. patens* cultures revealed a specificity primarily for *n*-8, but also for the *n*-9 position in 24:1;1 FAMES (see Figure 3.26.). The only other FA affected by PpSFD in *P. patens*, 26:1;1, was present in such low amounts in the samples that it could not be detected in DMDS-derivatized samples. In the frame of this work it was therefore not possible to determine the exact double bond preference of the enzyme in regards to front-end or methyl-end of the FA. There are two arguments to be considered when speculating about a possible positional preference for PpSFD. On the one hand, other analyzed FA-modifying bi-functional desaturases in bryophytes are all reported to be front-end desaturases, inserting double bonds close to the carboxyl-group of the FA (e.g.  $\Delta 5$  or  $\Delta 6$  position (Girke, Schmidt et al. 1998, Kaewsuwan, Cahoon et al. 2006)). PpSFD might therefore also rely on a similar mechanism to determine the double bond position. On the other hand, these front-end desaturases use unsaturated FAs as substrate (e.g. 18:2), not saturated very long chain FAs like PpSFD. Also, the position of the double bond inserted by PpSFD (*n*-8 or  $\Delta 16$ ) is actually located closer to the methyl-end of the FA than the carboxyl-end. Nevertheless, desaturases with at *n*-8 positional preference have not been reported before for plants.

All analyses were done on KO-mutant plant material and not with the isolated enzyme, so the exact substrate activity of PpSFD could not be determined. Purifying functional membrane-bound enzymes is nevertheless at the current state of research almost impossible to accomplish. Since no other effects on unsaturated FA or LCB moieties were detected in the KO-mutant it is assumed that sphingolipids, PC & PE are the only lipids that incorporate FAs desaturated by PpSFD. It also remains unclear if PpSFD acts on ceramides and phospholipids directly or if acyl-CoA or free FAs are desaturated and then built into these lipids. The double bond position in 24:1-moieties could also not be analyzed for stereochemistry with the tools available for this work, so it remains unclear if PpSFD catalyzes preferably the formation of *trans* or *cis* double bonds or a mixture of both, like some LCB desaturases do (Chen, Markham et al. 2012).

It was observed in this work that *sfd* KO-mutants did produce almost no 24:1 FAs (hydroxylated and non-hydroxylated, see Figure 3.9.). However, there were still very low residual amounts of 24:1 detectable in ceramides in this mutant line, which suggests that there might be another FA desaturase present in *P. patens* which has some minor activity on FAs in ceramides. The same was observed for PC and PE (see Figure 3.10.). It might be possible that the amount of 24:1 found in PS, which is present in relatively high amounts and not affected by the *sfd* KO-mutation, is caused by this other unknown FA desaturase or even another different desaturase. There must at least be one other FA desaturase with specificity for C24 FAs be present in *P. patens* so these high amounts of 24:1-PS species can be explained. It is, however, unclear which FA desaturase this might be. The gene homologue of PpSFD present in *P. patens* was shown by Beike (Beike 2013) to not be expressed under any analyzed condition, so this gene may be excluded as a responsible FA desaturase. Otherwise, any desaturase could potentially catalyze a similar reaction in *P. patens*. It is then possible that 24:1-FA moieties are reshuffled from PS to ceramides. However, these FAs additionally have to be hydroxylated, since FA in ceramides are present mostly this way, while in PS, they are not hydroxylated. It is also possible that shorter mono-unsaturated FAs like 18:1 are elongated to 24:1 by elongases to some degree and then built into sphingolipids and phospholipids.

#### 4.4. *Ppsfd* mutant does not significantly adjust lipid composition like wild type *P. patens* at cold stress

KO-mutants of *sfd* were analyzed on a lipid and phenotype level to determine the function of PpSFD in *P. patens*. When grown for several months on medium without tartrate, there is not much difference in phenotype observable for *sfd* KO-lines (see Appendix 9 & 10). Plate cultures look green and healthy at normal conditions and slightly more dried out at low temperature for both *sfd* and wild type, suggesting that *P. patens* retains apparently more water at normal temperatures than at low temperatures. This would be in line with reports about cold acclimatization and freezing stress in plants where water loss is a major concern for organisms at these conditions (Buchanan 2015). At gametophore-inducing conditions (without added tartrate), the moss is apparently well adapted to cold stress independent of the presence of unsaturated sphingolipids since both mutant and wild type appear equally healthy at these conditions. However, there is a significant difference detectable for moss cultures grown at protonema-inducing conditions (with added tartrate). At these conditions, the moss cultures develop less leaf-like structures and more of a sponge-like accumulation of filaments. At normal temperature, wild type moss protonema shows stronger signs of drying out compared to gametophore-induced plate cultures (see Figure 3.18.), indicating that the protonema filament of the moss might be less well adapted to long-term growth. Cold-stressed wild type plants actually appear more healthy and greener than those grown at normal temperature (see Figure 3.19.). It is not clear why this is the case, but possibly the special setup of a more sponge-like colony growth does also have some insulating effects on the plant, comparably to fur on animals. This theory remains however highly speculative. In *sfd* mutants, the effects of protonema-inducing conditions were observed as much more severe compared to wild type. The *sfd* lines showed much stronger bleaching of tissue and formation of even less gametophores,

both at normal and low temperatures. Also, chlorophyll content was much lower in *sfd* lines at normal temperature compared to wild type, but not at cold stress (see Figure 3.20.). Apparently, the *sfd* KO-mutant is much less viable on a general level when grown primarily as protonema and is more susceptible to drying out.

On lipid level, several differences between wild type *P. patens* and *sfd* were observed. First, the *sfd* KO-mutant produces even more ceramides with 24:0;1 as FA moiety after cold stress (see Figure 3.15.), possibly as a response to the absence of the second most abundant FA moiety in ceramides, 24:1;1. It is not clear if the absence of unsaturated ceramides is crucial for the cold stress response in *P. patens*, but in *A. thaliana*, the KO-mutant *ads2* which has a similar effect on sphingolipids in this organism, is severely compromised in growing at low temperature (Chen and Thelen 2013). Sphingolipids make up a major part of plasma membranes in plants up to 30 % (Buchanan 2015) and desaturation of these lipids might be important for maintaining membrane functionality at these low temperatures, possibly by increasing membrane fluidity. Sphingolipids are however special in that they are considered important for the formation of lipid rafts. These membrane microdomains have a higher density than the surrounding membrane and are possibly necessary for recruiting certain proteins to the plasma membrane (Bhat and Panstruga 2005). So far, desaturation of sphingolipids was not reported to be directly involved in the formation of lipid rafts in plants. However, in rice the hydroxylation of sphingolipid FA moieties has been shown to be crucial for lipid raft formation (Nagano, Ishikawa et al. 2016). A similar effect was observed in *A. thaliana* (Lenarčič, Albert et al. 2017). This could be an indication that small modifications of sphingolipids could have strong effects on lipid raft formation and might include the desaturation of these lipids as well.

A second effect on the lipidome in cold-stressed *sfd* is on the level of lipid classes other than sphingolipids. In wild type, significant changes in phospholipids and glycolipids appear regarding level of desaturation, FA chain length and the FA 20:4 (see Figures 3.12., 3.13., 3.14.). All three of these criteria in phospholipids and glycolipids are not significantly affected after cold stress in *sfd* KO-mutants. This is surprising, since *sfd* could not be shown to be directly involved in the synthesis of any lipids that did not contain 24:1 FA-moieties. Desaturation of PUFAs and incorporation of different FAs into non-sphingolipids should not be affected by the PpSFD enzyme directly. Nevertheless, PpSFD or the unsaturated ceramides appear to have a certain impact on how *P. patens* reorganizes its lipid composition when exposed to cold stress. In *sfd* KO mutants, the reaction towards cold stress seems to be delayed or disrupted when modifying lipids. However, when looking at the overall amount of some lipid classes, *sfd* and wild type *P. patens* have some other differences. Wild type *P. patens* was shown to not change the overall amount of any group of lipids after 24 h cold stress. In *sfd* cultures, the overall amount of glycolipids and sphingolipids was shown to be significantly decreased. Also, *sfd* contains about double the amount of TAGs compared to wild type, both at normal and cold stressed conditions.

Taking all this into account, it seems as if *sfd* mutants are not responding to cold stress in the same way as wild type *P. patens*, which results in a less healthy growth when grown primarily as protonema. The mutant looks even less healthy at normal temperature than at cold conditions. One theory for this phenotype is that the slower or inconsistent adjustment of lipids in *sfd* lines overall weakens the cell membranes of the moss, which is causing more water loss. Additionally, photosynthetic activity and viability of chloroplasts might also be impaired in *sfd* mutants, possibly for the inability to properly modify

plastid lipids. All these effects cannot be attributed solely to the missing activity of one desaturase on a plasma membrane lipid. Apparently, these desaturated sphingolipids are necessary for the functionality of complex intracellular communication pathways, possible in a function as lipid rafts. A theory would be that a sensor for cold stress in *P. patens* is located in lipid rafts of plasma membranes and that these lipid rafts cannot be formed properly in *sfd* KO-mutants. The mutant is then not capable of adjusting lipid composition normally when exposed to low temperatures. It is however unclear which exact signal pathway might be affected here.

## 4.5. PpSFD and AtADS2 function similarly in *A. thaliana*

Comparison between PpSFD and the *A. thaliana* desaturase AtADS2 revealed that both enzymes catalyze very similar reactions (Smith, Dauk et al. 2013). The activity of PpSFD on very long saturated FAs in sphingolipids and some phospholipids was also reported for AtADS2. Beike (Beike 2013) reported that PpSFD localizes to the ER, as AtADS2 does (Smith, Dauk et al. 2013). On top of that, both enzymes were reported to be involved in cold stress response in their respective organisms (Beike 2013, Chen and Thelen 2013), so it is easy to assume that there are a lot of functional similarities between these two enzymes. Nevertheless, both enzymes are very different on a structural and peptide level. AtADS2 is a mono-functional desaturase and contains three H residues in the third His-box of its desaturase domain (Smith, Dauk et al. 2013). PpSFD has all the typical characteristics of a front-end desaturase, including a cytochrome-*b5* domain and the typical Q/H amino acid switch in its desaturase domain (see Figure 3.7. (Meesapyodsuk and Qiu 2012)). Both enzymes share a peptide sequence identity of only 17 % (according to NCBI blastp (Johnson, Zaretskaya et al. 2008)).

The substrate specificity seems also to be slightly different between AtADS2 and PpSFD. In *A. thaliana*, 24:1-FAs appear in high amounts also in glycosyl-ceramides and GIPC (Markham and Jaworski 2007) and are reduced in *ads2* mutants (Smith, Dauk et al. 2013). Also, PS lipids containing 24:1 are strongly reduced in *ads2* KO mutants while in *P. patens*, these PS species are unaffected in *sfd* KO mutants (see Figure 3.10.). This suggests that AtADS2 is the only desaturase in *A. thaliana* that catalyzes the desaturation of C24 FAs, while in *P. patens*, there might at least be one other desaturase present with such a substrate specificity. Furthermore, on the matter of double bond position there are slight differences between AtADS2 and PpSFD. AtADS2 was reported to insert specifically at the *n*-9 position of FAs (Smith, Dauk et al. 2013), which was also confirmed in this work (see Figure 3.26.). PpSFD, however, has positional preference for *n*-8 position and also some *n*-9 position, with apparently both kinds of desaturations being formed in *P. patens* (see Figure 3.26.). The *n*-9 position is very common for desaturases in plants, since the first double bond inserted in C18 FAs is also inserted at the same position (Buchanan 2015). A *n*-8 position however is unusual in FAs.

KO-mutants of AtADS2 were shown to have reduced growth compared to wild type when grown at low temperatures and continuous light for several months (Chen and Thelen 2013). In this work, this phenotype was confirmed for *ads2.1* plants (see Figure 3.23.). When expressed under a 35S CaMV promoter in *A. thaliana ads2* KO-mutants, PpSFD was

capable of complementing the mutant phenotype with similar efficiency to AtADS2 complementation lines. The expression levels of both AtADS2 and PpSFD in the complementation lines far exceeded those occurring for AtADS2 in wild type *A. thaliana* wild type plants (see Figure 3.22.). The complementation lines can therefore be considered as overexpression lines. Lipid levels of unsaturated sphingolipids and phospholipids were on the level as wild type *A. thaliana* (see Figure 3.24.). However, the complementation lines did not quite reach the same plant size and weight in the cold stress experiment as the wild type plants did (see Figure 3.22.). This could be explained by the fact that the expression pattern of the 35S CaMV promoter might not be specific enough to guarantee proper expression of a gene in the necessary cellular compartment. Therefore, in the complementation lines there might not be the same level of 24:1-lipid species present in the correct membranes, causing them to not function properly at cold stress. It is still unclear which ones of the lipid species affected by AtADS2 are actually most important for the cold stress phenotype: sphingolipids or phospholipids. In either case, the lipids containing 24:1-FA-moieties would be predominantly present in the plasma membrane and some other membranes, but probably not in the chloroplasts of the plants since these contain only minor amounts of phospholipids and sphingolipids (Buchanan 2015). Therefore we can assume that photosynthesis activity might not be significantly impaired in *ads2* plants and instead some other kind of cell homeostasis might be affected. Additionally, since sphingolipids are involved, one must consider a regulatory role of the lipids in responding to cold stress, perhaps via so-called lipid raft microdomains (Bhat and Panstruga 2005). Since no tests were performed on *ads2* lines concerning lipid microdomains in this work or others, this theory remains however purely speculative.

Remarkably, PpSFD is apparently fully functional when expressed in *A. thaliana*. There was no significant difference detectable on a lipid level between PpSFD and AtADS2 complementation lines, only for 24:1-containing PE, which were slightly higher in AtADS2 complementation lines (see Figure 3.24.). PpSFD complementation lines were also slightly lighter, but still both types of complementation lines did have a significantly higher weight than *ads2.1* (see Figure 3.23.). For all intents and purposes, PpSFD and AtADS2 complementation seems to be very similar, meaning that PpSFD can fully substitute the function of AtADS2. The exact position of the double bond inserted into the C24 FA moiety does not seem to play a big role in this context, since PpSFD complementation lines contain 24:1;1 FAMES with mostly *n*-8 position double bonds and lesser amounts of the *n*-9 position, which is exclusively appearing in *A. thaliana* wild type (see Figure 3.26.). If both types of double bonds appear in the same stereochemistry (*trans* or *cis*) for both desaturases, the difference of one C-atom might not have a strong enough impact on the physical attributes of the FA to change its functionality in a membrane. However, the exact function of the double bond in sphingolipids is not known. It may be for adjusting membrane fluidity, or for allowing other types of lipid (like sterols) to better mix into the membranes, which could be important for lipid raft formation (Bhat and Panstruga 2005).

## 4.6. PpSFD might be part of a yet unknown class of bi-functional desaturases

PpSFD is a bi-functional desaturase and therefore structurally different from mono-functional desaturases. The FA desaturase AtADS2, which has a similar enzymatic function as PpSFD, is a monofunctional desaturase and therefore not closely related to PpSFD or other bi-functional desaturases. Phylogenetically, *PpSFD* clusters broadly with other bi-functional desaturases from plants, but it is definitely located in a separate cluster within this group (see Figure 3.8.). Neither LCB-desaturases nor front-end desaturases that are known from plants seem to be very closely related to *PpSFD*. Instead, the desaturases that are most closely related to *PpSFD* were all considered hypothetical proteins by the NCBI database (Coordinators 2016) and most derived from non-plant organisms. It is not known if any of the other enzymes from the same cluster have a similar enzymatic activity as *PpSFD*, since none of these enzymes have been analyzed in any way before. Since the closest relative to *PpSFD* is a gene from the liverwort *M. polymorpha*, it could be possible that this type of enzyme evolved already in early bryophytes. However, the presence of similar genes in diatoms, fungi and choanoflagellates would hint towards an even earlier ancestor if all these genes actually derived from the same kind of desaturase. The closest relation to desaturases of known function are those of the  $\Delta 5$  front-end desaturases, which form a separate cluster on the phylogenetic tree (see Figure 3.8.). It is possible that there exists an early common ancestor of  $\Delta 5$  desaturase and the new undefined cluster. It was already proposed before that most front-end desaturases might derive from a single type of desaturase, possibly a  $\Delta 5$  or  $\Delta 6$  desaturase (Meesapyodsuk and Qiu 2012). However, to the knowledge of the author, there is no front-end desaturase yet been reported that catalyzes a similar reaction as PpSFD: the formation of the first double bond into a C24 FA. This type of desaturase might have evolved independently in bryophytes and diatoms, while the same function in vascular plants evolved from mono-functional desaturases.

## 4.7. Outlook

In this work, the bryophyte model organism *P. patens* was analyzed for its lipid composition in a scale and detail that has not been performed for any other non-vascular plant to date. However, there are still many open questions about lipid synthesis in this organism that lied beyond the scope of this work. Especially the exact composition of those lipid classes that were only detected in traces in *P. patens* – namely betaines, SQDG and GIPC – requires further work. Overcoming limiting factors for analysis with the techniques applied in this study come down to two major points: 1) Extracting lipids from more moss sample material to raise signal intensity for minor lipid compounds, and 2) developing additional MRM transitions of the compounds in question to better distinguish them from other lipids in the extracts. Especially the composition of GIPC will be of high interest here and how they differ from other sphingolipid classes in *P. patens*. To further investigate the development of lipid synthesis from marine plants to vascular plants, more other plant organisms should be analyzed for their lipidome. Obvious candidates would be the liverwort *M. polymorpha*, which is closely related to mosses, and the early vascular plant



*Selaginella moellendorffii*. It would be interesting to see whether sphingolipid composition and function is similar in these organisms that share more physiological features with *P. patens* than *A. thaliana*.

The compared to *A. thaliana* very different sphingolipid composition in *P. patens* should also be the topic of further studies in the future. The presence of virtually no GIPCs is of course interesting, but also the fact that the glycosyl-ceramides in *P. patens* are dominated by only one single lipid species. This single lipid species could be of crucial importance for *P. patens* and knocking out genes for its synthesis could yield strong phenotypes in *P. patens*. The same can also be applied to other sphingolipid modifying genes, like LCB-hydroxylases and -desaturases. Future work on *P. patens* sphingolipids should focus on the synthesis of glycosyl-ceramides and how important they are for survival in *P. patens*.

Also of interest would be what reaction the hypothetical proteins catalyze that were discovered in the phylogenetic comparison of PpSFD to other desaturases. If the cluster of unknown desaturases with genes from *M. polymorpha* and diatoms also desaturate sphingolipids or very long chain FAs like PpSFD does, this cluster could be considered a new type of bi-functional desaturases besides front-end desaturases and LCB desaturases. The analysis of just one desaturase from this cluster is certainly not sufficient to characterize this novel cluster in more general terms, so more work has to be done on other genes in this cluster. Other questions surrounding these unknown bi-functional desaturases are: Do they have similar double bond position preference as PpSFD (*n*-8)? Are KO-mutants of these genes involved in the stress response? Do some of these genes even fulfill completely different functions? How far back in plant evolution do these desaturases appear? Is it a stringent evolution or does the function of sphingolipid FA desaturation in bi-functional desaturases evolve multiple times? Since non-vascular plants are still only superficially studied for their lipid composition, many more questions might arise once more studies are done on this topic.

In this work, the importance of sphingolipid desaturation was shown to not only appear in vascular plants like *A. thaliana*, but also in bryophytes. But still, there is no good model available on why the desaturation of sphingolipids has these effects in plants. The comparison between the *n*-8 desaturase PpSFD and the *n*-9 desaturase AtADS2 also showed that the exact position of the double bond does not seem to affect its functionality as long as the double bond is present at all. It would be interesting to see whether FA desaturases with a stronger difference in position preference would still be able of rescuing the phenotype of *ads2* plants at cold stress. A possible candidate for such a desaturase could be the  $\Delta 5$  desaturase BsDES from *Bacillus subtilis* (Aguilar, Cronan et al. 1998). Since the topic of lipid rafts is of high interest when researching sphingolipids, analysis of lipid raft formation in *A. thaliana* and *P. patens* could lead to new insights into which lipid attributes are necessary for microdomain formation. As a technique, the lipid probe approach used by Nagano (Nagano, Ishikawa et al. 2016) could be useful in this regard. Since hydroxylation of glycosyl-ceramides has been shown in this work to be crucial for lipid raft formation in rice, sphingolipid FA desaturation (and possibly LCB desaturation) could also be important in membrane microdomain formation.

*P. patens* wild type and KO-mutants were tested in this work only on cold stress conditions, which is comparable to a long-term cold acclimatization (Buchanan 2015). However, the stronger abiotic stress of freezing was not tested, which could have an even bigger influence on *P. patens*, including mortality rate, lipid composition and other factors.

Therefore, further studies on *P. patens* should include freezing stress, dry stress and other abiotic stresses and evaluate differences in lipid modifications under each condition. This would give us a broader overview on which exact roles different lipids play to maintain cell viability in bryophytes, which have less developed root systems or cuticulae compared to vascular plants.

## 5. References

---

- Aguilar, P. S., J. E. Cronan and D. De Mendoza (1998). "A *Bacillus subtilis* gene induced by cold shock encodes a membrane phospholipid desaturase." *Journal of bacteriology* **180**(8): 2194-2200.
- Alonso, D. L., F. Garcia-Maroto, J. Rodriguez-Ruiz, J. Garrido and M. Vilches (2003). "Evolution of the membrane-bound fatty acid desaturases." *Biochemical systematics and ecology* **31**(10): 1111-1124.
- Andreou, A., F. Brodhun and I. Feussner (2009). "Biosynthesis of oxylipins in non-mammals." *Progress in lipid research* **48**(3): 148-170.
- Artimo, P., M. Jonnalagedda, K. Arnold, D. Baratin, G. Csardi, E. De Castro, S. Duvaud, V. Flegel, A. Fortier and E. Gasteiger (2012). "ExpASY: SIB bioinformatics resource portal." *Nucleic acids research* **40**(W1): W597-W603.
- Ashton, N. and D. Cove (1977). "The isolation and preliminary characterisation of auxotrophic and analogue resistant mutants of the moss, *Physcomitrella patens*." *Molecular and General Genetics MGG* **154**(1): 87-95.
- Badea, C. and S. K. Basu (2009). "The effect of low temperature on metabolism of membrane lipids in plants and associated gene expression." *Plant Omics* **2**(2): 78.
- Beike, A. K. (2013). *The Transcriptomic and Physiological Cold Stress Response of Physcomitrella Patens*, Albert-Ludwigs-Universität Freiburg im Breisgau.
- Beike, A. K., C. Jaeger, F. Zink, E. L. Decker and R. Reski (2014). "High contents of very long-chain polyunsaturated fatty acids in different moss species." *Plant cell reports* **33**(2): 245-254.
- Benhassaine-Kesri, G., F. Aid, C. Demandre, J. C. Kader and P. Mazliak (2002). "Drought stress affects chloroplast lipid metabolism in rape (*Brassica napus*) leaves." *Physiologia Plantarum* **115**(2): 221-227.
- Benveniste, P. (2004). "Biosynthesis and accumulation of sterols." *Annu. Rev. Plant Biol.* **55**: 429-457.
- Bertani, G. (1951). "STUDIES ON LYSOGENESIS I.: The Mode of Phage Liberation by Lysogenic *Escherichia coli*1." *Journal of bacteriology* **62**(3): 293.
- Bhat, R. A. and R. Panstruga (2005). "Lipid rafts in plants." *Planta* **223**(1): 5.
- Bigogno, C., I. Khozin-Goldberg, S. Boussiba, A. Vonshak and Z. Cohen (2002). "Lipid and fatty acid composition of the green oleaginous alga *Parietochloris incisa*, the richest plant source of arachidonic acid." *Phytochemistry* **60**(5): 497-503.
- Bohn, M., S. Lühje, P. Sperling, E. Heinz and K. Dörffling (2007). "Plasma membrane lipid alterations induced by cold acclimation and abscisic acid treatment of winter wheat seedlings differing in frost resistance." *Journal of plant physiology* **164**(2): 146-156.

- Bohnert, H. J., D. E. Nelson and R. G. Jensen (1995). "Adaptations to environmental stresses." The plant cell **7**(7): 1099.
- Buchanan, B. B. (2015). Biochemistry and molecular biology of plants, John Wiley & Sons.
- Buré, C., J.-L. Cacas, S. Mongrand and J.-M. Schmitter (2014). "Characterization of glycosyl inositol phosphoryl ceramides from plants and fungi by mass spectrometry." Analytical and bioanalytical chemistry **406**(4): 995-1010.
- Chen, M., J. E. Markham and E. B. Cahoon (2012). "Sphingolipid  $\Delta 8$  unsaturation is important for glucosylceramide biosynthesis and low-temperature performance in Arabidopsis." The Plant Journal **69**(5): 769-781.
- Chen, M., J. E. Markham, C. R. Dietrich, J. G. Jaworski and E. B. Cahoon (2008). "Sphingolipid long-chain base hydroxylation is important for growth and regulation of sphingolipid content and composition in Arabidopsis." The Plant Cell **20**(7): 1862-1878.
- Chen, M. and J. J. Thelen (2013). "ACYL-LIPID DESATURASE2 is required for chilling and freezing tolerance in Arabidopsis." The plant cell **25**(4): 1430-1444.
- Christie, W. W. (1989). Gas chromatography and lipids, Oily.
- Christie, W. W. (1998). "Gas chromatography-mass spectrometry methods for structural analysis of fatty acids." Lipids **33**(4): 343-353.
- Christie, W. W. (2009). Methylation of fatty acids—a beginner's guide.
- Clarke, J. T., R. C. Warnock and P. C. Donoghue (2011). "Establishing a time-scale for plant evolution." New Phytol **192**(1): 266-301.
- Coordinators, N. R. (2016). "Database resources of the national center for biotechnology information." Nucleic acids research **44**(Database issue): D7.
- Cove, D. (2005). "The moss *Physcomitrella patens*." Annu. Rev. Genet. **39**: 339-358.
- Cuming, A. (2011). "Molecular bryology: mosses in the genomic era." Field Bryology **103**(9): e13.
- De Palma, M., S. Grillo, I. Massarelli, A. Costa, G. Balogh, L. Vigh and A. Leone (2008). "Regulation of desaturase gene expression, changes in membrane lipid composition and freezing tolerance in potato plants." Molecular Breeding **21**(1): 15-26.
- Decker, E. L., G. Gorr and R. Reski (2003). "Moss—an innovative tool for protein production." BIOforum Europe **2**(2003): 96-97.
- Decker, E. L. and R. Reski (2004). "The moss bioreactor." Current Opinion in Plant Biology **7**(2): 166-170.
- Degenkolbe, T., P. Giavalisco, E. Zuther, B. Seiwert, D. K. Hinch and L. Willmitzer (2012). "Differential remodeling of the lipidome during cold acclimation in natural accessions of *Arabidopsis thaliana*." The Plant Journal **72**(6): 972-982.
- Dembitsky, V. M. (1993). "Lipids of bryophytes." Progress in lipid research **32**(3): 281-356.
- Dembitsky, V. M. (1996). "Betaine ether-linked glycerolipids: chemistry and biology." Progress in lipid research **35**(1): 1-51.

- Dunn, J. L., J. D. Turnbull and S. A. Robinson (2004). "Comparison of solvent regimes for the extraction of photosynthetic pigments from leaves of higher plants." Functional Plant Biology **31**(2): 195-202.
- Engel, P. P. (1968). "The induction of biochemical and morphological mutants in the moss *Physcomitrella patens*." American Journal of Botany: 438-446.
- Eskelinen, O. (2002). Diet of the wood lemming *Myopus schisticolor*. Annales Zoologici Fennici, JSTOR.
- Francis, G. W. and K. Veland (1987). "Alkylthiolation for the determination of double-bond positions in linear alkenes." Journal of Chromatography A **219**(3): 379-384.
- Gigon, A., A.-R. Matos, D. Laffray, Y. Zuily-Fodil and A.-T. Pham-Thi (2004). "Effect of drought stress on lipid metabolism in the leaves of *Arabidopsis thaliana* (ecotype Columbia)." Annals of botany **94**(3): 345-351.
- Girke, T., H. Schmidt, U. Zähringer, R. Reski and E. Heinz (1998). "Identification of a novel D6-acyl-group desaturase by targeted gene disruption in *Physcomitrella patens*." The Plant Journal **15**(1): 39-48.
- Glime, J. M. (2007). *Bryophyte ecology*. Vol. 1. Physiological ecology. E-book sponsored by Michigan Technological University and the International Association of Bryologists.
- Griffiths, W. J. and Y. Wang (2009). "Mass spectrometry: from proteomics to metabolomics and lipidomics." Chemical Society Reviews **38**(7): 1882-1896.
- Grimsley, N. H., J. M. Grimsley and E. Hartmann (1981). "Fatty acid composition of mutants of the moss *Physcomitrella patens*." Phytochemistry **20**(7): 1519-1524.
- Guschina, I. A. and J. L. Harwood (2006). "Lipids and lipid metabolism in eukaryotic algae." Progress in lipid research **45**(2): 160-186.
- Hartmann, E., P. Beutelmann, O. Vandekerkhove, R. Euler and G. Kohn (1986). "Moss cell cultures as sources of arachidonic and eicosapentaenoic acids." FEBS letters **198**(1): 51-55.
- Harwood, J. L. and I. A. Guschina (2009). "The versatility of algae and their lipid metabolism." Biochimie **91**(6): 679-684.
- Hashimoto, M., M. S. Hossain, H. Yamasaki, K. Yazawa and S. Masumura (1999). "Effects of eicosapentaenoic acid and docosahexaenoic acid on plasma membrane fluidity of aortic endothelial cells." Lipids **34**(12): 1297-1304.
- Henry, R. J. (1997). Practical applications of plant molecular biology, Nelson Thornes.
- Hiss, M., O. Laule, R. M. Meskauskiene, M. A. Arif, E. L. Decker, A. Erxleben, W. Frank, S. T. Hanke, D. Lang and A. Martin (2014). "Large-scale gene expression profiling data for the model moss *Physcomitrella patens* aid understanding of developmental progression, culture and stress conditions." The Plant Journal **79**(3): 530-539.
- Hodgetts, H. (2010). *Aphanorrhagma patens (Physcomitrella patens)*, spreading earth-moss. . Mosses and liverworts of Britain and Ireland: a field guide. I. B. Atherton, S; Lawley, M. London, British Bryological Society: 567.
- Hohe, A. and R. Reski (2002). "Optimisation of a bioreactor culture of the moss *Physcomitrella patens* for mass production of protoplasts." Plant Science **163**(1): 69-74.

- Holthuis, J. C. and A. K. Menon (2014). "Lipid landscapes and pipelines in membrane homeostasis." Nature **510**(7503): 48.
- Ishikawa, T., Y. Ito and M. Kawai-Yamada (2016). "Molecular characterization and targeted quantitative profiling of the sphingolipidome in rice." The Plant Journal **88**(4): 681-693.
- Johnson, M., I. Zaretskaya, Y. Raytselis, Y. Merezhuik, S. McGinnis and T. L. Madden (2008). "NCBI BLAST: a better web interface." Nucleic acids research **36**(suppl\_2): W5-W9.
- Kaewsuwan, S., E. B. Cahoon, P.-F. Perroud, C. Wiwat, N. Panvisavas, R. S. Quatrano, D. J. Cove and N. Bunyapraphatsara (2006). "Identification and functional characterization of the moss *Physcomitrella patens*  $\Delta 5$ -desaturase gene involved in arachidonic and eicosapentaenoic acid biosynthesis." Journal of Biological Chemistry **281**(31): 21988-21997.
- Karg, S. R. and P. T. Kallio (2009). "The production of biopharmaceuticals in plant systems." Biotechnology advances **27**(6): 879-894.
- Karunen, P. (1977). "Determination of fatty acid composition of spore lipids of the moss *Polytrichum commune* by glass capillary column gas chromatography." Physiologia Plantarum **40**(4): 239-243.
- Karunen, P. and E. ARO (1979). "Fatty acid composition of polar lipids in *Ceratodon purpureus* and *Pleurozium schreberi*." Physiologia Plantarum **45**(2): 265-269.
- Kenrick, P. and P. R. Crane (1997). "The origin and early evolution of plants on land." Nature **389**(6646): 33.
- Khozin-Goldberg, I., H. Z. Yu, D. Adlerstein, S. Didi-Cohen, Y. M. Heimer and Z. Cohen (2000). "Triacylglycerols of the red microalga *Porphyridium cruentum* can contribute to the biosynthesis of eukaryotic galactolipids." Lipids **35**(8): 881-889.
- Klug, L., P. Tarazona, C. Gruber, K. Grillitsch, B. Gasser, M. Trötz Müller, H. Köfeler, E. Leitner, I. Feussner and D. Mattanovich (2014). "The lipidome and proteome of microsomes from the methylotrophic yeast *Pichia pastoris*." Biochimica Et Biophysica Acta (BBA)-Molecular and Cell Biology of Lipids **1841**(2): 215-226.
- Knight, C. D., D. J. Cove, A. C. Cuming and R. S. Quatrano (2002). "Moss gene technology." Molecular plant biology **2**: 285-301.
- König, S., K. Feussner, M. Schwarz, A. Kaefer, T. Iven, M. Landesfeind, P. Ternes, P. Karlovsky, V. Lipka and I. Feussner (2012). "Arabidopsis mutants of sphingolipid fatty acid  $\alpha$ -hydroxylases accumulate ceramides and salicylates." New Phytologist **196**(4): 1086-1097.
- Künzler, K. and W. Eichenberger (1997). "Betaine lipids and zwitterionic phospholipids in plants and fungi." Phytochemistry **46**(5): 883-892.
- Lenarčič, T., I. Albert, H. Böhm, V. Hodnik, K. Pirc, A. B. Zavec, M. Podobnik, D. Pahovnik, E. Žagar and R. Pruitt (2017). "Eudicot plant-specific sphingolipids determine host selectivity of microbial NLP cytolysins." Science **358**(6369): 1431-1434.
- Li, J., P. Nagpal, V. Vitart, T. C. McMorris and J. Chory (1996). "A role for brassinosteroids in light-dependent development of *Arabidopsis*." Science **272**(5260): 398-401.
- Luttgeharm, K. D., A. N. Kimberlin and E. B. Cahoon (2016). Plant sphingolipid metabolism and function. Lipids in Plant and Algae Development, Springer: 249-286.

- Marchler-Bauer, A., M. K. Derbyshire, N. R. Gonzales, S. Lu, F. Chitsaz, L. Y. Geer, R. C. Geer, J. He, M. Gwadz and D. I. Hurwitz (2014). "CDD: NCBI's conserved domain database." Nucleic acids research **43**(D1): D222-D226.
- Markham, J. E. and J. G. Jaworski (2007). "Rapid measurement of sphingolipids from *Arabidopsis thaliana* by reversed-phase high-performance liquid chromatography coupled to electrospray ionization tandem mass spectrometry." Rapid Communications in Mass Spectrometry **21**(7): 1304-1314.
- Markham, J. E., J. Li, E. B. Cahoon and J. G. Jaworski (2006). "Separation and identification of major plant sphingolipid classes from leaves." Journal of Biological Chemistry **281**(32): 22684-22694.
- Markham, J. E., D. V. Lynch, J. A. Napier, T. M. Dunn and E. B. Cahoon (2013). "Plant sphingolipids: function follows form." Current opinion in plant biology **16**(3): 350-357.
- Markham, J. E., D. Molino, L. Gissot, Y. Bellec, K. Hématy, J. Marion, K. Belcram, J.-C. Palauqui, B. Satiat-JeuneMaître and J.-D. Faure (2011). "Sphingolipids containing very-long-chain fatty acids define a secretory pathway for specific polar plasma membrane protein targeting in *Arabidopsis*." The Plant Cell **23**(6): 2362-2378.
- Markham, N. R. and M. Zuker (2008). UNAFold. Bioinformatics, Springer: 3-31.
- Matyash, V., G. Liebisch, T. V. Kurzchalia, A. Shevchenko and D. Schwudke (2008). "Lipid extraction by methyl-tert-butyl ether for high-throughput lipidomics." Journal of lipid research **49**(5): 1137-1146.
- Meesapyodsuk, D. and X. Qiu (2012). "The Front-end Desaturase: Structure, Function, Evolution and Biotechnological Use." Lipids **47**(3): 227-237.
- Miquel, M. (1992). "Browse J (1992) *Arabidopsis* mutants deficient in polyunsaturated fatty acid synthesis." Biochemical and genetic characterization of a plant oleoyl-phosphatidylcholine desaturase. J. Biol. Chem **267**(3): 1502-1509.
- Morikawa, T., H. Saga, H. Hashizume and D. Ohta (2009). "CYP710A genes encoding sterol C22-desaturase in *Physcomitrella patens* as molecular evidence for the evolutionary conservation of a sterol biosynthetic pathway in plants." Planta **229**(6): 1311-1322.
- Mullis, K. B. (1987). Process for amplifying nucleic acid sequences, Google Patents.
- Murphy, D. J. (1999). "Production of novel oils in plants." Current opinion in biotechnology **10**(2): 175-180.
- Nagano, M., T. Ishikawa, M. Fujiwara, Y. Fukao, Y. Kawano, M. Kawai-Yamada and K. Shimamoto (2016). "Plasma membrane microdomains are essential for Rac1-RbohB/H-mediated immunity in rice." The Plant Cell **28**(8): 1966-1983.
- O'Neill, C. M., S. Gill, D. Hobbs, C. Morgan and I. Bancroft (2003). "Natural variation for seed oil composition in *Arabidopsis thaliana*." Phytochemistry **64**(6): 1077-1090.
- Oñate-Sánchez, L. and J. Vicente-Carbajosa (2008). "DNA-free RNA isolation protocols for *Arabidopsis thaliana*, including seeds and siliques." BMC research notes **1**(1): 93.
- Porra, R., W. Thompson and P. Kriedemann (1989). "Determination of accurate extinction coefficients and simultaneous equations for assaying chlorophylls a and b extracted with four

- different solvents: verification of the concentration of chlorophyll standards by atomic absorption spectroscopy." *Biochimica et Biophysica Acta (BBA)-Bioenergetics* **975**(3): 384-394.
- Proctor, M. C. F., R. Ligrone and J. G. Duckett (2007). "Desiccation Tolerance in the Moss *Polytrichum formosum*: Physiological and Fine-structural Changes during Desiccation and Recovery" Proctor et al. — Desiccation Tolerance in the Moss *Polytrichum formosum* Proctor et al. — Desiccation Tolerance in the Moss *Polytrichum formosum*." *Annals of Botany* **99**(1): 75-93.
- Reich, M., C. Göbel, A. Kohler, M. Buée, F. Martin, I. Feussner and A. Polle (2009). "Fatty acid metabolism in the ectomycorrhizal fungus *Laccaria bicolor*." *New Phytologist* **182**(4): 950-964.
- Rensing, S. A., D. Lang, A. D. Zimmer, A. Terry, A. Salamov, H. Shapiro, T. Nishiyama, P.-F. Perroud, E. A. Lindquist and Y. Kamisugi (2008). "The *Physcomitrella* genome reveals evolutionary insights into the conquest of land by plants." *Science* **319**(5859): 64-69.
- Repellin, A., A. P. Thi, A. Tashakorje, Y. Sahseh, C. Daniel and Y. Zuily-Fodil (1997). "Leaf membrane lipids and drought tolerance in young coconut palms (*Cocos nucifera* L.)." *European Journal of Agronomy* **6**(1-2): 25-33.
- Reski, R. and W. O. Abel (1985). "Induction of budding on chloronemata and caulonemata of the moss, *Physcomitrella patens*, using isopentenyladenine." *Planta* **165**(3): 354-358.
- Roads, E., R. E. Longton and P. Convey (2014). "Millennial timescale regeneration in a moss from Antarctica." *Current Biology* **24**(6): R222-R223.
- Ruiz-Lopez, N., R. P. Haslam, J. A. Napier and O. Sayanova (2014). "Successful high-level accumulation of fish oil omega-3 long-chain polyunsaturated fatty acids in a transgenic oilseed crop." *The Plant Journal* **77**(2): 198-208.
- Rutten, D. and K. A. Santarius (1992). "Relationship between frost tolerance and sugar concentration of various bryophytes in summer and winter." *Oecologia* **91**(2): 260-265.
- Schaefer, D., J.-P. Zryd, C. Knight and D. Cove (1991). "Stable transformation of the moss *Physcomitrella patens*." *Molecular and General Genetics MGG* **226**(3): 418-424.
- Schaeffer, A., R. Bronner, P. Benveniste and H. Schaller (2001). "The ratio of campesterol to sitosterol that modulates growth in *Arabidopsis* is controlled by *STEROL METHYLTRANSFERASE 2; 1*." *The Plant Journal* **25**(6): 605-615.
- Scholz, J., F. Brodhun, E. Hornung, C. Herrfurth, M. Stumpe, A. K. Beike, B. Faltin, W. Frank, R. Reski and I. Feussner (2012). "Biosynthesis of allene oxides in *Physcomitrella patens*." *BMC plant biology* **12**(1): 228.
- Shanklin, J. and E. B. Cahoon (1998). "Desaturation and related modifications of fatty acids." *Annual review of plant biology* **49**(1): 611-641.
- Smallwood, M. and D. J. Bowles (2002). "Plants in a cold climate." *Philosophical Transactions of the Royal Society B: Biological Sciences* **357**(1423): 831-847.
- Smith, M. A., M. Dauk, H. Ramadan, H. Yang, L. E. Seamons, R. P. Haslam, F. Beaudoin, I. Ramirez-Erosa and L. Forseille (2013). "Involvement of *Arabidopsis* *ACYL-COENZYME A DESATURASE-LIKE2* (*At2g31360*) in the biosynthesis of the very-long-chain monounsaturated fatty acid components of membrane lipids." *Plant physiology* **161**(1): 81-96.
- Spolaore, P., C. Joannis-Cassan, E. Duran and A. Isambert (2006). "Commercial applications of microalgae." *Journal of bioscience and bioengineering* **101**(2): 87-96.

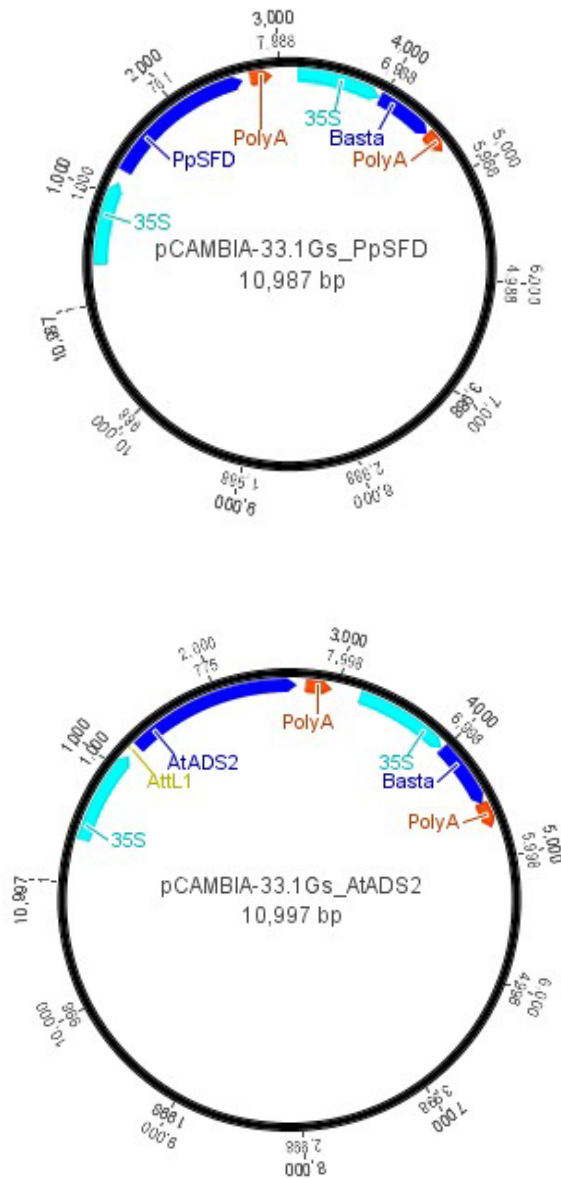


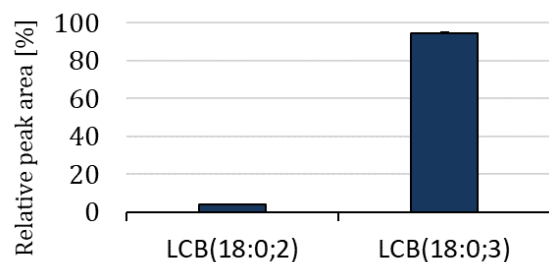
- Stumpe, M., C. Göbel, B. Faltin, A. K. Beike, B. Hause, K. Himmelsbach, J. Bode, R. Kramell, C. Wasternack and W. Frank (2010). "The moss *Physcomitrella patens* contains cyclopentenones but no jasmonates: mutations in allene oxide cyclase lead to reduced fertility and altered sporophyte morphology." *New Phytologist* **188**(3): 740-749.
- Tarazona, P., K. Feussner and I. Feussner (2015). "An enhanced plant lipidomics method based on multiplexed liquid chromatography–mass spectrometry reveals additional insights into cold- and drought-induced membrane remodeling." *The Plant Journal* **84**(3): 621-633.
- Tasseva, G., J. D. de Virville, C. Cantrel, F. Moreau and A. Zachowski (2004). "Changes in the endoplasmic reticulum lipid properties in response to low temperature in *Brassica napus*." *Plant Physiology and Biochemistry* **42**(10): 811-822.
- Thompson, J. D., T. J. Gibson and D. G. Higgins (2003). "Multiple sequence alignment using ClustalW and ClustalX." *Current protocols in bioinformatics*(1): 2.3. 1-2.3. 22.
- Tjellström, H., L. I. Hellgren, Å. Wieslander and A. S. Sandelius (2010). "Lipid asymmetry in plant plasma membranes: phosphate deficiency-induced phospholipid replacement is restricted to the cytosolic leaflet." *The FASEB Journal* **24**(4): 1128-1138.
- Touchstone, J. C. (1995). "Thin-layer chromatographic procedures for lipid separation." *Journal of Chromatography B: Biomedical Sciences and Applications* **671**(1-2): 169-195.
- Uemura, M., R. A. Joseph and P. L. Steponkus (1995). "Cold acclimation of *Arabidopsis thaliana* (effect on plasma membrane lipid composition and freeze-induced lesions)." *Plant physiology* **109**(1): 15-30.
- Untergasser, A., I. Cutcutache, T. Koressaar, J. Ye, B. C. Faircloth, M. Remm and S. G. Rozen (2012). "Primer3—new capabilities and interfaces." *Nucleic acids research* **40**(15): e115-e115.
- Voet, D. and J. G. Voet (2004). "Biochemistry. Hoboken." *John Wiley & Sons* **1**: 591.
- Vogel, G. and W. Eichenberger (1992). "Betaine lipids in lower plants. Biosynthesis of DGTS and DGTA in *Ochromonas danica* (Chrysophyceae) and the possible role of DGTS in lipid metabolism." *Plant and cell physiology* **33**(4): 427-436.
- Volkman, J., S. Jeffrey, P. Nichols, G. Rogers and C. Garland (1989). "Fatty acid and lipid composition of 10 species of microalgae used in mariculture." *Journal of Experimental Marine Biology and Ecology* **128**(3): 219-240.
- Wang, T. L., D. J. Cove, P. Beutelmann and E. Hartmann (1980). "Isopentenyladenine from mutants of the moss, *Physcomitrella patens*." *Phytochemistry* **19**(6): 1103-1105.
- Wang, X., P. Yang, X. Zhang, Y. Xu, T. Kuang, S. Shen and Y. He (2009). "Proteomic analysis of the cold stress response in the moss, *Physcomitrella patens*." *Proteomics* **9**(19): 4529-4538.
- Wasternack, C. (2007). "Jasmonates: an update on biosynthesis, signal transduction and action in plant stress response, growth and development." *Annals of botany* **100**(4): 681-697.
- Welti, R., W. Li, M. Li, Y. Sang, H. Biesiada, H.-E. Zhou, C. Rajashekar, T. D. Williams and X. Wang (2002). "Profiling membrane lipids in plant stress responses role of phospholipase D $\alpha$  in freezing-induced lipid changes in *Arabidopsis*." *Journal of Biological Chemistry* **277**(35): 31994-32002.

- Welti, R. and X. Wang (2004). "Lipid species profiling: a high-throughput approach to identify lipid compositional changes and determine the function of genes involved in lipid metabolism and signaling." Current opinion in plant biology **7**(3): 337-344.
- Wewer, V., I. Dombrink, K. vom Dorp and P. Dörmann (2011). "Quantification of sterol lipids in plants by quadrupole time-of-flight mass spectrometry." Journal of lipid research **52**(5): 1039-1054.
- Xie, C. F. and H. X. Lou (2009). "Secondary metabolites in bryophytes: an ecological aspect." Chemistry & biodiversity **6**(3): 303-312.
- Yordanov, I., V. Velikova and T. Tsonev (2000). "Plant responses to drought, acclimation, and stress tolerance." Photosynthetica **38**(2): 171-186.
- Yu, B., C. Xu and C. Benning (2002). "Arabidopsis disrupted in SQD2 encoding sulfolipid synthase is impaired in phosphate-limited growth." Proceedings of the National Academy of Sciences **99**(8): 5732-5737.
- Yuanyuan, M., Z. Yali, L. Jiang and S. Hongbo (2009). "Roles of plant soluble sugars and their responses to plant cold stress." African Journal of Biotechnology **8**(10).
- Zank, T. K., U. Zähringer, C. Beckmann, G. Pohnert, W. Boland, H. Holtorf, R. Reski, J. Lerchl and E. Heinz (2002). "Cloning and functional characterisation of an enzyme involved in the elongation of  $\Delta$ 6-polyunsaturated fatty acids from the moss *Physcomitrella patens*." The Plant Journal **31**(3): 255-268.
- Zhu, S. Q., C. M. Yu, X. Y. Liu, B. H. Ji and D. M. Jiao (2007). "Changes in unsaturated levels of fatty acids in thylakoid PSII membrane lipids during chilling-induced resistance in rice." Journal of Integrative Plant Biology **49**(4): 463-471.

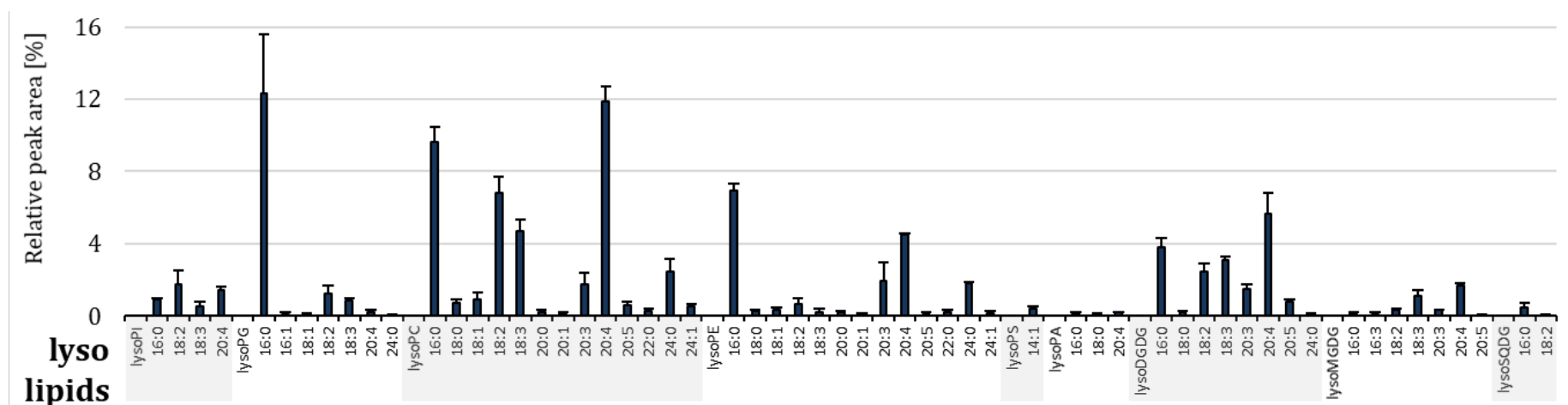
## 6. Appendix

**Appendix 1. Structure of plasmid constructs used for *Agrabacterium*-mediated transformation in *A. thaliana* *ads2.1* lines.** All constructs were based on the pCambia-33.1Gs plasmid.

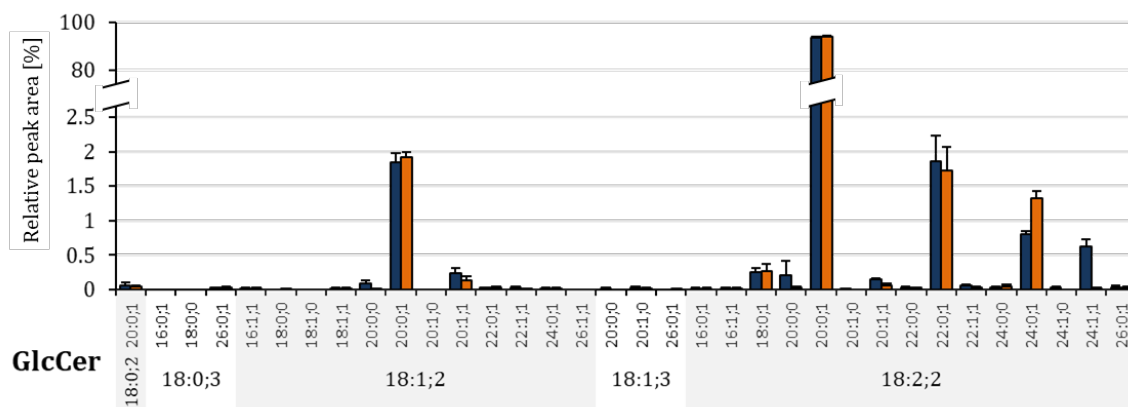
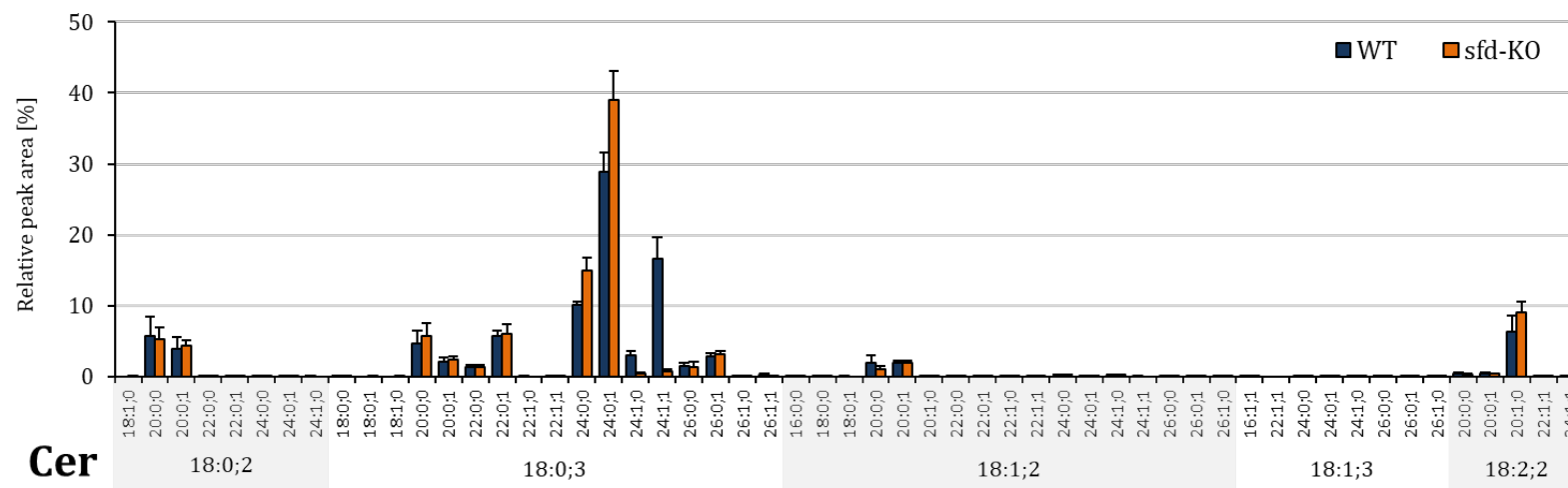




**Appendix 2. Free LCB composition in *P. patens* wild type.** Moss cultures were started by inoculation with disrupted moss tissue and grown in aerated (1% CO<sub>2</sub>) liquid cultures for 7 days. Lipids were extracted from lyophilized moss material using a one-phase isopropanol/hexane/water extraction. Lipid species were characterized via MRM-based UPLC-QTrap-ESI-MS analysis. Only lipid species detected with a relative peak area of > 0.01 % were included in the dataset. Data represents mean values with standard deviations of 4 biological replicates.



**Appendix 3. Lyso-lipid composition in *P. patens* wild type.** Subclasses include: lyso-phosphatidic acid (lysoPA), lyso-phosphatidyl-choline (lysoPC), lyso-phosphatidyl-ethanolamine (lysoPE), lyso-phosphatidyl-glycerol (lysoPG), lyso-phosphatidyl-inositol (lysoPI), lyso-phosphatidyl-serine (lysoPS), lyso-monogalactosyl-diacylglycerol (lysoMGDg), lyso-digalactosyl-diacylglycerol (lysoDGDG), lyso-sulfoquinovosyl-diacylglycerol (lysoSQDG). Moss cultures were started by inoculation with disrupted moss tissue and grown in aerated (1% CO<sub>2</sub>) liquid cultures for 7 days. Lipids were extracted from lyophilized moss material using a one-phase isopropanol/hexane/water extraction. Lipid species were characterized via MRM-based UPLC-QTrap-ESI-MS analysis. Only lipid species detected with a relative peak area of > 0.01 % were included in the dataset. Data represents mean values with standard deviations of 4 biological replicates.



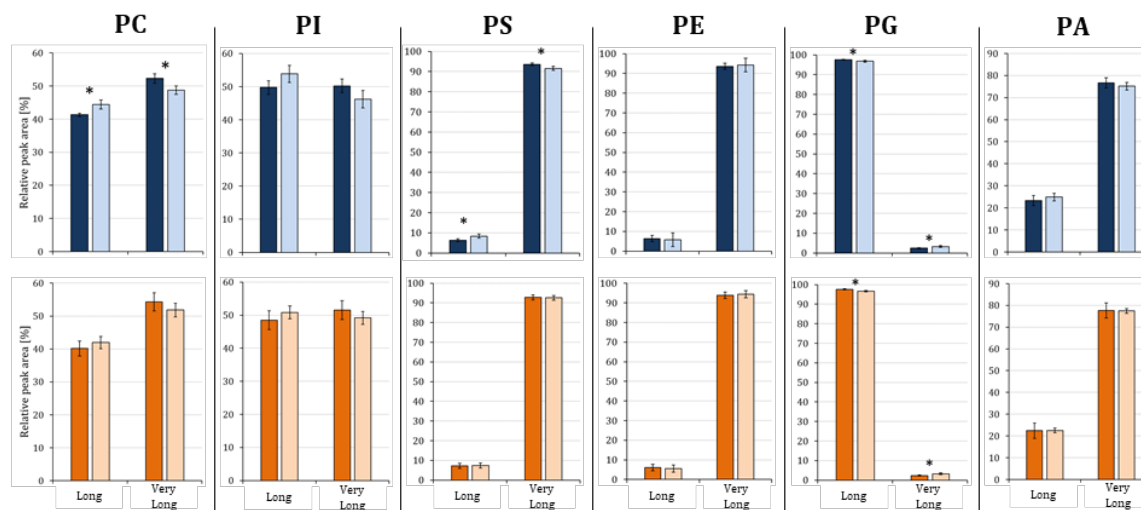
**Appendix 4. Sphingolipid composition in *P. patens* wild type & sfd-KO line.** Subclasses include: Ceramides (Cer), and glycosyl-ceramides (GlcCer). Moss cultures were started by inoculation with disrupted moss tissue and grown in aerated (1% CO<sub>2</sub>) liquid cultures for 7 days. Lipids were extracted from lyophilized moss material using a one-phase isopropanol/hexane/water extraction. Lipid species were characterized via MRM-based UPLC-QTrap-ESI-MS analysis. Only lipid species detected with a relative peak area of > 0.01 % were included in the dataset. Data represents mean values with standard deviations of 4 biological replicates.

**Appendix 5. Effects of cold stress on FAs chain length in combined lipid species of glycerolipids (phospholipids, glycolipids, neutral lipids).**

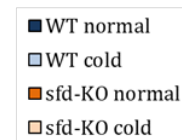
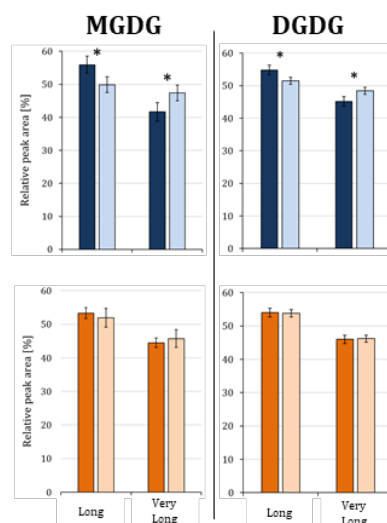
Samples were taken from *P. patens* wild type & *sfd*-KO plants, grown at normal conditions or treated with cold stress. Moss cultures were started by inoculation with disrupted moss tissue and grown in aerated (1% CO<sub>2</sub>) liquid cultures for 7 days. Cold treated samples were grown 1 additional day at 4 °C. Lipids were extracted from lyophilized moss material using a one-phase

isopropanol/hexane/water extraction. Lipid species were characterized via MRM-based UPLC-QTrap-ESI-MS analysis. Only lipid species detected with a relative peak area of > 0.01 % were included in the dataset. Data represent mean values with standard deviations of 4 biological replicates. “Long” lipids include all lipid species that contain only C16 & C18 fatty acids, but no C20 or longer fatty acids; “Very Long” lipids contain at least one C20-24 fatty acid moiety. Asterisks represent results of student *t*-test performed for the difference in relative peak area between normal & cold-stressed wild type or normal & cold-stressed KO-line. \* =  $p < 0.05$ , \*\* =  $p < 0.01$ , \*\*\* =  $p < 0.001$ .

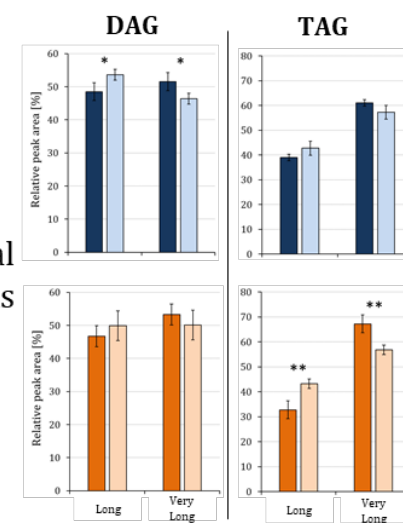
**Phospho-  
lipids**



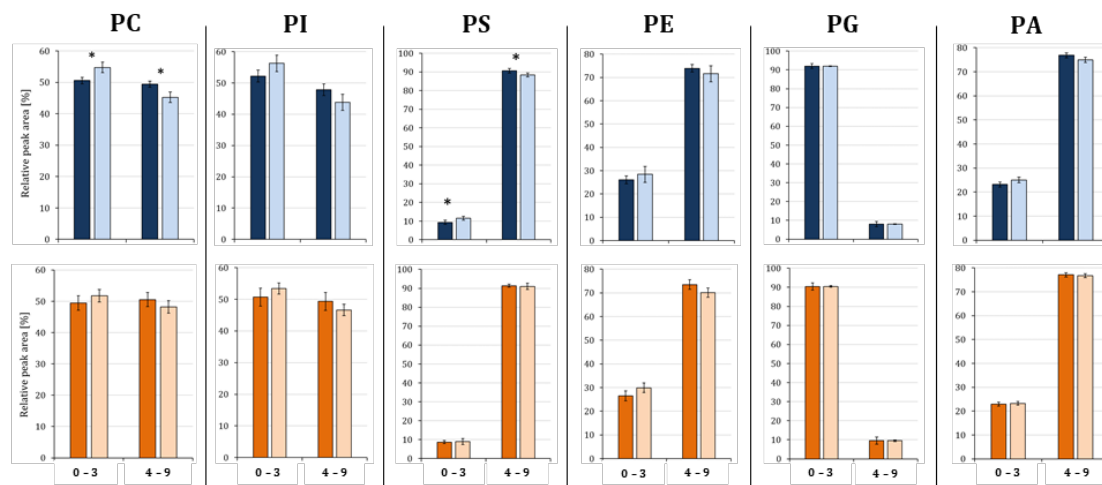
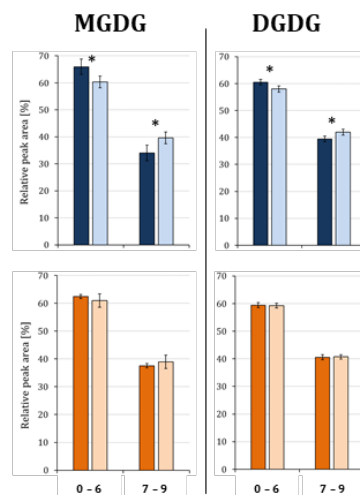
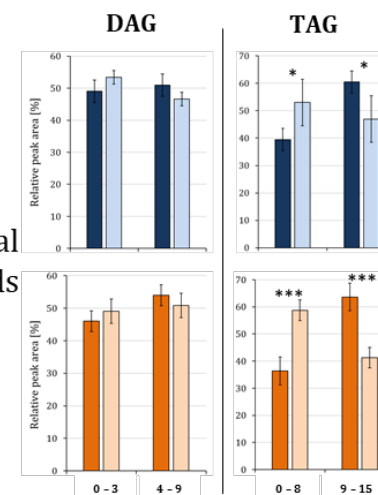
**Glyco-  
lipids**



**Neutral  
lipids**



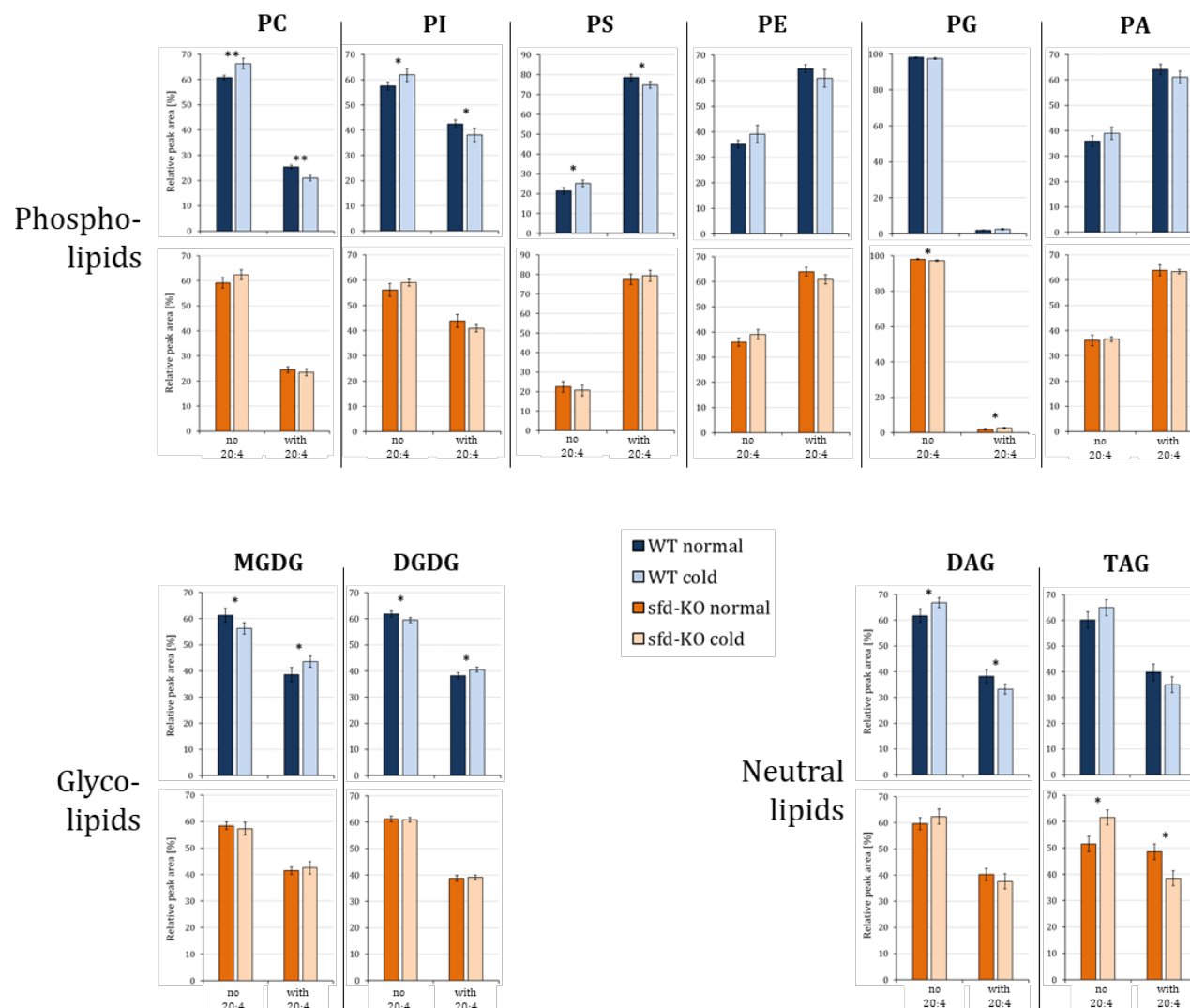
**Appendix 6. Effects of cold stress on total number of double bonds in combined lipid species of glycerolipids (phospholipids, glycolipids, neutral lipids).** Samples were taken from *P. patens* wild type & *sfd*-KO plants, grown at normal conditions or treated with cold stress. Moss cultures were started by inoculation with disrupted moss tissue and grown in aerated (1% CO<sub>2</sub>) liquid cultures for 7 days. Cold treated samples were grown 1 additional day at 4 °C. Lipids were extracted from lyophilized moss material using a one-phase isopropanol/hexane/water extraction. Lipid species were characterized via MRM-based UPLC-QTrap-ESI-MS analysis. Only lipid species detected with a relative peak area of > 0.01 % were included in the dataset. Data represent mean values with standard deviations of 4 biological replicates. Asterisks represent results of student *t*-test performed for the difference in relative peak area between normal & cold-stressed wild type or normal & cold-stressed KO-line. \* =  $p < 0.05$ , \*\* =  $p < 0.01$ , \*\*\* =  $p < 0.001$ .

Phospho-  
lipidsGlyco-  
lipidsNeutral  
lipids

**Appendix 7. Effects of cold stress on the amount of the FA 20:4 in combined lipid species of glycerolipids (phospholipids, glycolipids, neutral lipids).**

Samples were taken from *P. patens* wild type & *sfd*-KO plants, grown at normal conditions or treated with cold stress. Moss cultures were started by inoculation with disrupted moss tissue and grown in aerated (1% CO<sub>2</sub>) liquid cultures for 7 days. Cold treated samples were grown 1 additional day at 4 °C. Lipids were extracted from lyophilized moss material using a one-phase

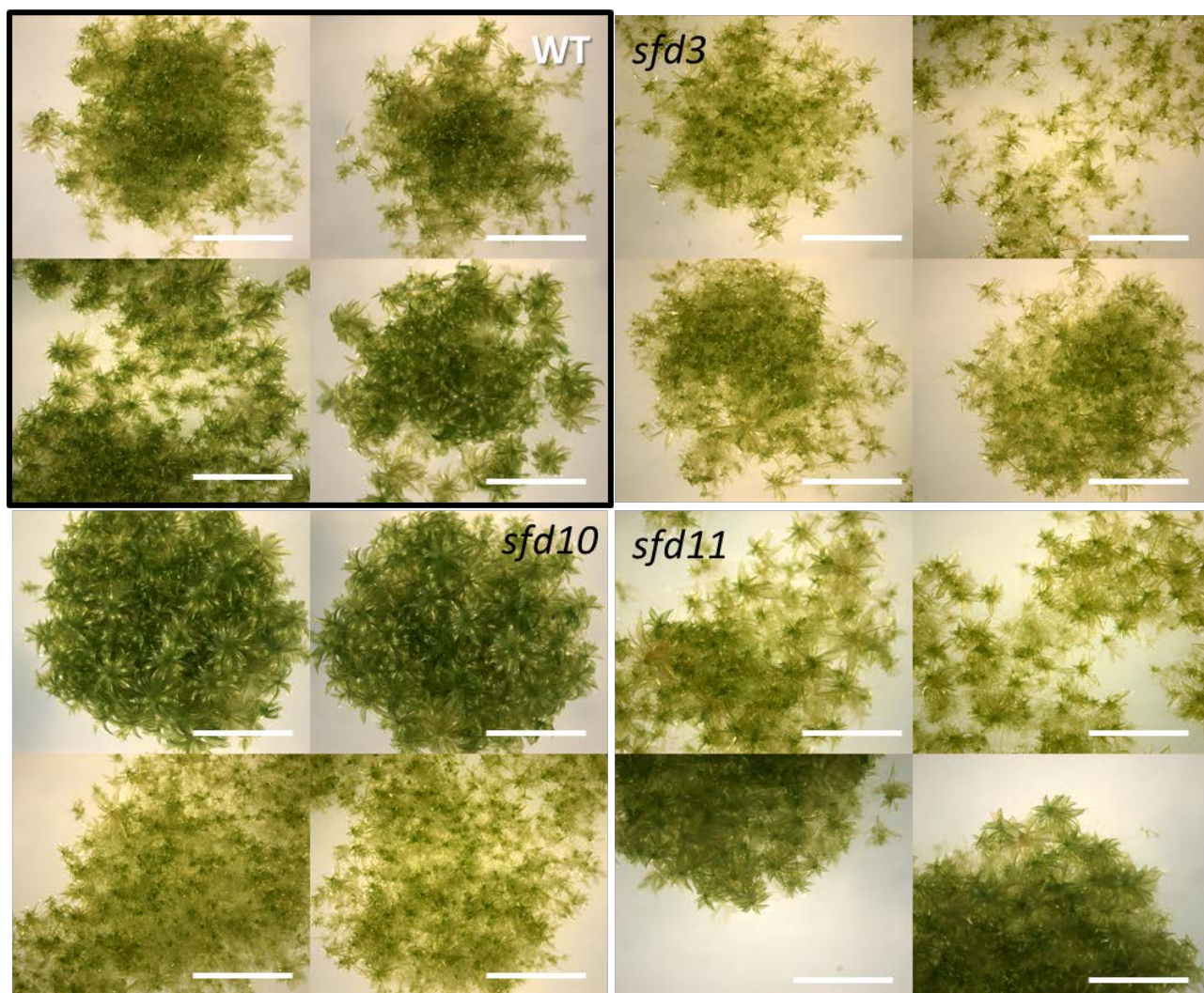
isopropanol/hexane/water extraction. Lipid species were characterized via MRM-based UPLC-QTrap-ESI-MS analysis. Only lipid species detected with a relative peak area of > 0.01% were included in the dataset. Data represent mean values with standard deviations of 4 biological replicates. Asterisks represent results of student *t*-test performed for the difference in relative peak area between normal & cold-stressed wild type or normal & cold-stressed KO-line. \* =  $p < 0.05$ , \*\* =  $p < 0.01$ , \*\*\* =  $p < 0.001$ .



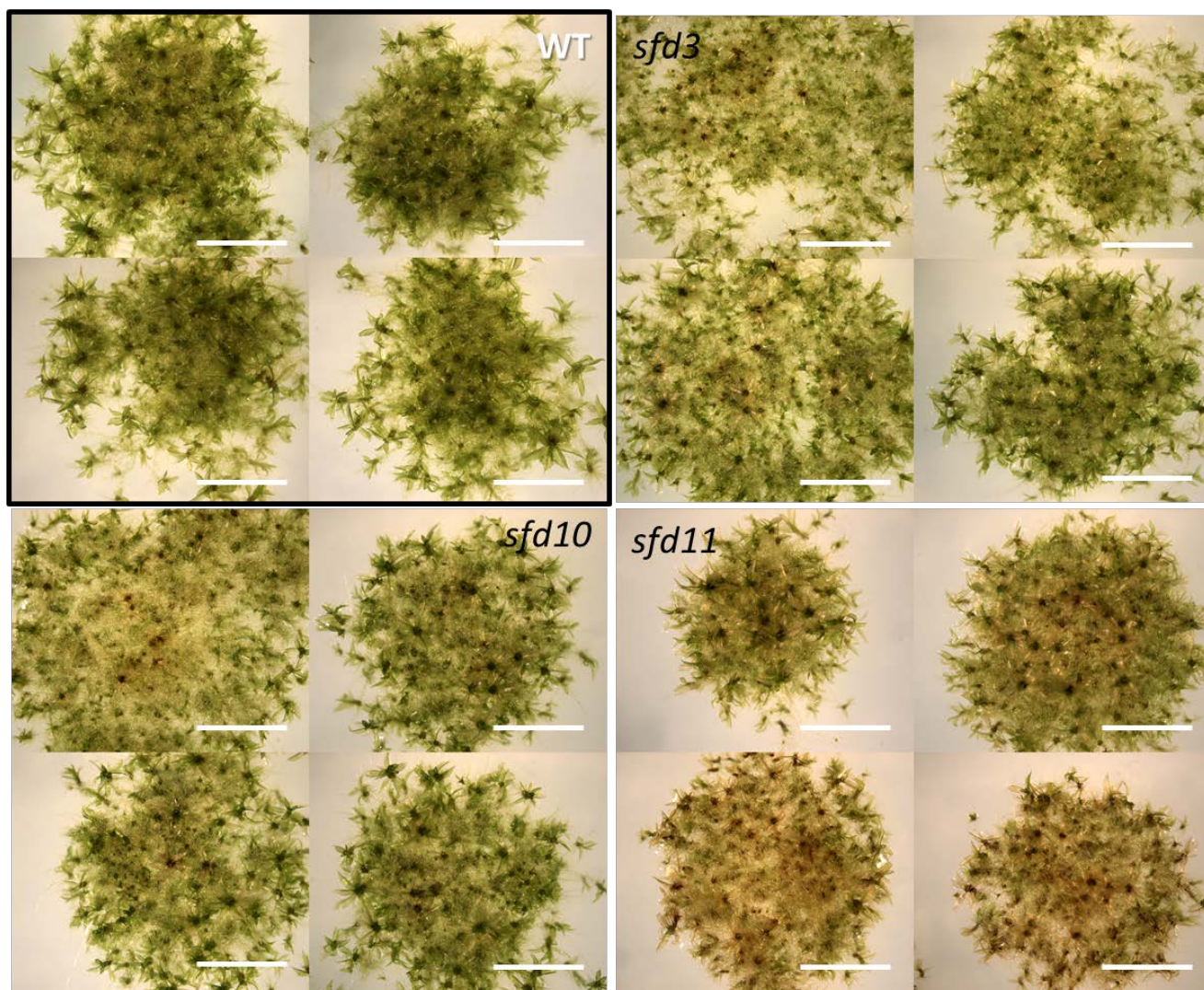


**Appendix 8. Protein IDs of peptides used for building a phylogenetic tree (see Figure 3.8).** Protein IDs were retrieved from NCBI (Johnson, Zaretskaya et al. 2008).

<b>Protein designation</b>	<b>ID (NCBI)</b>
P. patens o6-FADS	XP_024390435
<b>A.thaliana d9-ADS2</b>	NP_565721
<b>P. patens SFD</b>	XP_024359978
<b>P. patens SFD [pseudogene]</b>	PNR35346
M. polymorpha hyp. protein	OAE24732
T. oceanica hyp. protein	EJK64693
T. pseudonana hyp. protein	XP_002290058
R. allomycis hyp. protein	EPZ35951
S. rosetta d5-FADS [put]	XP_004998044
L. incisa d5-FADS	ADB81956
M. squamata d5-FADS	CAQ30478
M. polymorpha d5-FADS	AAT85663
P. patens d5-FADS	XP_024396886
M. alpina d5-FADS	ADE06661
N. gaditana hyp. protein	XP_005852476
P. tricornutum hyp. protein	XP_002183026
P. tricornutum d5-FADS	AAL92562
A. thaliana d8-SLD1	NP_191717
A. thaliana d8-SLD2	OAP10850
C. sativa d8-SLD [put]	XP_010506617
B. napus d8-SLD	NP_001302507
B. officinalis d8-SLD	Q9FR82
N. tabacum d8-SLD [put]	XP_009790286
Z. mays d8-SLD [put]	NP_00114588
M. polymorpha d8-SLD [put]	OAE27975
P. patens d8-SLD	XP_024364920
S. moellendorffii d8-SLD [put]	XP_002968817
C. purpureus Acet6	Q9LENO
C. purpureus d6-DES	Q9LEM9
P. patens d6-FADS	XP_024379482
P. tricornutum d6-FADS	ADI49419
M. squamata d6-FADS	CAQ30479

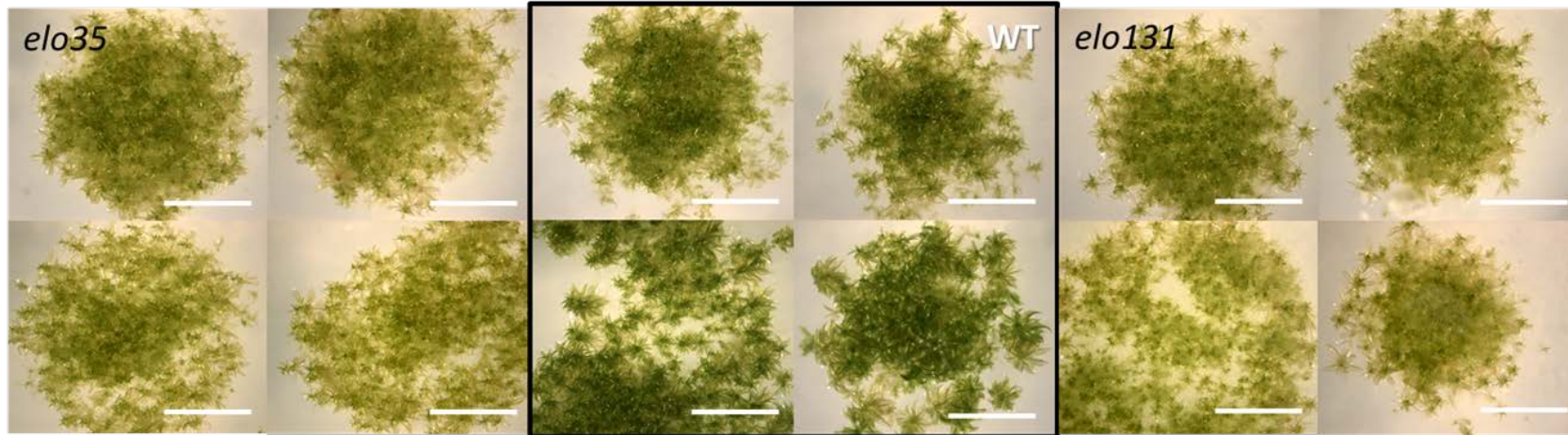


**Appendix 9. Moss plate cultures at normal temperature and gametophore-inducing growth conditions (without tartrate).** *P. patens* strains used are wild type (WT) and *PpSFD* KO-lines *sfd3*, *sfd10* and *sfd11*. Agar plate cultures were grown for 3 months at continuous light. Pictures were taken from two independent plate cultures for each strain. Scale bar = 0.5 cm

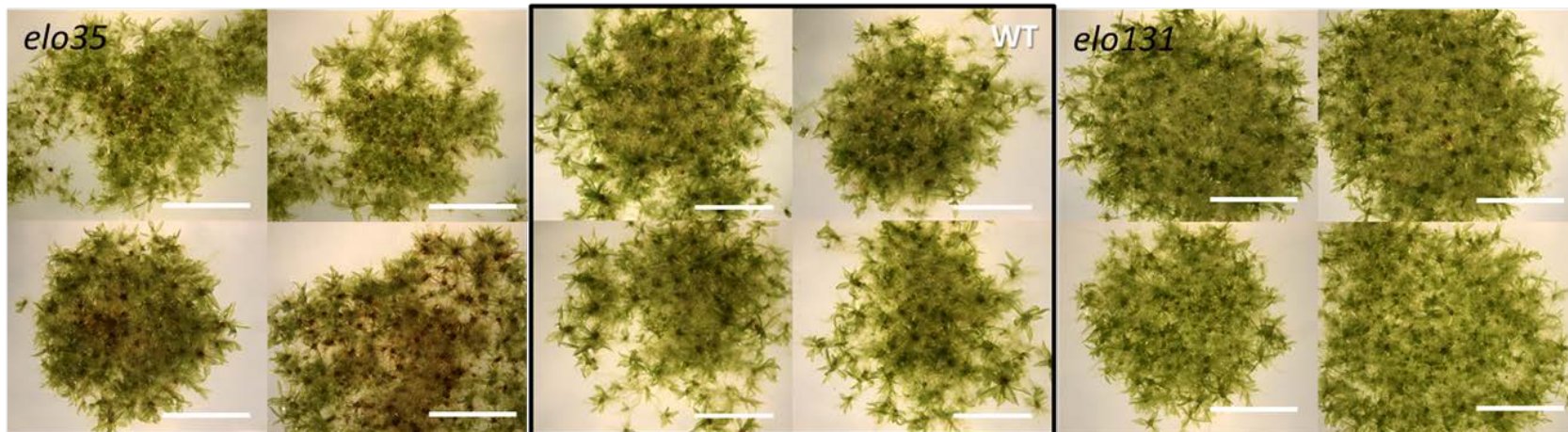


**Appendix 10. Moss plate cultures at cold stress temperature (6°C) and gametophore-inducing growth conditions (without tartrate).** *P. patens* strains used are wild type (WT) and *PpSFD* KO-lines *sfd3*, *sfd10* and *sfd11*. Agar plate cultures were grown for 3 months at continuous light. Pictures were taken from two independent plate cultures for each strain. Scale bar = 0.5 cm

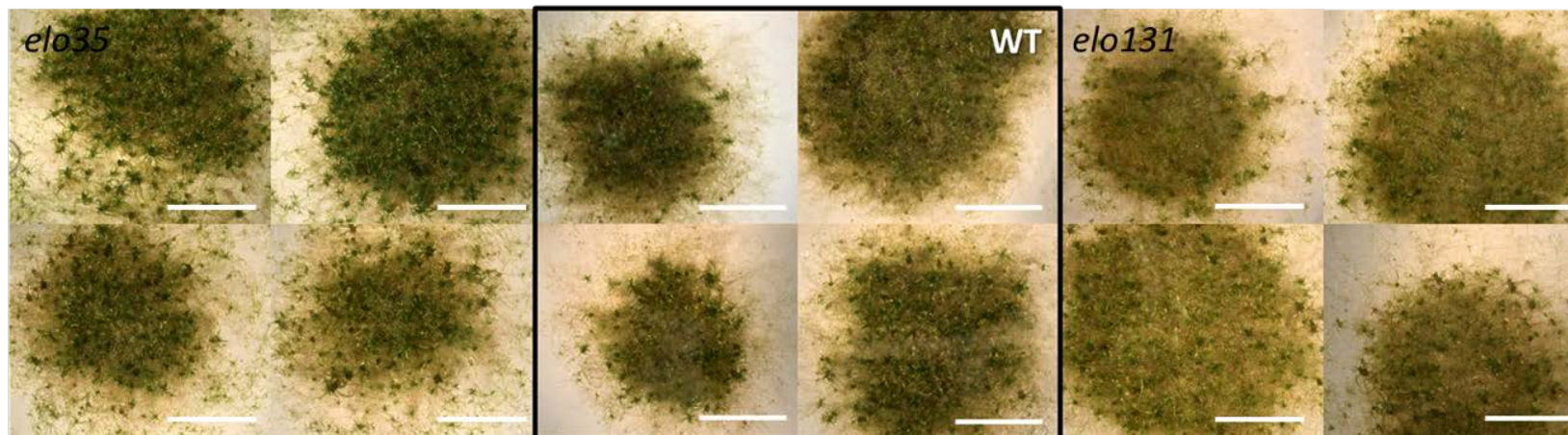
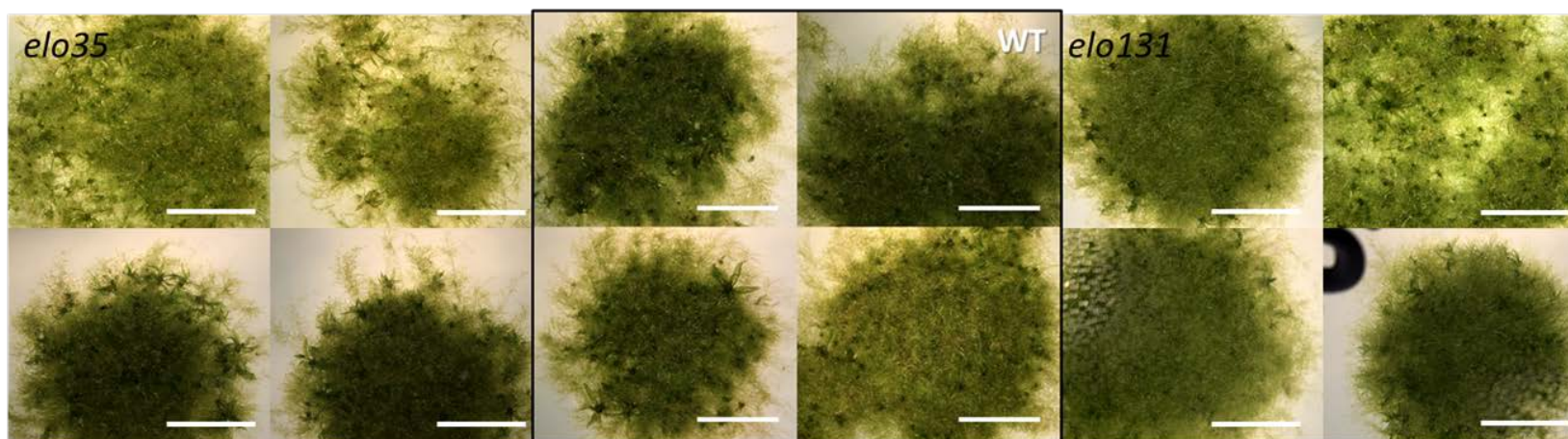
## Normal



## Cold stressed



**Appendix 11. Moss plate cultures at normal grown (24°C) and cold stress temperature (6°C) and gametophore-inducing growth conditions (without tartrate).** *P. patens* strains used are wild type (WT) and *PpELO* KO-lines *elo35* & *elo131*. Agar plate cultures were grown for 3 months at continuous light. Pictures were taken from two independent plate cultures for each strain. Scale bar = 0.5 cm

**Normal****Cold stressed**

**Appendix 12. Moss plate cultures at normal grown (24°C) and cold stress temperature (6°C) and protonema-inducing growth conditions (with tartrate).** *P. patens* strains used are wild type (WT) and *PpELO* KO-lines *elo35* & *elo131*. Agar plate cultures were grown for 3 months at continuous light. Pictures were taken from two independent plate cultures for each strain. Scale bar = 0.5 cm

# **Declaration of independent work**

I hereby confirm that I have written the attached thesis on my own and that I did not use any resources than those specified above. This work has not been previously submitted, either in the same or in a similar form to any other examination committee and has not yet been published.

Hanno Christoph Resemann  
Göttingen, April 2018

